Multiwavelength campaign of OJ287 in 2005-2010

M. Valtonen, HIP

8th INTEGRAL/BART Workshop
April 29, 2011

OJ287 binary black hole system?

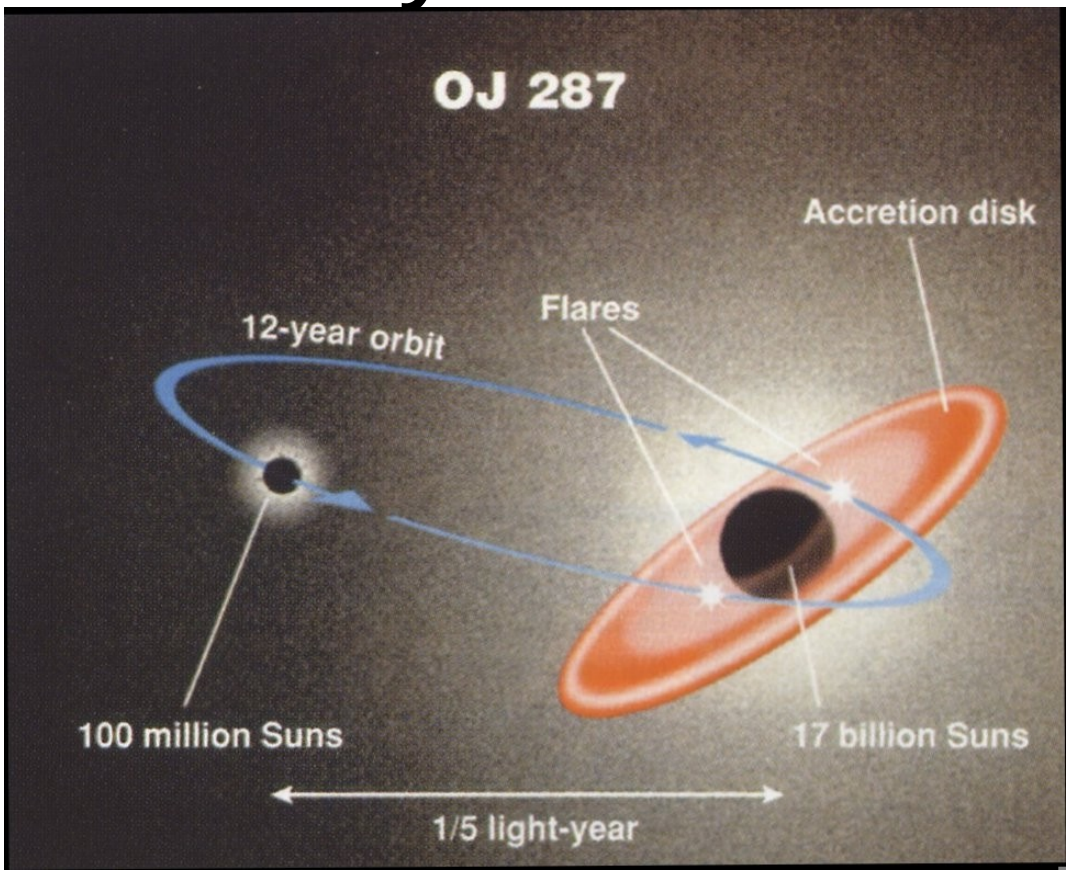

Sillanpää, Haarala, S., Valtonen, M. J., Sundelius, B. & Byrd, G. G., 1988, ApJ, 325, 628

Light curve

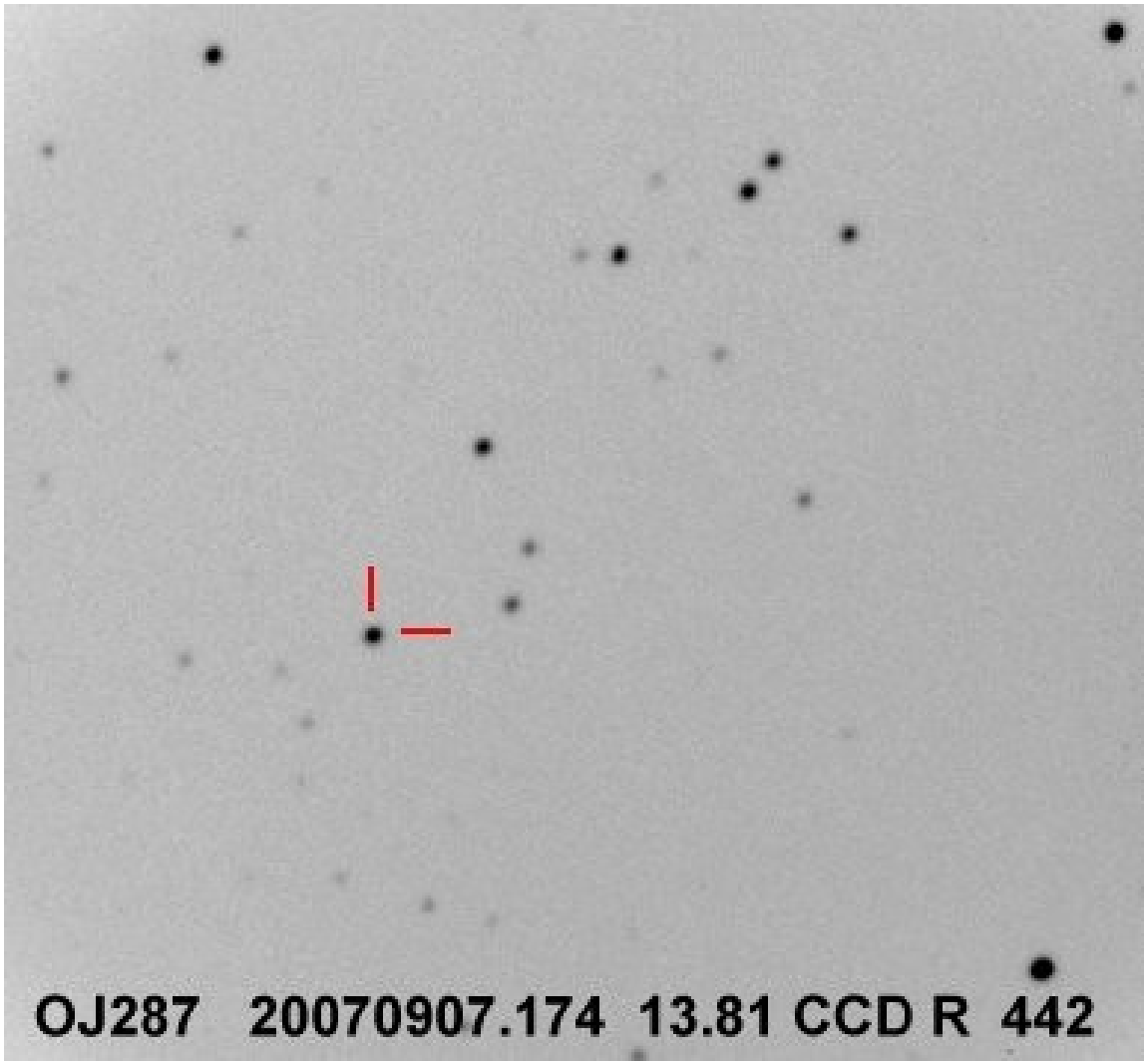

Optical light curve: 1891 -

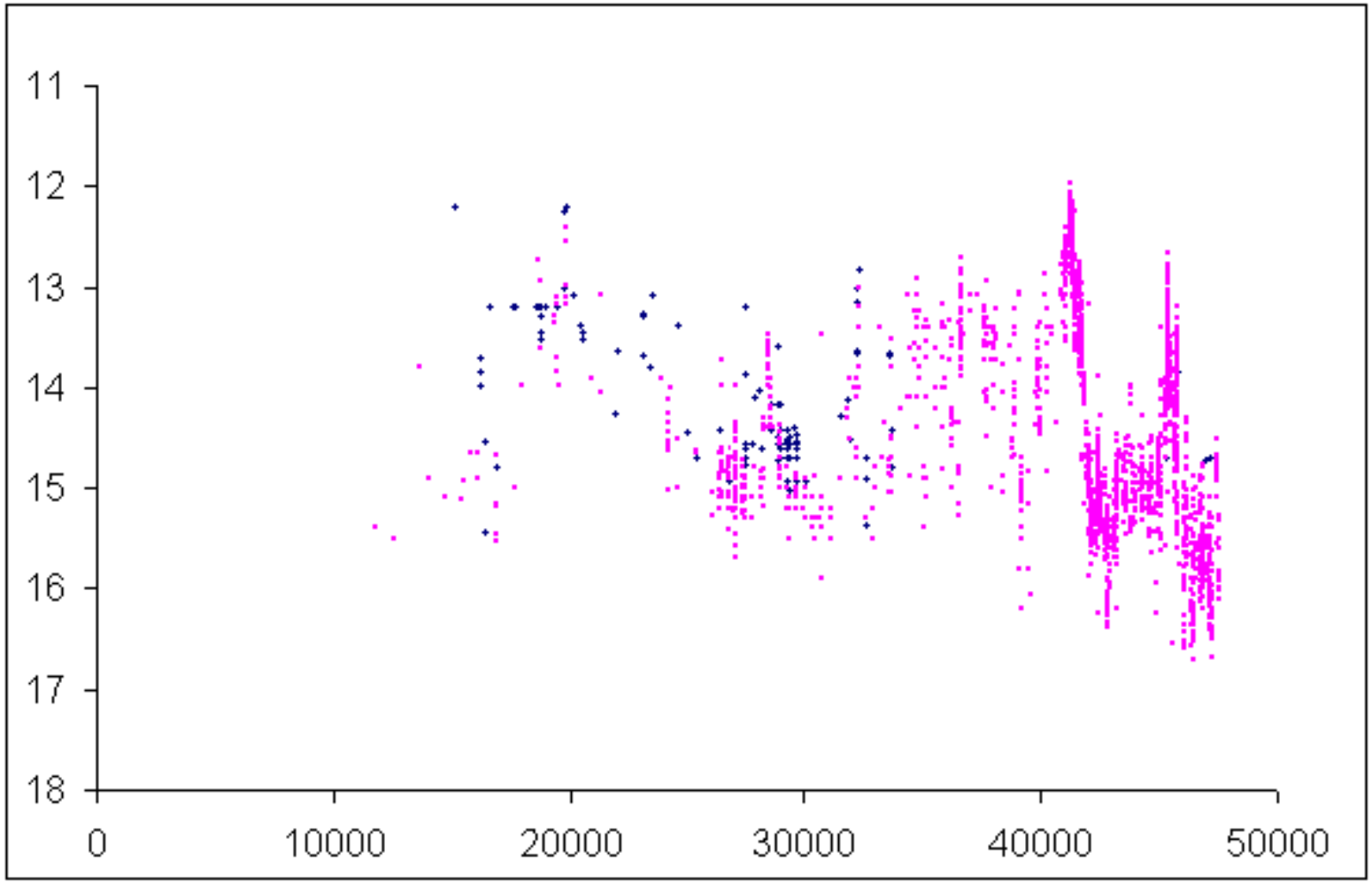

1. Signature of binary black holes: precession

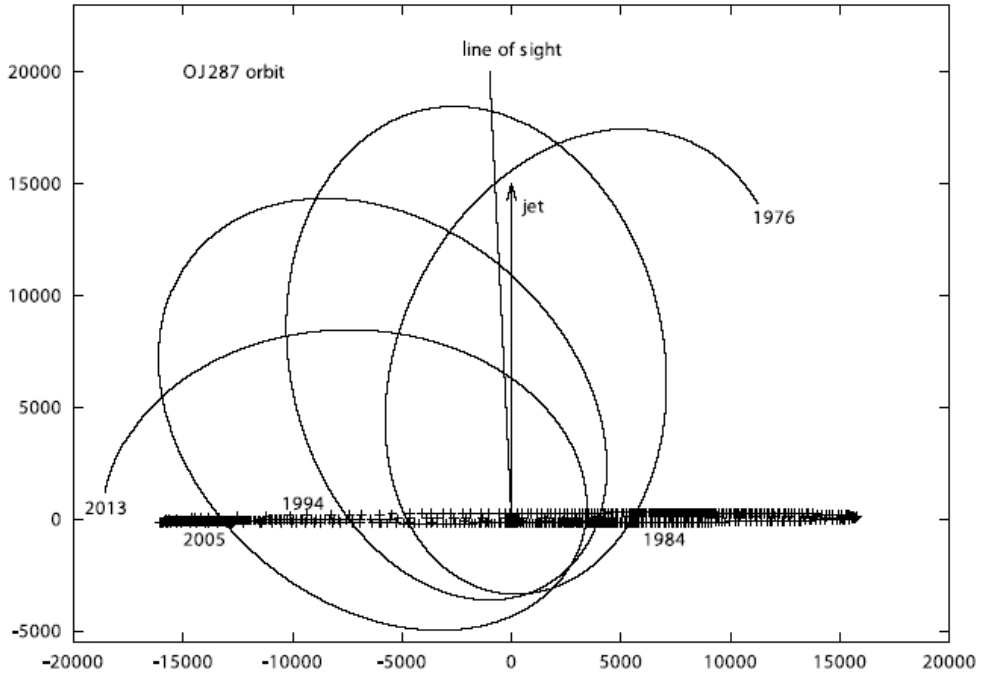

FIG. 1.—Precessing-binary model of OJ 287. The primary black hole is at coordinates (0, 0). The secondary black hole traces out a precessing elliptical orbit counterclockwise around the primary, illustrated here from 1976 to 2013. The secondary crosses the accretion disk of the primary (*horizontal set of points*) at impact sites; the 1984, 1994, and 2005 impacts are labeled. The axis of the accretion disk is labeled "jet." Not far from the jet is the line of sight to the observer. The binary orbit is at right angles to the accretion disk; Sundelius et al. (1997) have shown that this is not a restriction on the generality of the model, i.e., different relative inclinations would produce very similar results.

$$\Delta\phi = 39.1 \pm 0.1$$

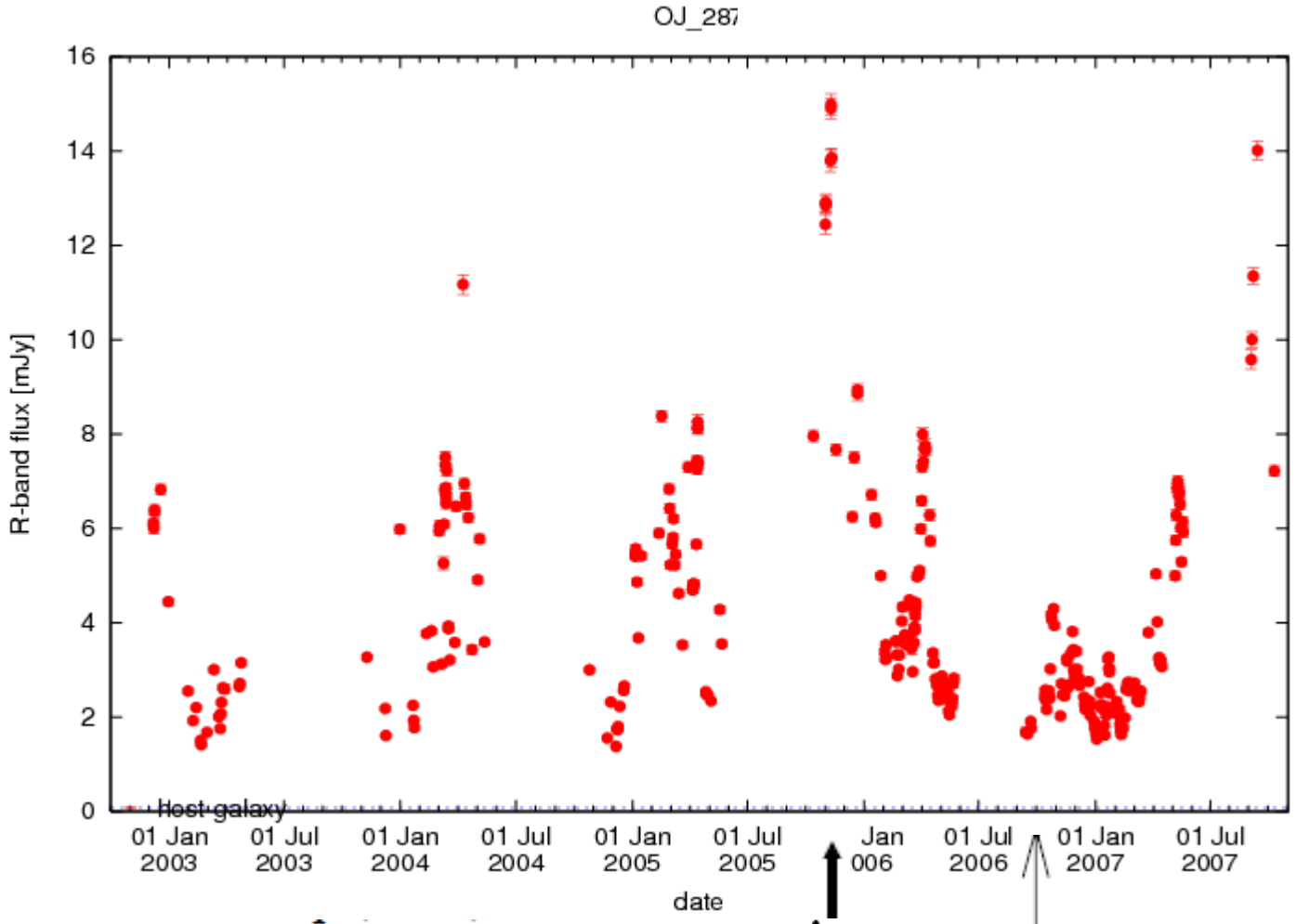

Sillanpää, A. et al. precession

no precession

Igumenschev, I. V., & Abramowicz, M. A. 1999

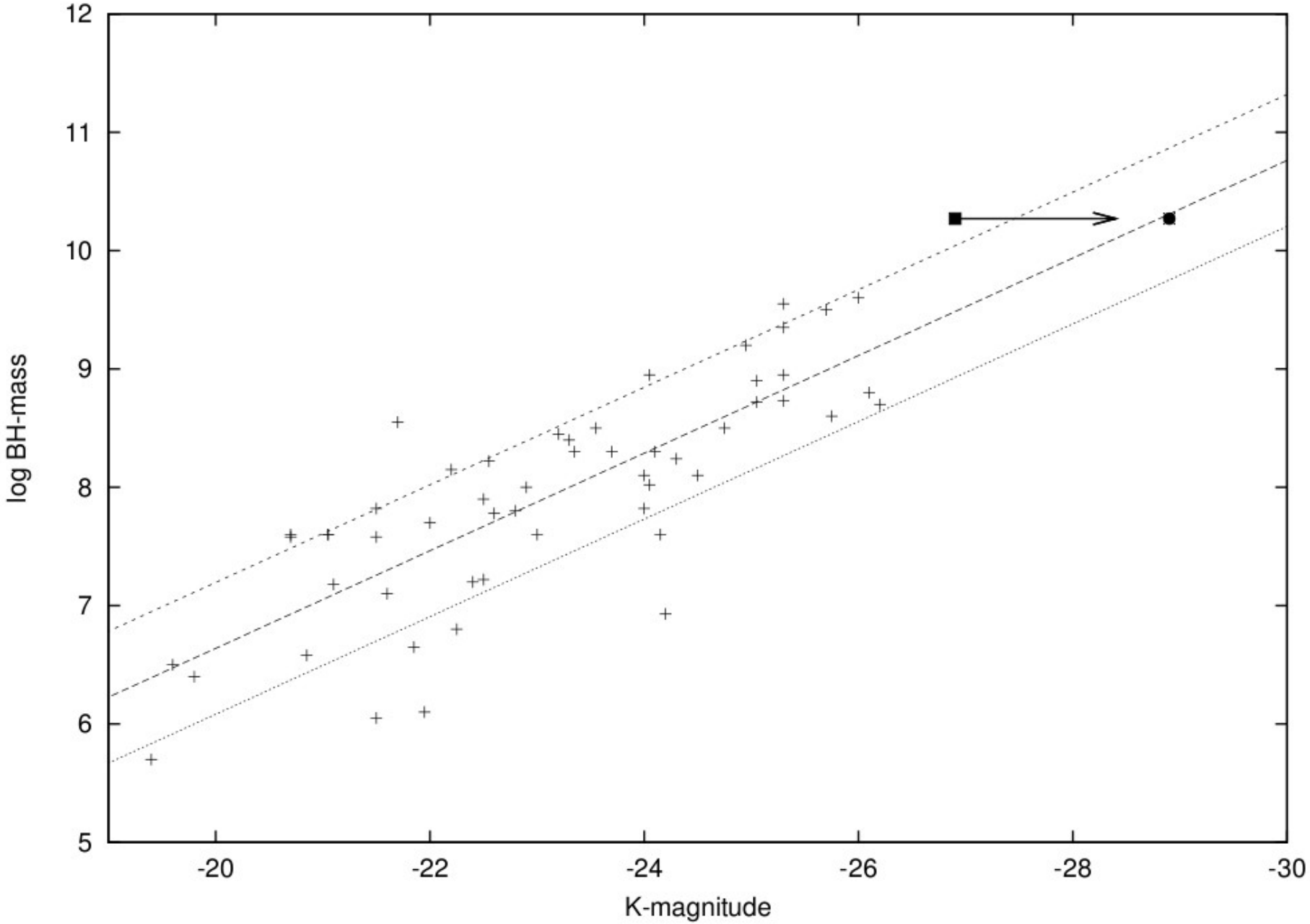
12
11
10
9
8
7
6
5
log BH-mass
-20
-22
-24
-26
-28
-30
K-magnitude

Nature Letter, 20 January 2011, 000, 000–000

Supermassive black holes do not correlate with dark matter halos of galaxies

John Kormendy[1,2,3] & Ralf Bender[2,3]

OJ 287

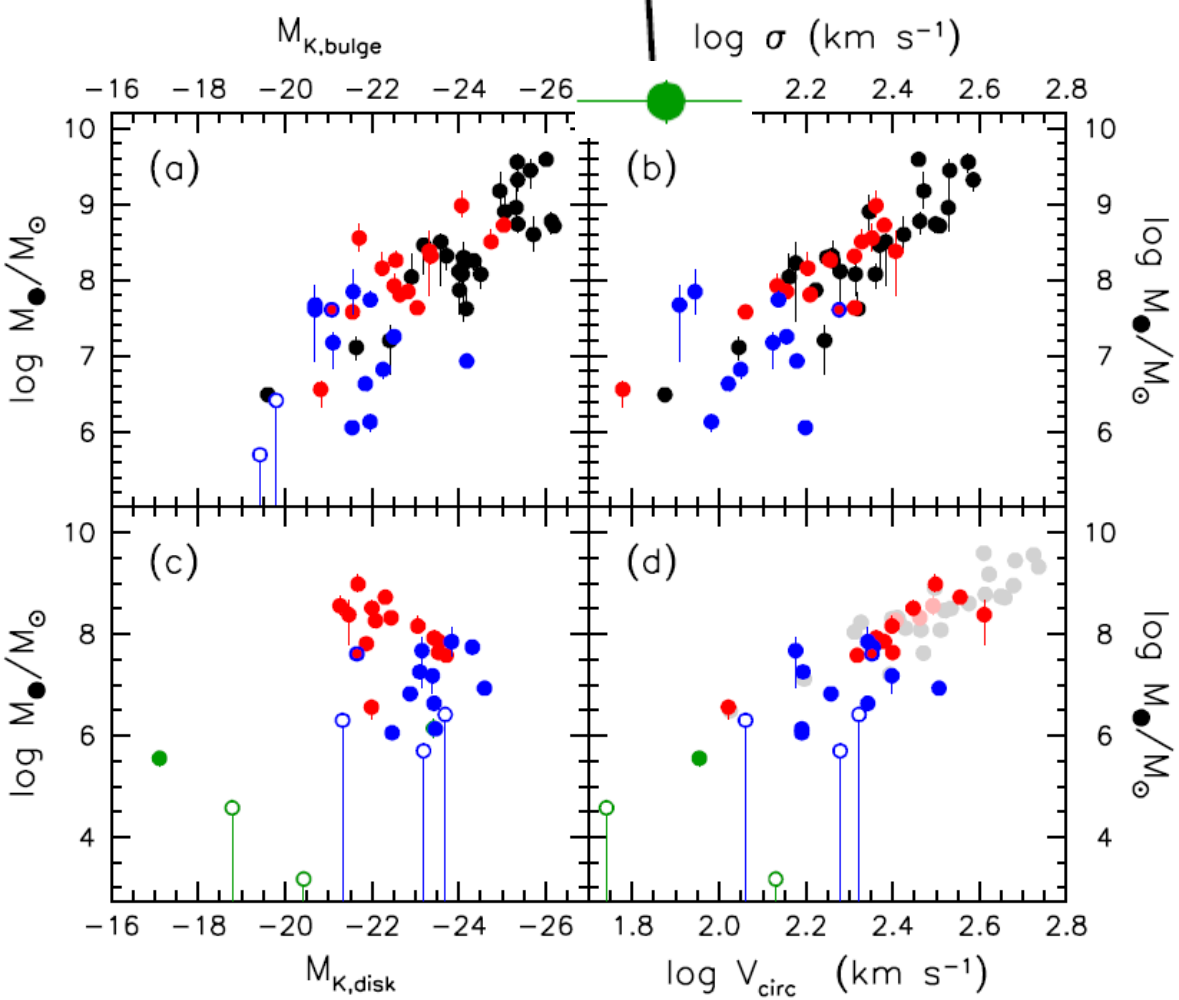

2. Black hole – Accretion disk collision

Ivanov et al. 1998

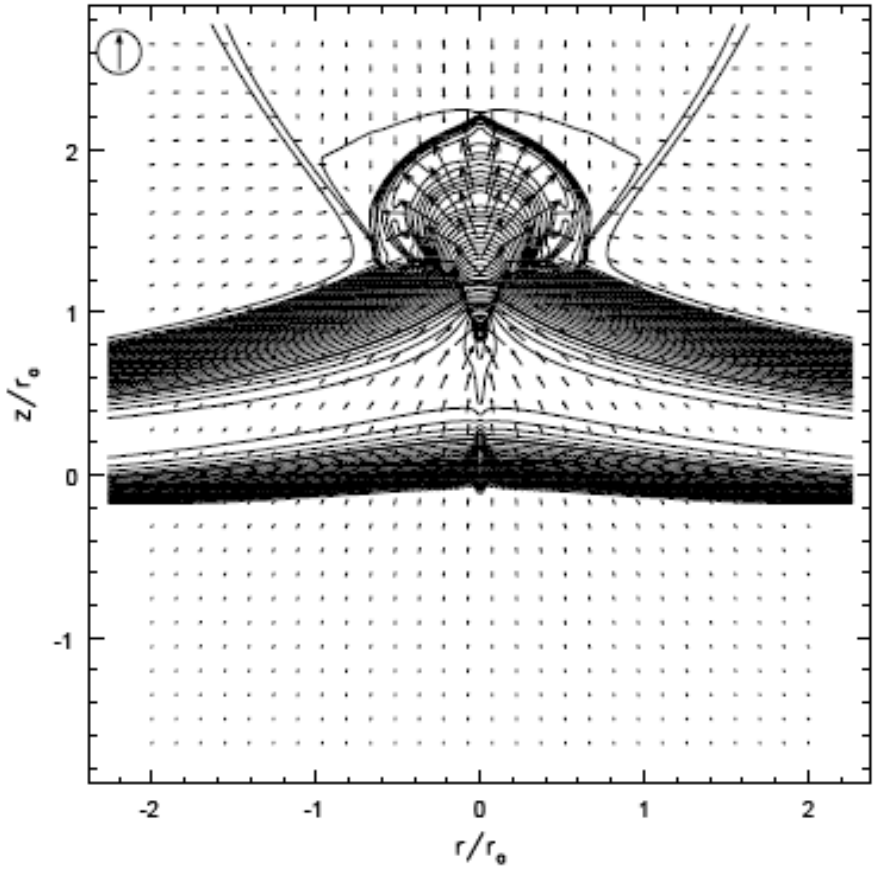

Collision 2

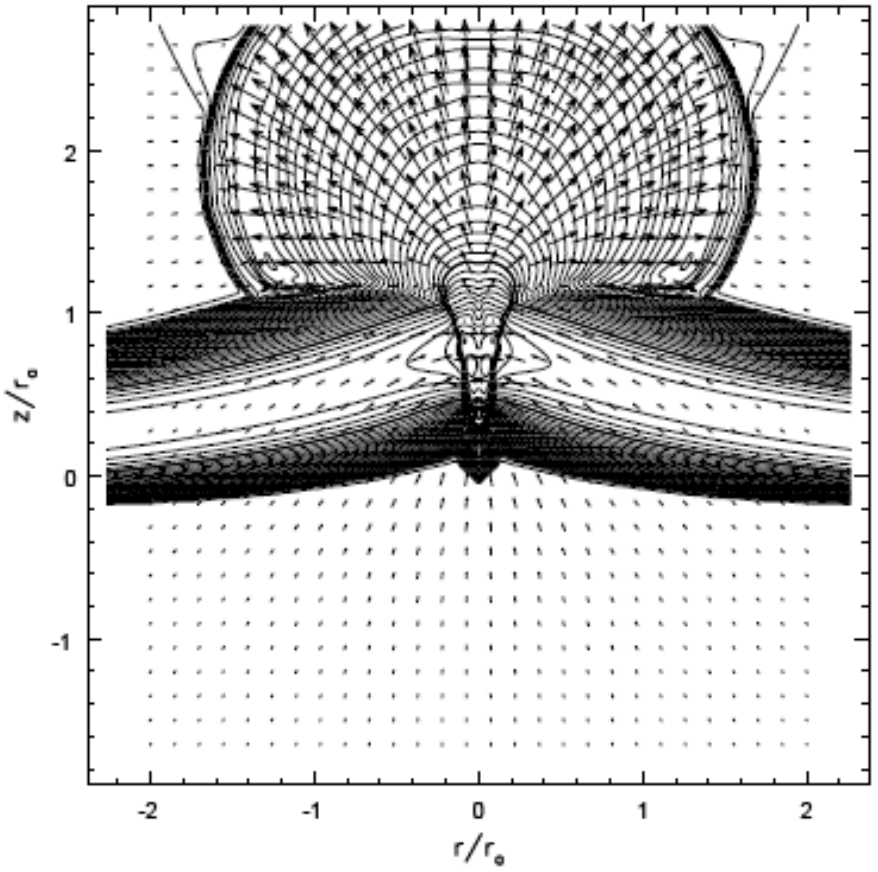

Collision 3

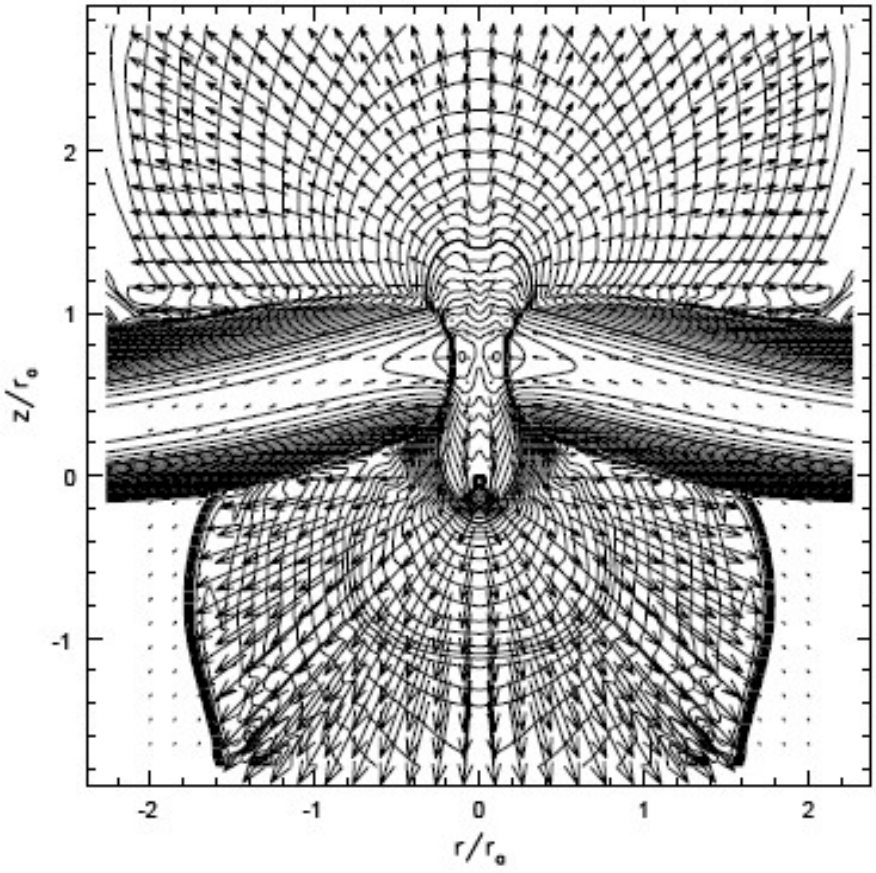

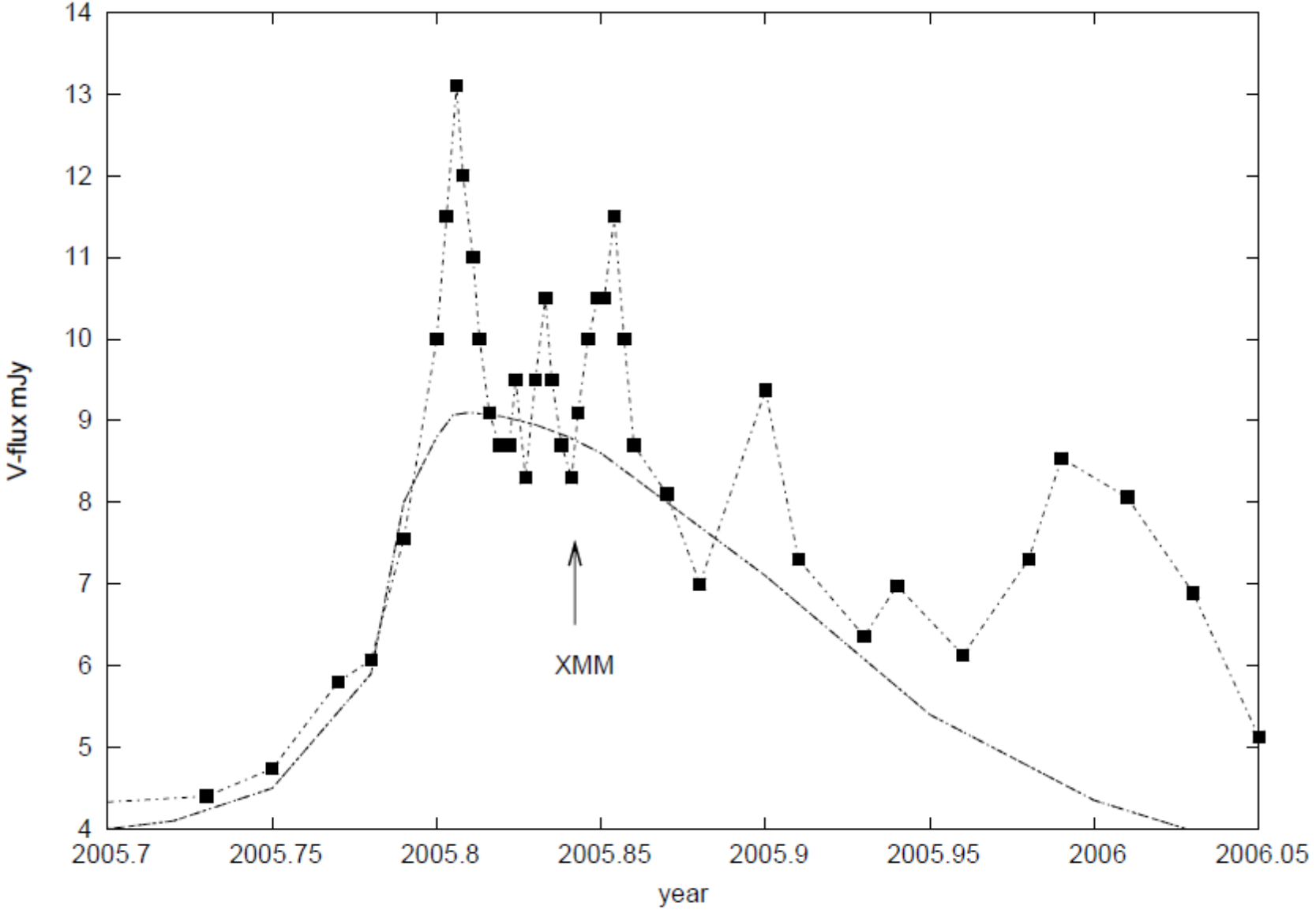
V-flux mJy
year
XMM
14
13
12
11
10
9
8
7
6
5
4
2005.7
2005.75
2005.8
2005.85
2005.9
2005.95
2006
2006.05

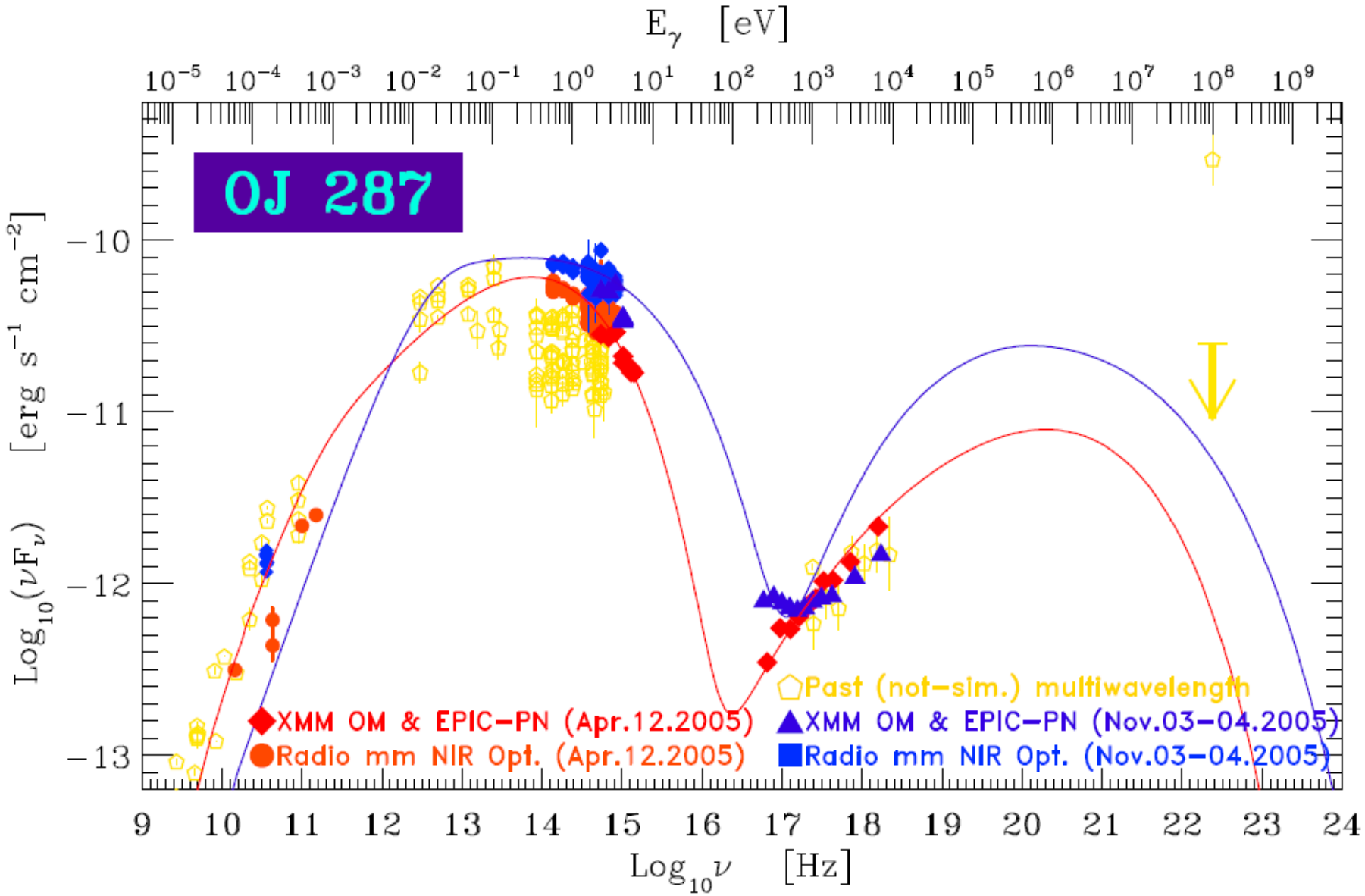
E$_\gamma$ [eV]
10^{-5} 10^{-4} 10^{-3} 10^{-2} 10^{-1} 10^{0} 10^{1} 10^{2} 10^{3} 10^{4} 10^{5} 10^{6} 10^{7} 10^{8} 10^{9}
OJ 287
Log$_{10}(\nu F_\nu)$ [erg s^{-1} cm^{-2}]
−10
−11
−12
−13
Past (not−sim.) multiwavelength
XMM OM & EPIC−PN (Apr.12.2005)
Radio mm NIR Opt. (Apr.12.2005)
XMM OM & EPIC−PN (Nov.03−04.2005)
Radio mm NIR Opt. (Nov.03−04.2005)
9 10 11 12 13 14 15 16 17 18 19 20 21 22 23 24
Log$_{10}\nu$ [Hz]

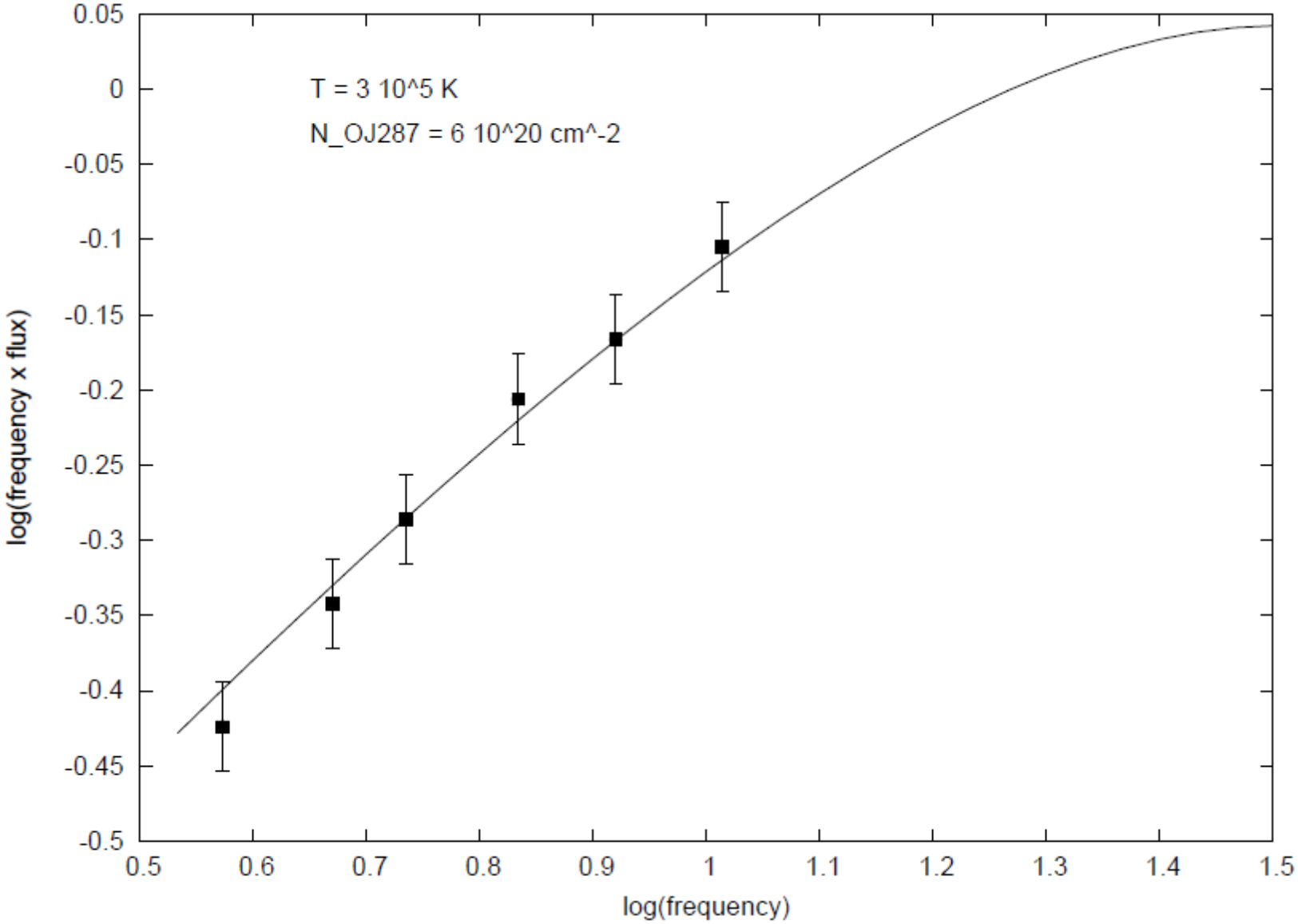
T = 3 10^5 K
N_OJ287 = 6 10^20 cm^-2
log(frequency x flux)
log(frequency)
0.05
0
-0.05
-0.1
-0.15
-0.2
-0.25
-0.3
-0.35
-0.4
-0.45
-0.5
0.5
0.6
0.7
0.8
0.9
1
1.1
1.2
1.3
1.4
1.5

3. Prediction: 2nd outburst Sept 2007 unpolarized

OJ287 in September 2007

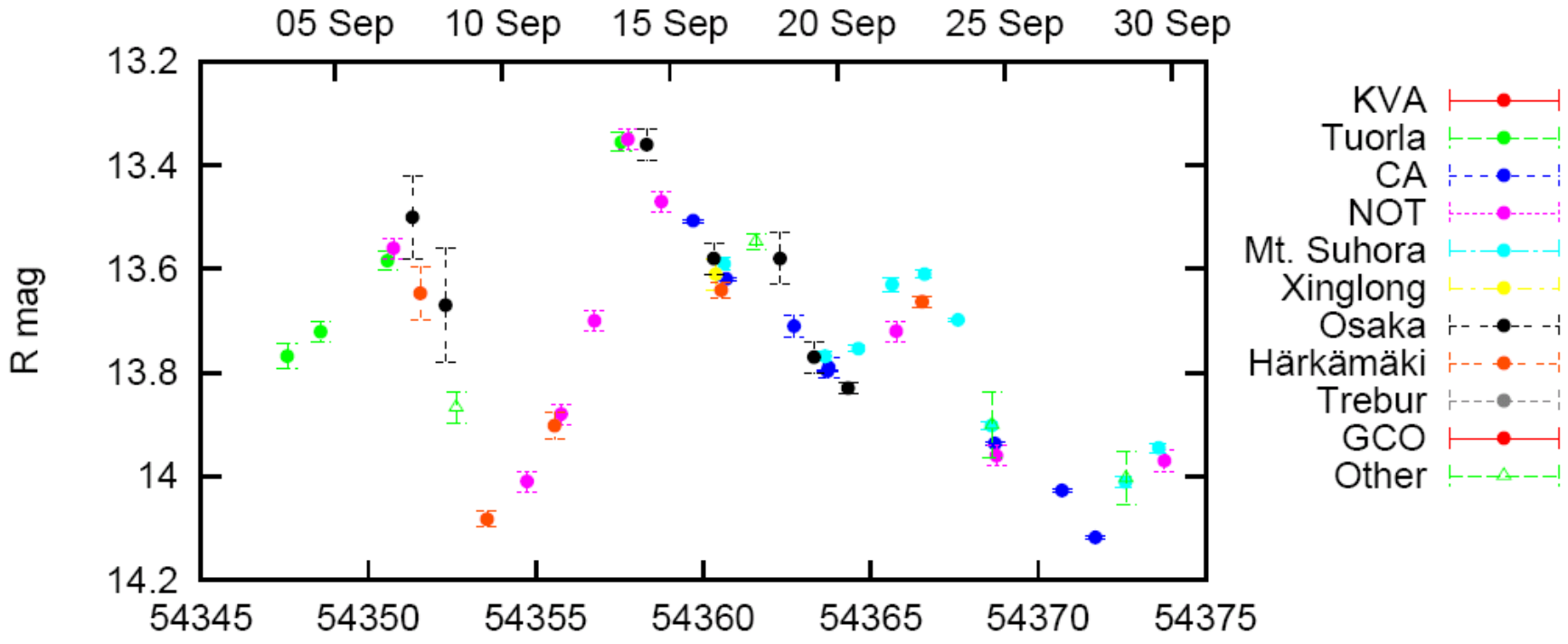

Polarization

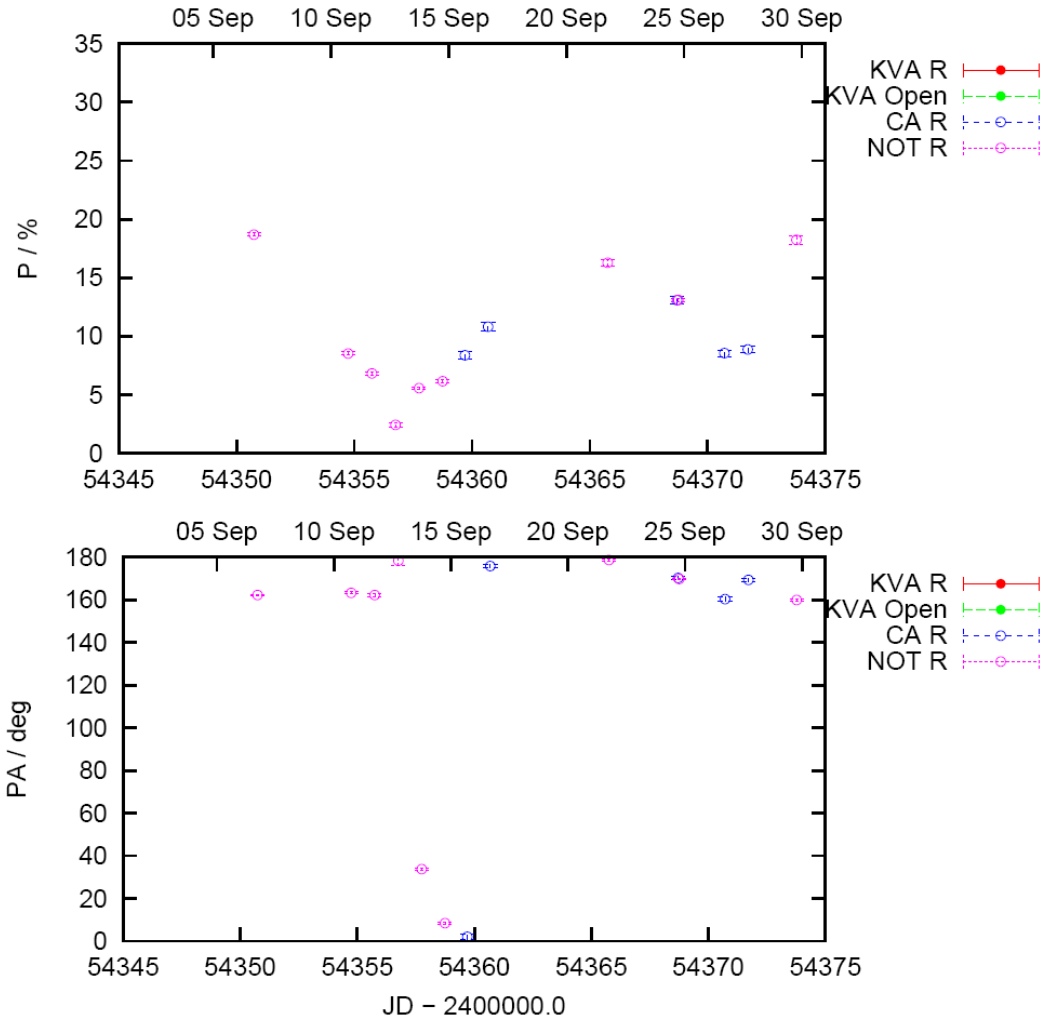

Vol 452|17 April 2008|doi:10.1038/nature06896

nature

LETTERS

A massive binary black-hole system in OJ 287 and a test of general relativity

M. J. Valtonen[1], H. J. Lehto[1], K. Nilsson[1], J. Heidt[2], L. O. Takalo[1], A. Sillanpää[1], C. Villforth[1], M. Kidger[3], G. Poyner[4], T. Pursimo[5], S. Zola[6,7], J.-H. Wu[8], X. Zhou[8], K. Sadakane[9], M. Drozdz[7], D. Koziel[6], D. Marchev[10], W. Ogloza[7], C. Porowski[6], M. Siwak[6], G. Stachowski[7], M. Winiarski[6], V.-P. Hentunen[11], M. Nissinen[11], A. Liakos[12] & S. Dogru[13]

1 Department of Physics and Tuorla Observatory, University of Turku, Vaisäläntie 20, FI-21500 Piikkiö, Finland

2 Landessternwarte Heidelberg, Königstuhl, 69117 Heidelberg, Germany

3 Herschel Science Centre, European Space Astronomy Centre, European Space Agency, Villafrance del Castillo Satellite Tracking Station, P.O.Box 78, 28691 Villanueva de la Canada, Madrid, Spain, and INSA, Paseo del Pintor Rosales 34, 28008 Madrid, Spain

4 British Astronomical Association Variable Star Section, 67 Ellerton Road, Kingstanding, Birmingham B44 0QE, England

5 Nordic Optical Telescope, Apartado 474, E-38700 S/C de La Palma, Spain

6 Astronomical Observatory of the Jagiellonian University, u1. Orla 171, 30-224 Cracow, Poland

7 Mt.Suhora Observatory, Pedagogical University, ul. Podchorazych 2, 30-084, Cracow, Poland

8 National Astronomical Observatories, Chinese Academy of Sciences, 20A Datun Road, Beijing 100012, China

9 Astronomical Institute, Osaka-Kyoiku University, Asahigaoka, Kashiwara, Osaka 582-8582, Japan

10 Department of Physics, Shoumen University, 9700 Shoumen, Bulgaria

11 Warkauden Kassiopeia ry, Härkämäentie 88, 79480 Kangaslampi, Finland

12 Department of Astrophysics, Astronomy and Mechanics, Faculty of Physics, University of Athens, Panepistimiopolis, GR-15784 Zografos, Athens, Greece

13 Canakkale Onsekiz Mart University, Faculty of Physics, TR-17020 Canakkale, Turkey

4. Rotation of radio jet

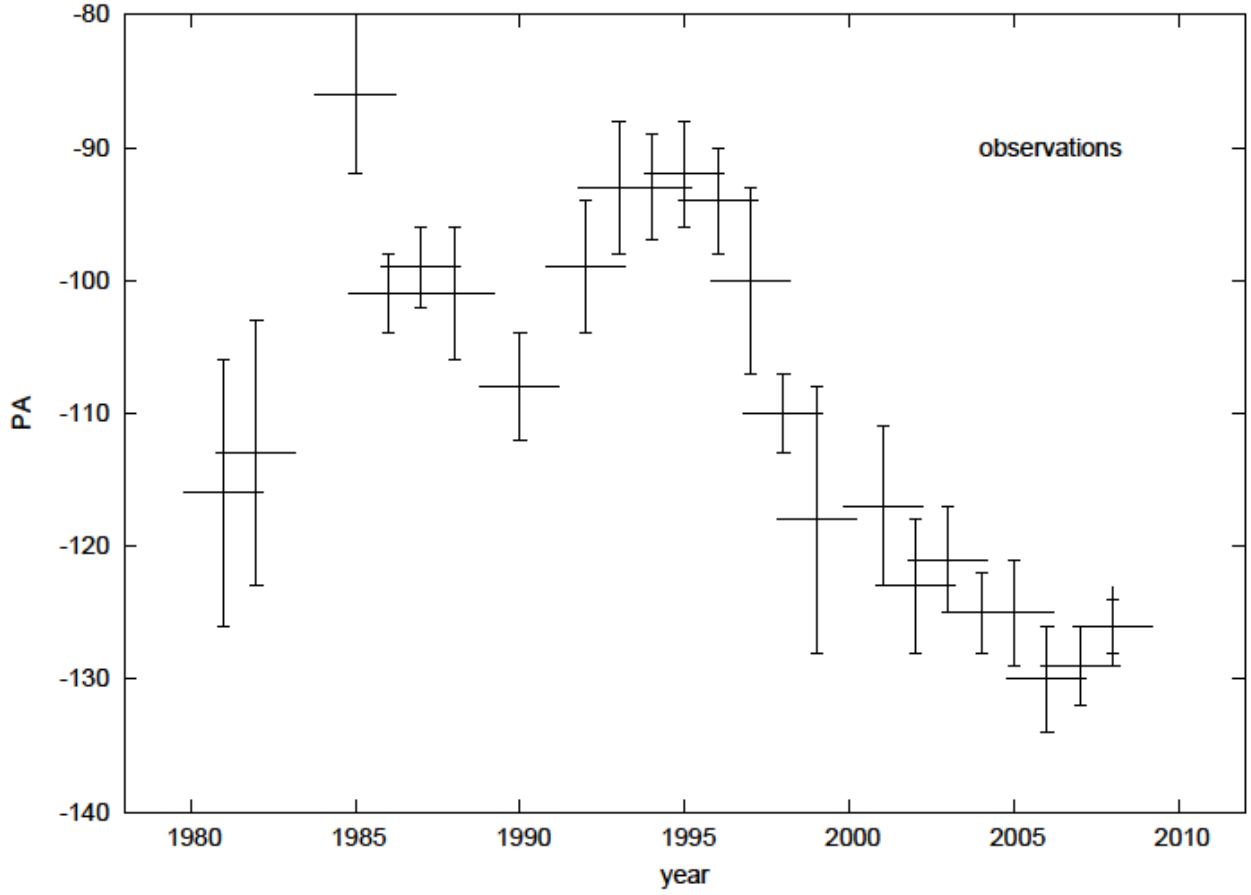

Binary model

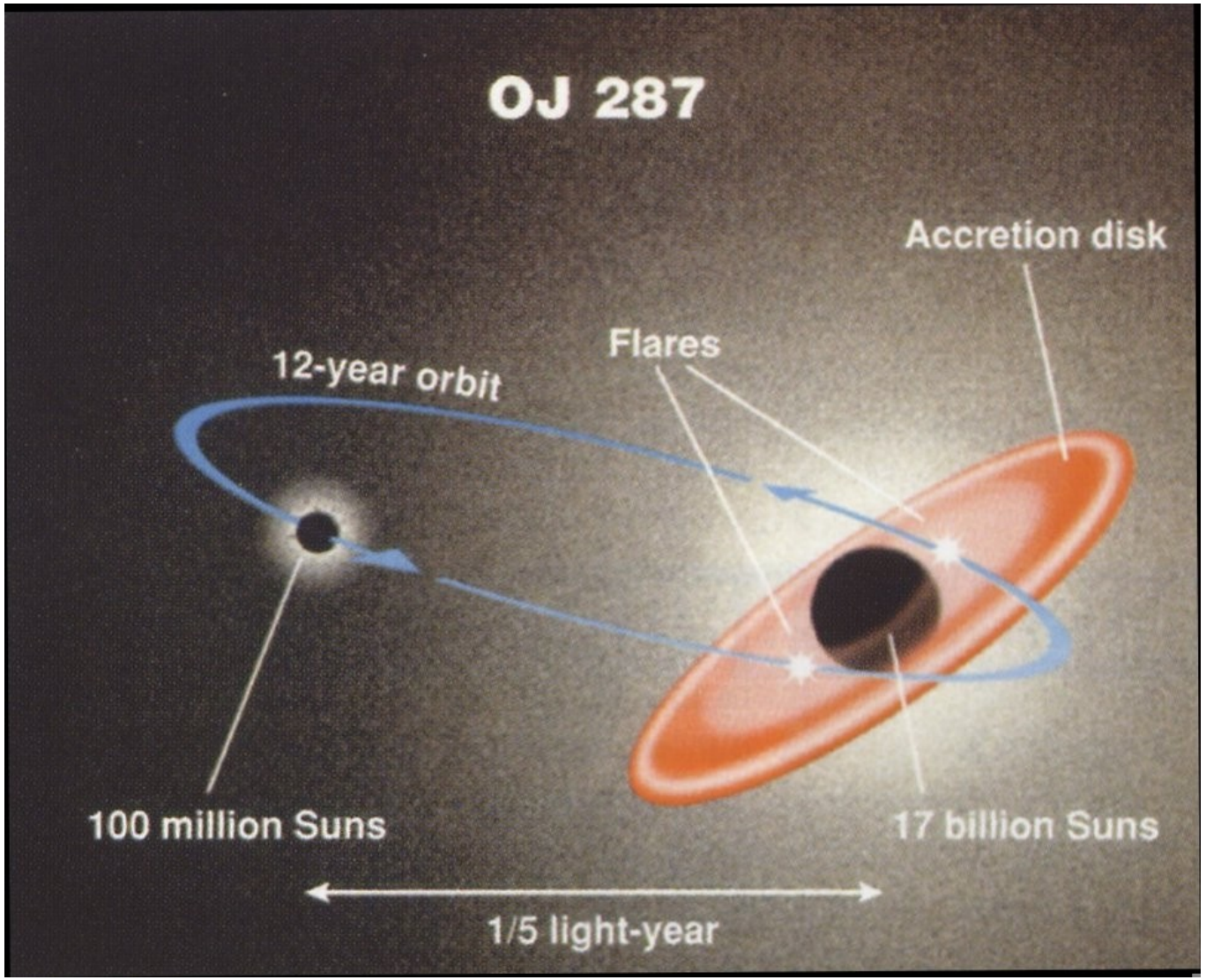

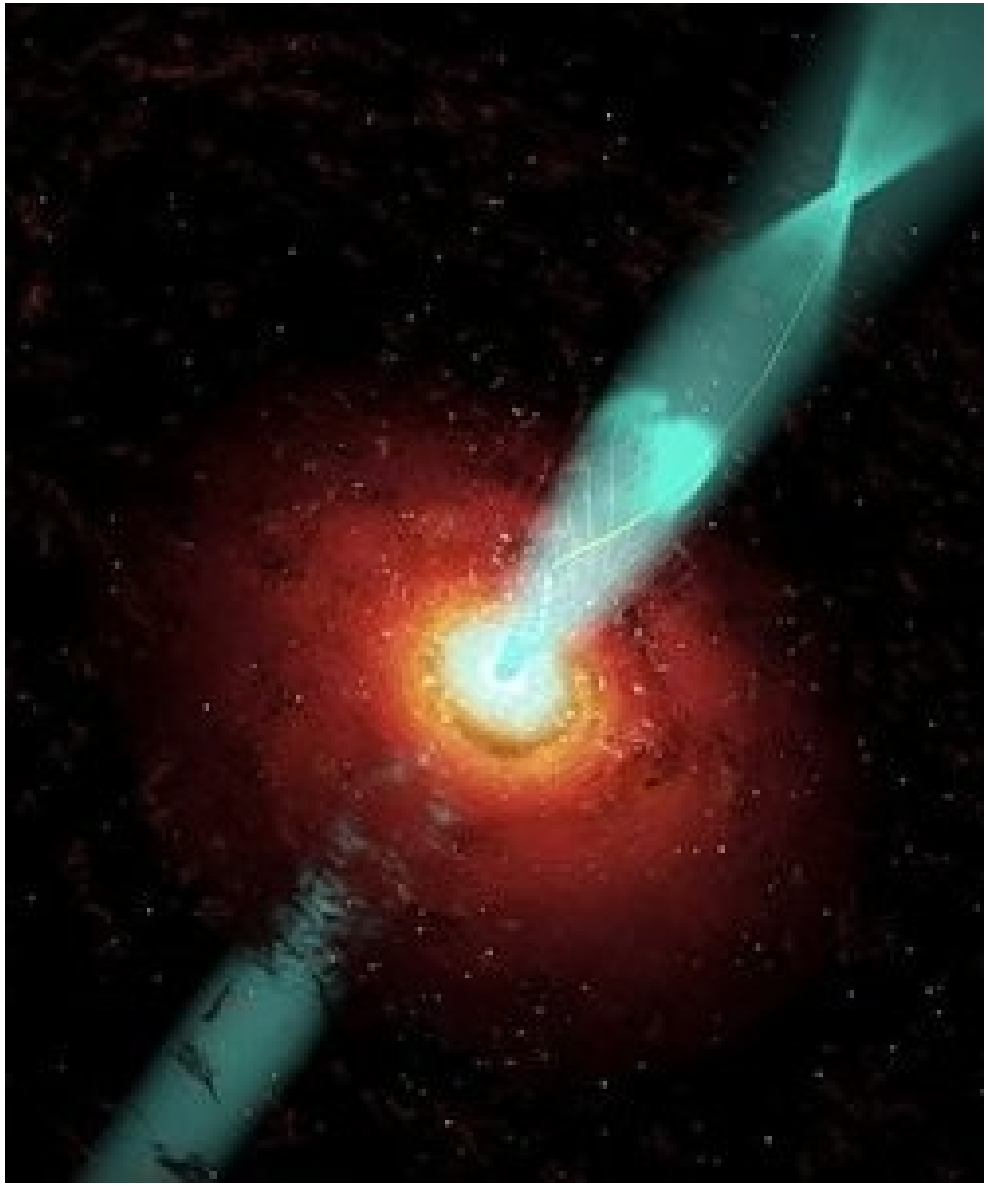

Jorstad et al. 2005

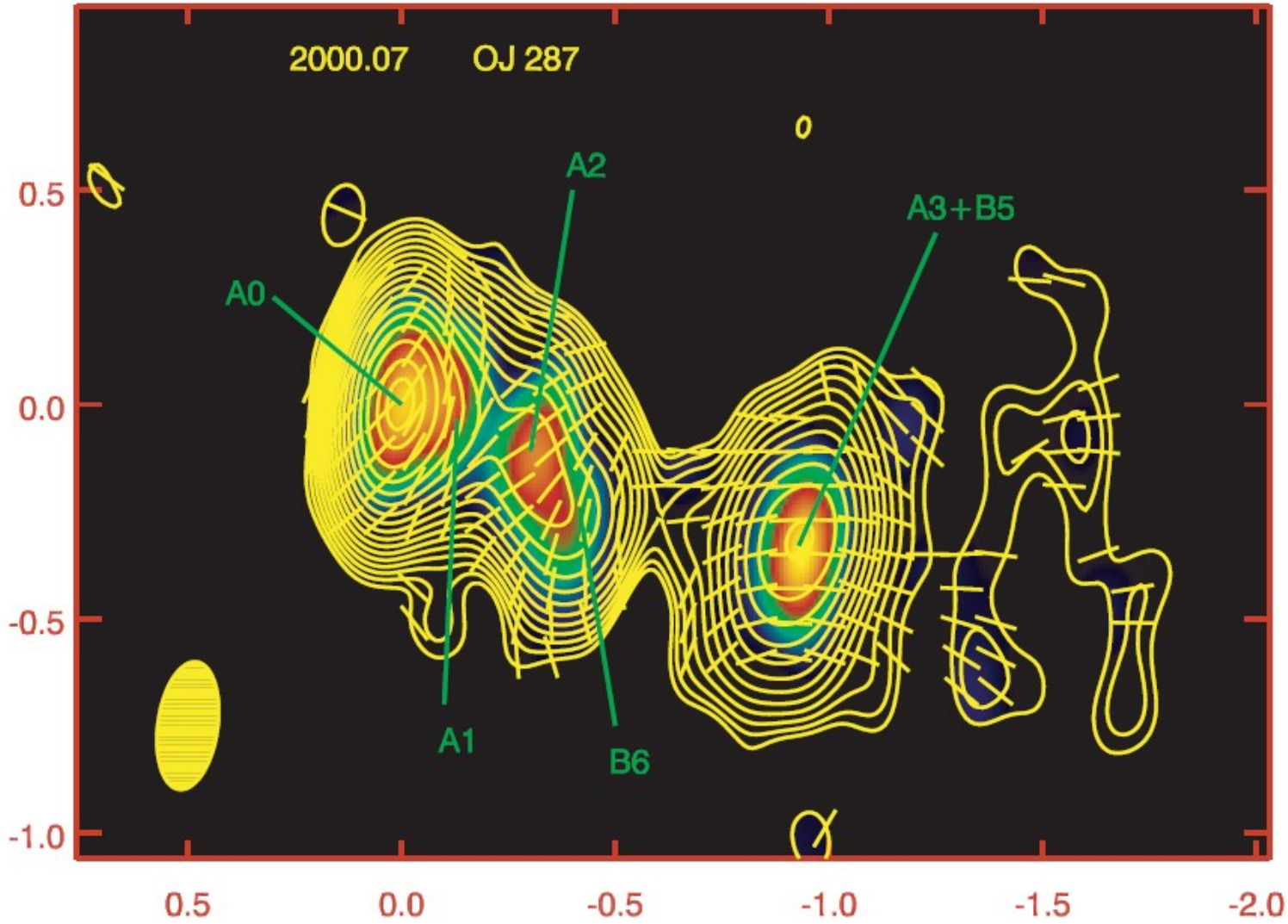

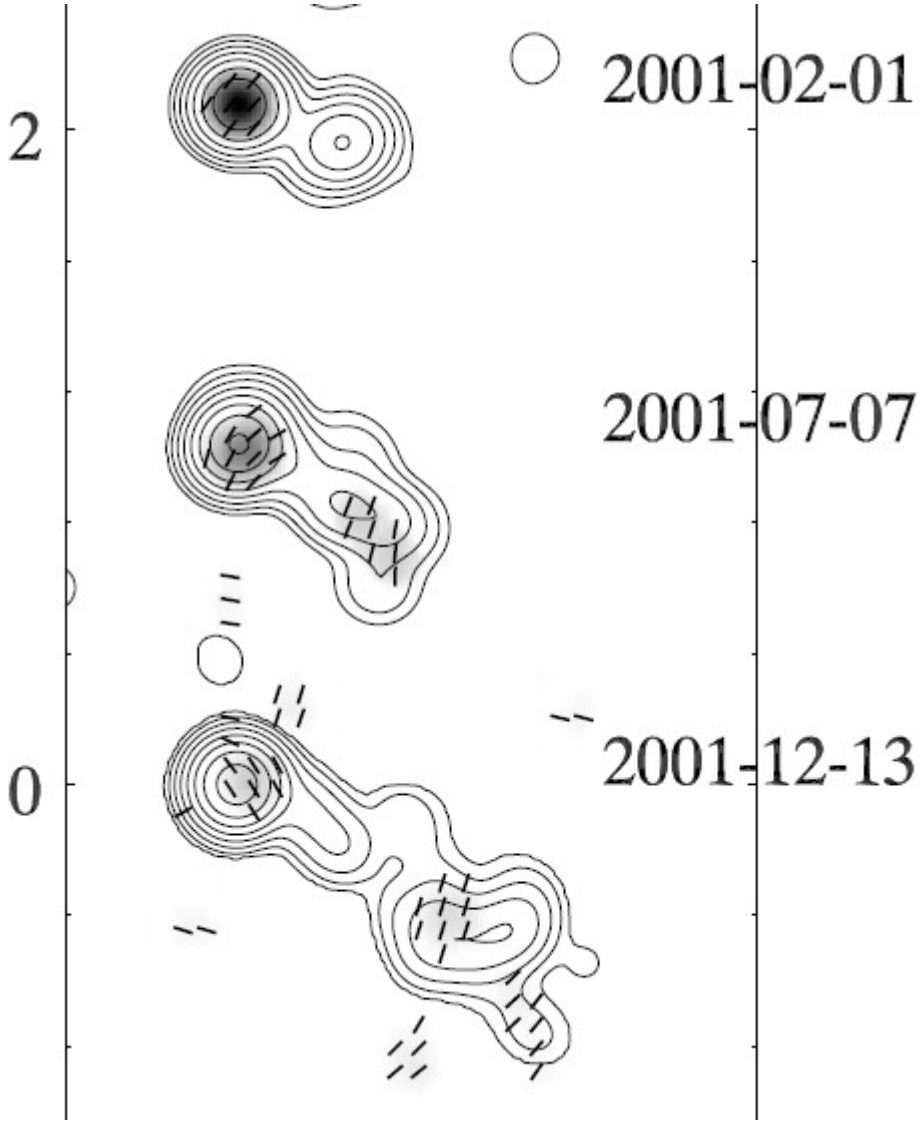
2001-02-01
2001-07-07
2001-12-13
2
0

LOCATION OF γ-RAY FLARE EMISSION IN THE JET OF THE BL LACERTAE OBJECT OJ287 MORE THAN 14 PC FROM THE CENTRAL ENGINE

IVÁN AGUDO[1], SVETLANA G. JORSTAD[1,2], ALAN P. MARSCHER[1], VALERI M. LARIONOV[2,3], JOSÉ L. GÓMEZ[4], ANNE LÄHTEENMÄKI[5], MARK GURWELL[6], PAUL S. SMITH[7], HELMUT WIESEMEYER[8], CLEMENS THUM[9], JOCHEN HEIDT[10], DMITRIY A. BLINOV[2,3], FRANCESCA D. D'ARCANGELO[1,11], VLADIMIR A. HAGEN-THORN[2,3], DARIA A. MOROZOVA[2], ELINA NIEPPOLA[5,12], MAR ROCA–SOGORB[4], GARY D. SCHMIDT[13], BRIAN TAYLOR[1,14], MERJA TORNIKOSKI[5], IVAN S. TROITSKY[2]

Accepted for publication in The Astrophysical Journal Letters

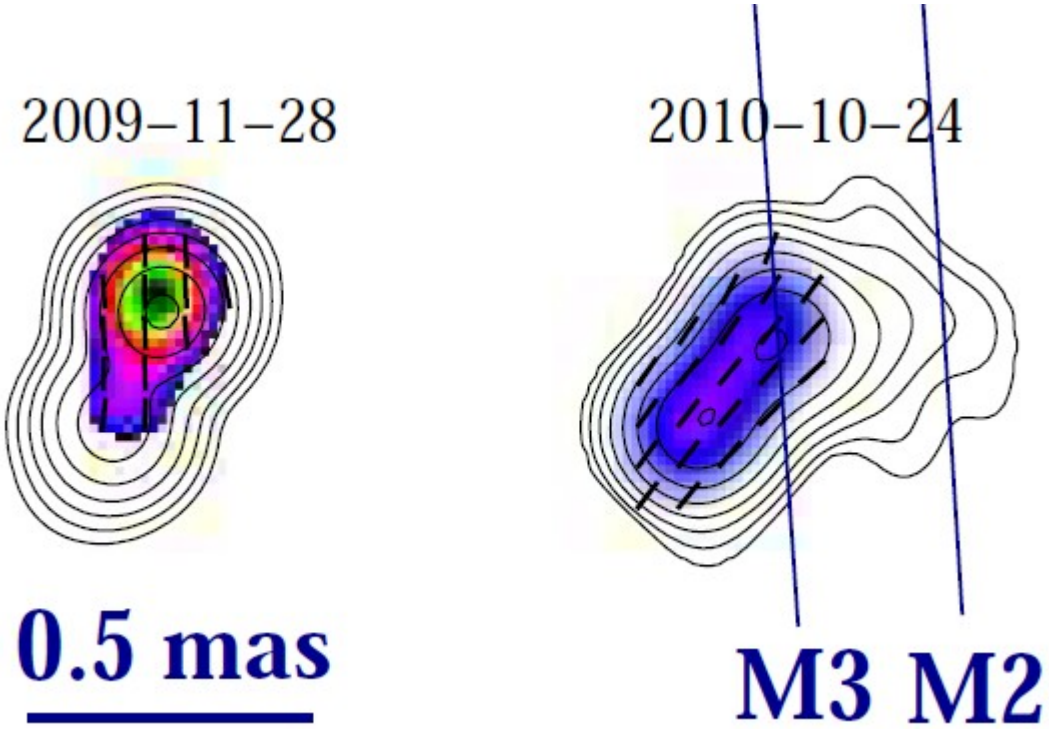

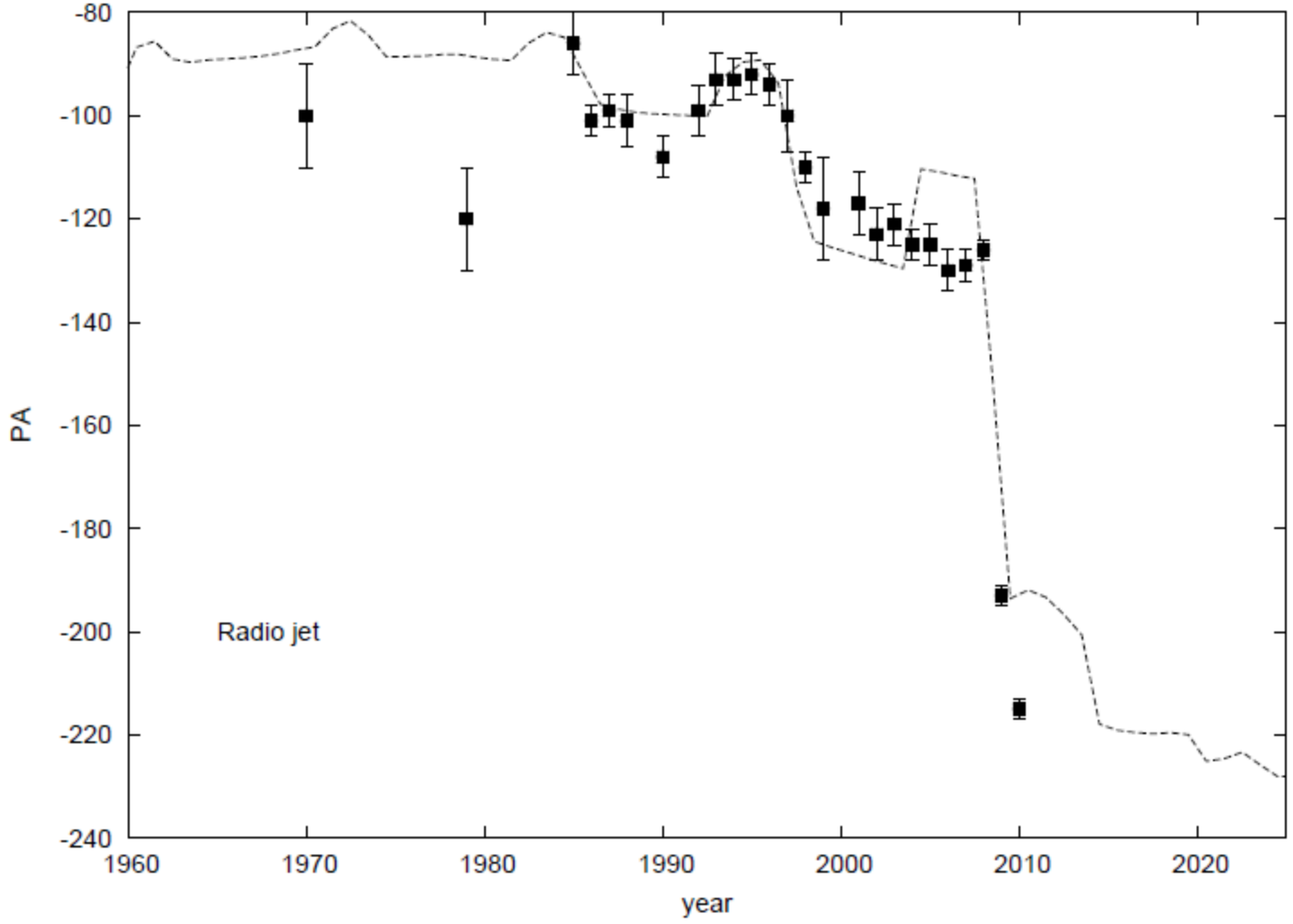

Figure 4. The variation of the position angle of the radio jet in

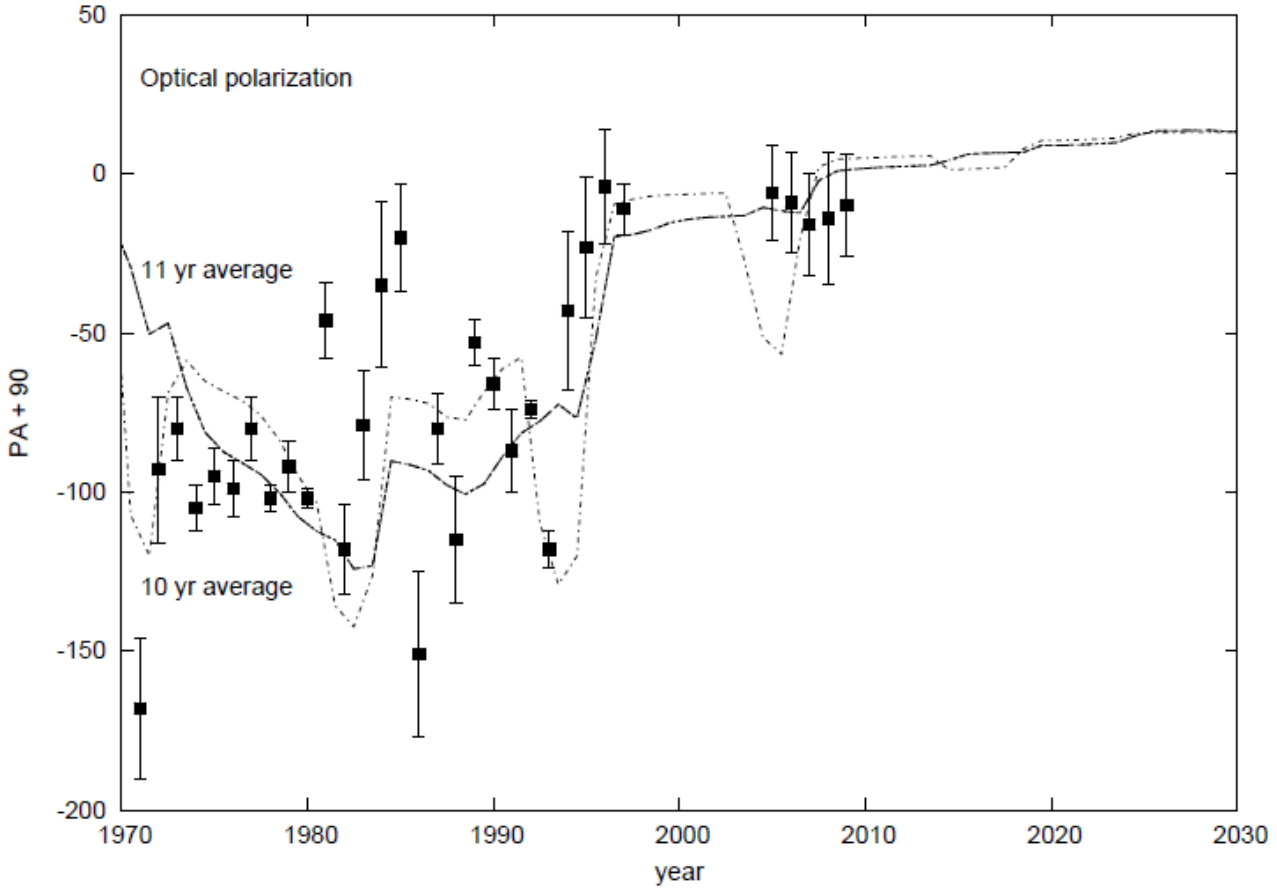

Figure 6. The evolution of the optical polarization angle compared with the model. The curves are for a 10 yr (dash-dot line) and for an 11 yr (dashed line) average. Observations refer to the values in Table 1 minus 180°. The theoretical lines are shifted by adding 90° since the electric vector does not project parallel to the jet axis.

5. Tidal outbursts

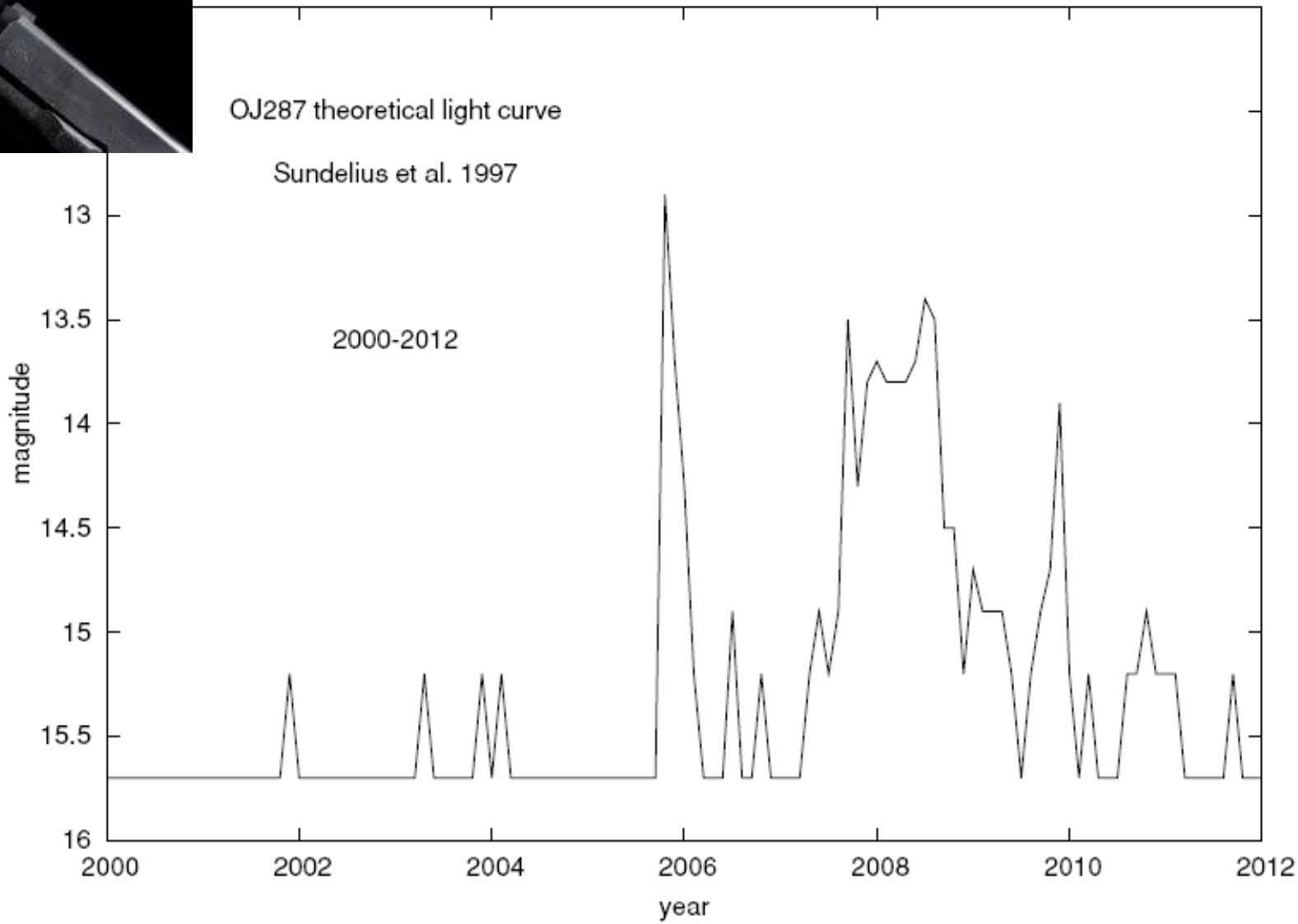

Binary model

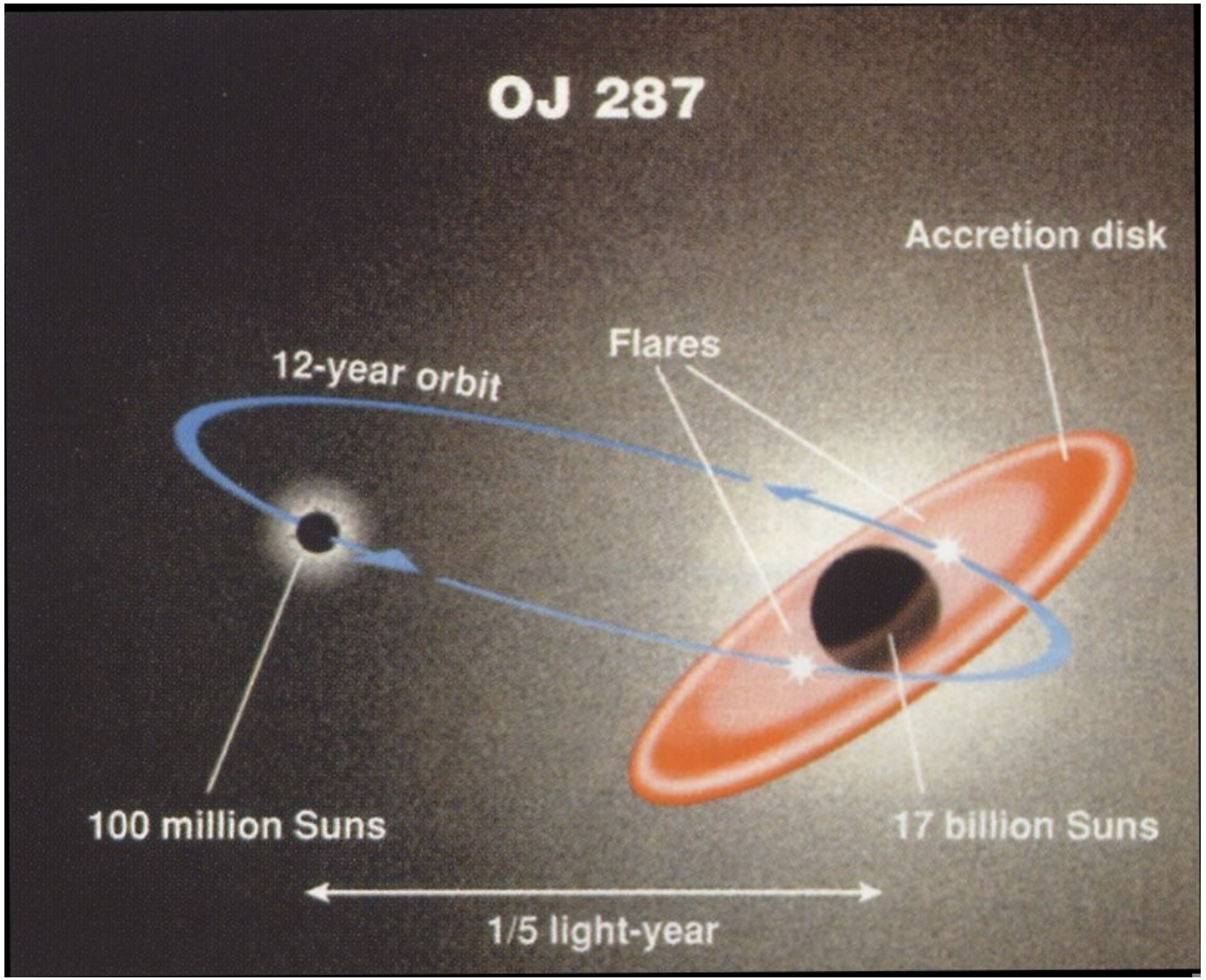

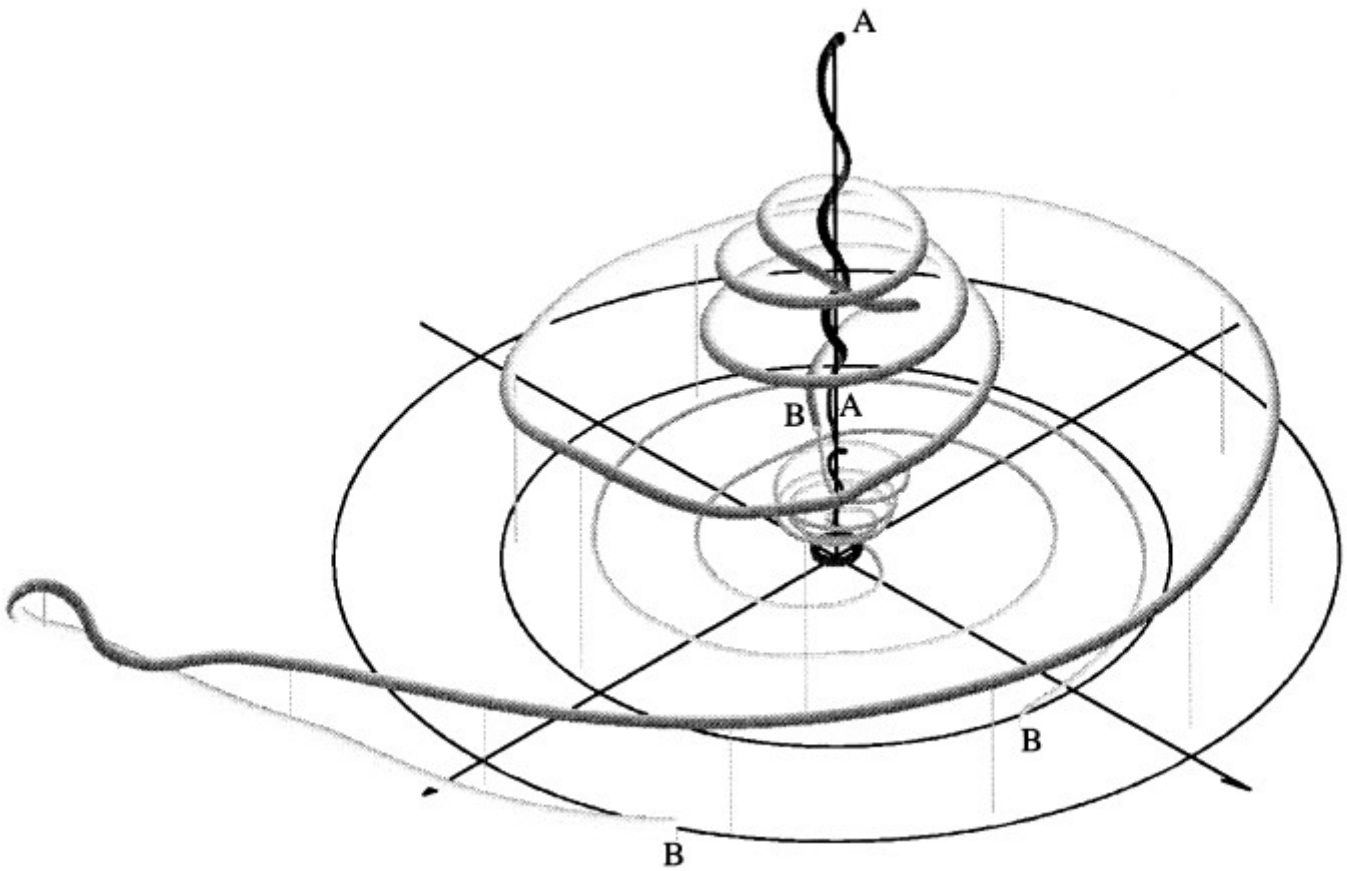
A
B
A
B
B

Testing the 1995 binary black hole model of OJ287

M. J. Valtonen[1,2], H. J. Lehto[1], L. O. Takalo[1], A. Sillanpää[1]

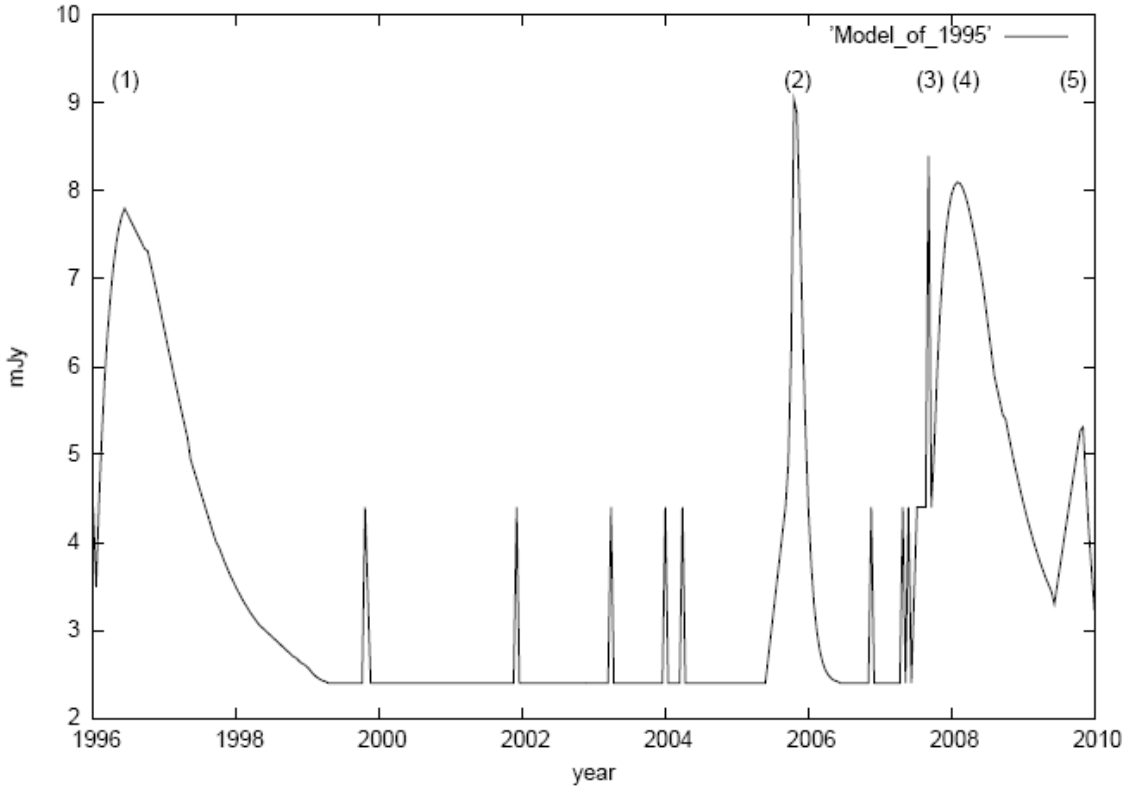

Fig. 1.— The 1995 light curve of OJ287. Five ma-

Observed optical brightness 1996-2010

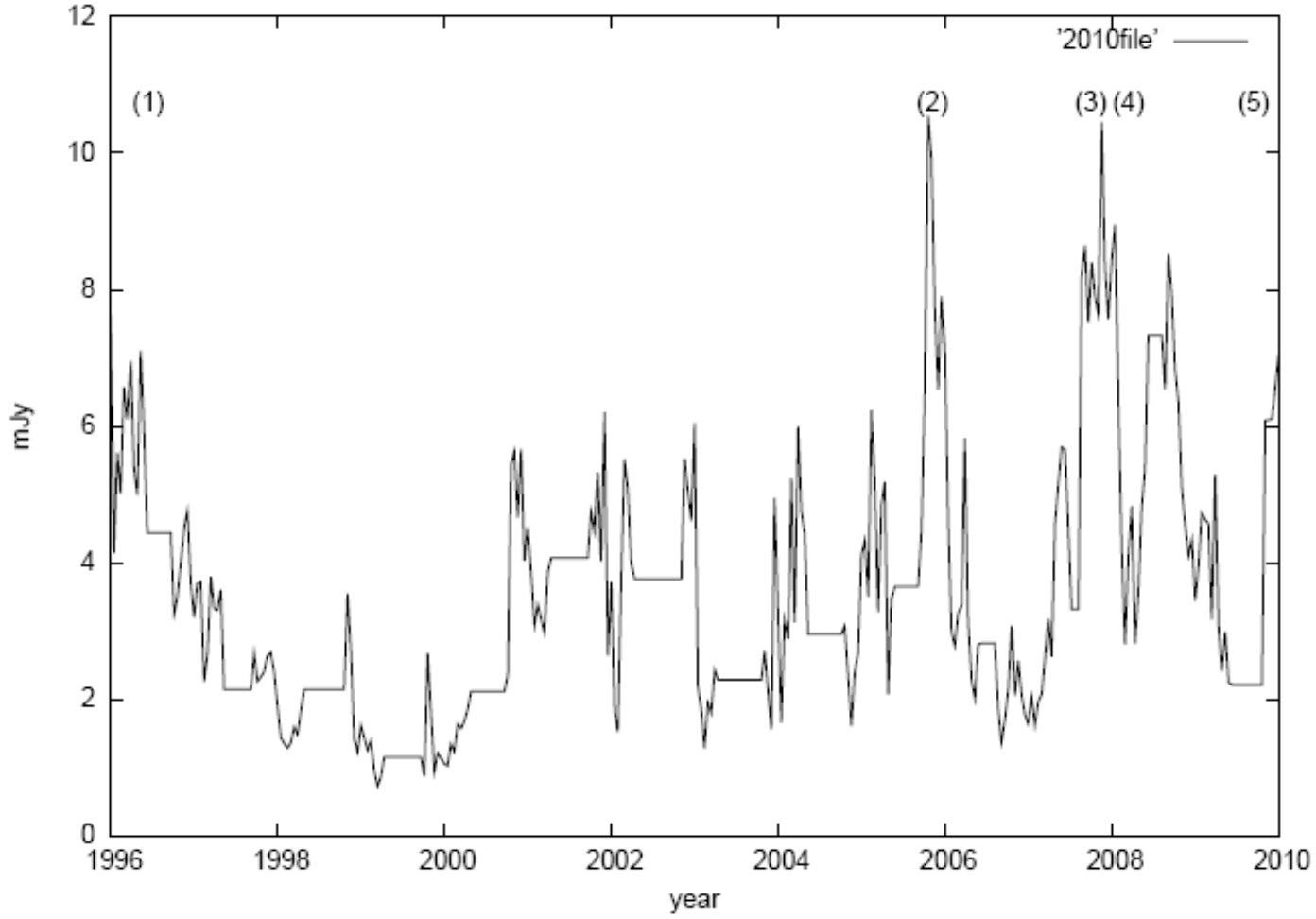

Fig. 2.— The observations of OJ287 during 1996

Residuals: quasi-periodic oscillations: probability < 10^-8

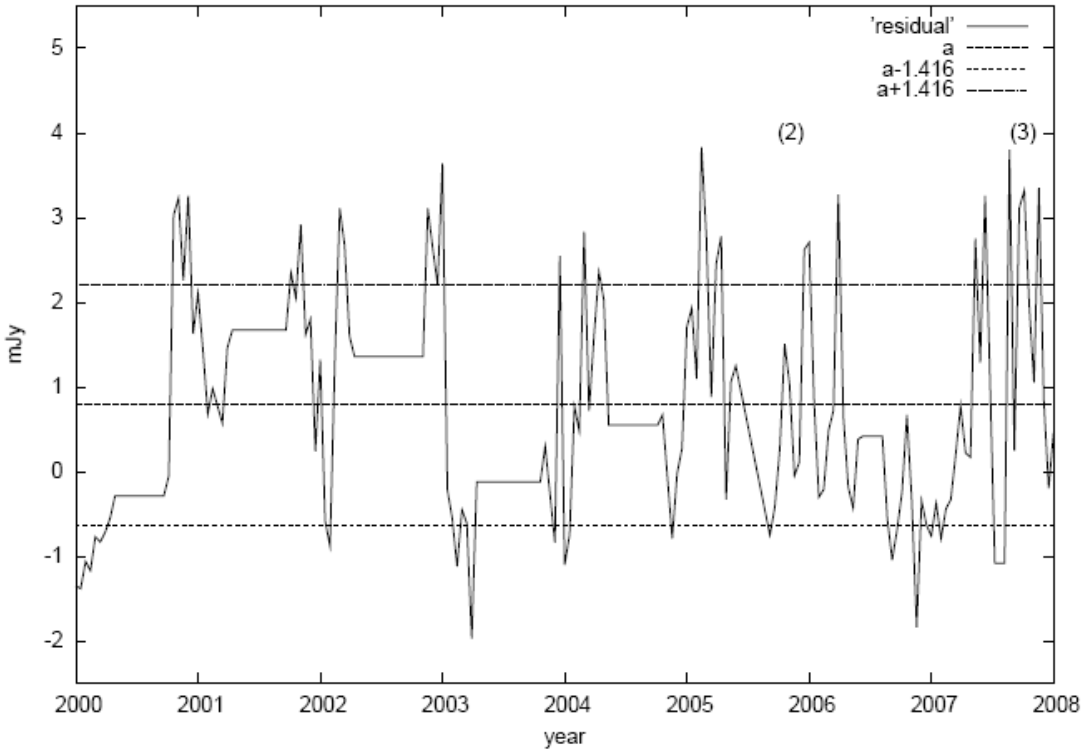

Fig. 3.— The residuals observations minus the model for OJ287 during the 2000 - 2008.

Next: 2015 – 2022 campaign

2015: accurate spin value

2019: test of no-hair –theorem

2022: confirmation of precession

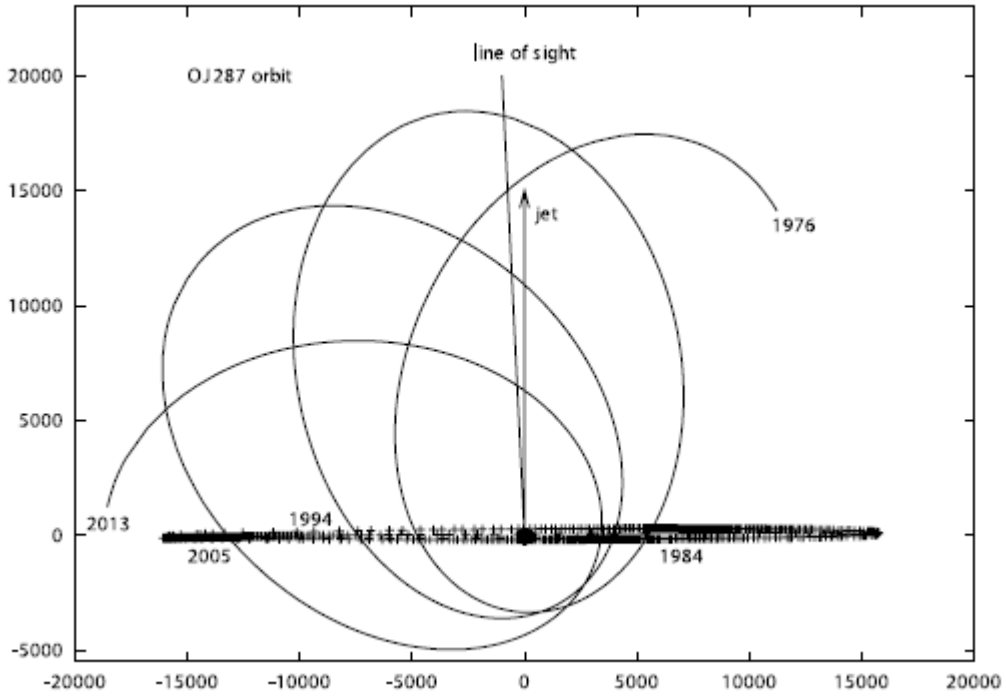

PN acceleration

.

$$\ddot{\boldsymbol{x}} \equiv \frac{d^2\boldsymbol{x}}{dt^2} = \ddot{\boldsymbol{x}}_0 + \ddot{\boldsymbol{x}}_{1\mathrm{PN}} + \ddot{\boldsymbol{x}}_{\mathrm{SO}} + \ddot{\boldsymbol{x}}_Q + \ddot{\boldsymbol{x}}_{2\mathrm{PN}} + \ddot{\boldsymbol{x}}_{2.5\mathrm{PN}},$$

$$\ddot{\boldsymbol{x}}_0 = -\frac{G\,m}{r^3}\,\boldsymbol{x}$$

$$\ddot{\boldsymbol{x}}_{1\mathrm{PN}} = -\frac{Gm}{c^2 r^2}\left\{\boldsymbol{n}\left[-2(2+\eta)\frac{Gm}{r} + (1+3\eta)v^2 - \frac{3}{2}\eta\dot{r}^2\right] - 2(2-\eta)\dot{r}\boldsymbol{v}\right\},$$

$$\begin{aligned}\ddot{\boldsymbol{x}}_{2\mathrm{PN}} = -\frac{G\,m}{c^4 r^2}\Bigg\{\boldsymbol{n}\Bigg[&\frac{3}{4}(12+29\eta)\left(\frac{G\,m}{r}\right)^2 \\ &+ \eta(3-4\eta)v^4 + \frac{15}{8}\eta(1-3\eta)\dot{r}^4 \\ &- \frac{3}{2}\eta(3-4\eta)v^2\dot{r}^2 - \frac{1}{2}\eta(13-4\eta)\left(\frac{G\,m}{r}\right)v^2 \\ &- (2+25\eta+2\eta^2)\left(\frac{G\,m}{r}\right)\dot{r}^2\Bigg] \\ &- \frac{1}{2}\dot{r}\boldsymbol{v}\left[\eta(15+4\eta)v^2 - (4+41\eta+8\eta^2)\left(\frac{G\,m}{r}\right)\right. \\ &\left.-3\eta(3+2\eta)\dot{r}^2\right]\Bigg\},\end{aligned}$$

Spin-orbit term

$$\ddot{\boldsymbol{x}}_{\rm SO} = \frac{G\,m}{r^2}\left(\frac{G\,m}{c^3\,r}\right)\left(\frac{1+\sqrt{1-4\,\eta}}{4}\right)$$
$$\times\,\chi\left\{\left[12\,\left[\boldsymbol{s}_1\cdot(\boldsymbol{n}\times\boldsymbol{v})\right]\right]\boldsymbol{n}\right.$$
$$+\left[\left(9+3\sqrt{1-4\,\eta}\right)\,\dot{r}\right](\boldsymbol{n}\times\boldsymbol{s}_1)$$
$$\left.-\left[7+\sqrt{1-4\,\eta}\right](\boldsymbol{v}\times\boldsymbol{s}_1)\right\},$$

$$\ddot{\boldsymbol{x}}_{2.5\mathrm{PN}} = \frac{8}{15}\frac{G^2 m^2 \eta}{c^5 r^3}\left\{\left[9v^2 + 17\frac{G\,m}{r}\right]\dot{r}\boldsymbol{n} - \left[3v^2 + 9\frac{G\,m}{r}\right]\boldsymbol{v}\right\},$$

$$\ddot{\mathbf{x}}_Q = q\,\chi^2\,\frac{3\,G^3\,m_1^2 m}{2\,c^4\,r^4}\left\{\left[5(\mathbf{n}\cdot\mathbf{s_1})^2 - \mathbf{1}\right]\mathbf{n} - \mathbf{2}(\mathbf{n}\cdot\mathbf{s_1})\mathbf{s_1}\right\}$$

no-hair theorem

quadrupole moment Q

$$Q = -q\frac{S^2}{Mc^2} \qquad \mathbf{S}_1 = G\,m_1^2\,\chi\,\mathbf{s}_1/c$$

unit vector $\mathbf{s}_1$

For black holes $q = 1$

for neutron stars $q > 2$

Parameters

$\Delta\phi^\circ$	39.1 ± 0.1
m_1	$(1.83 \pm 0.01) \cdot 10^{10} M_\odot$
m_2	$(1.4 \pm 0.1) \cdot 10^{8} M_\odot$
χ	0.28 ± 0.08
ϕ_0	$56^\circ.5 \pm 1.^\circ 2$
e_0	0.6584 ± 0.001
q	1.0 ± 0.3
t_d	0.75 ± 0.04

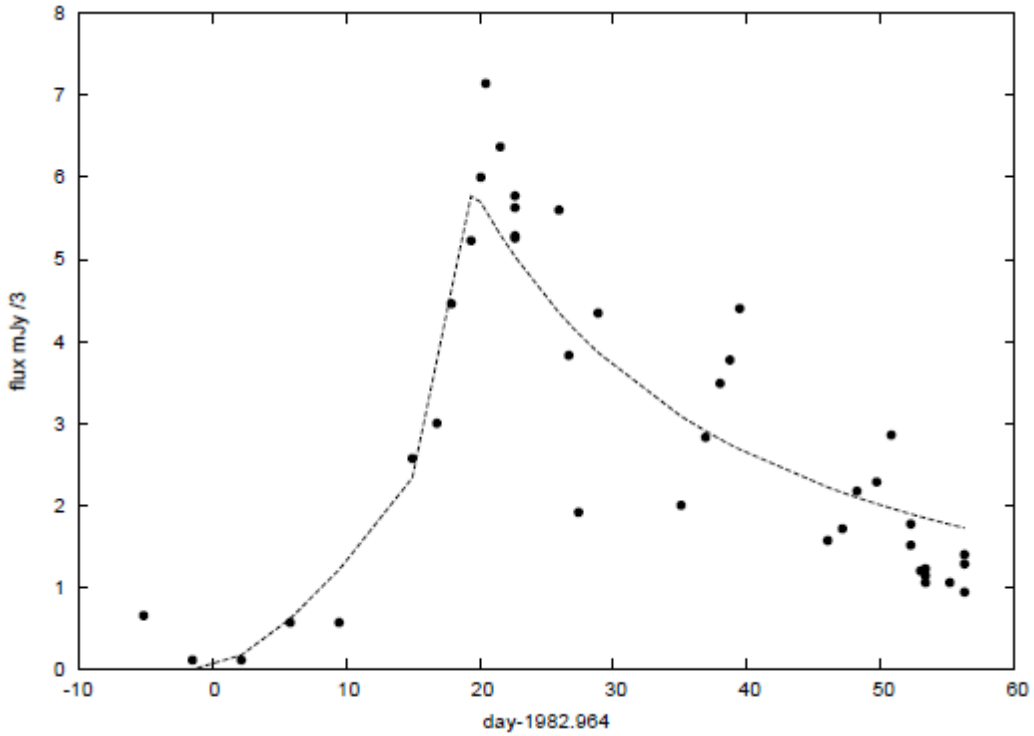
flux mJy /3
day-1982.964
8
7
6
5
4
3
2
1
0
-10
0
10
20
30
40
50
60

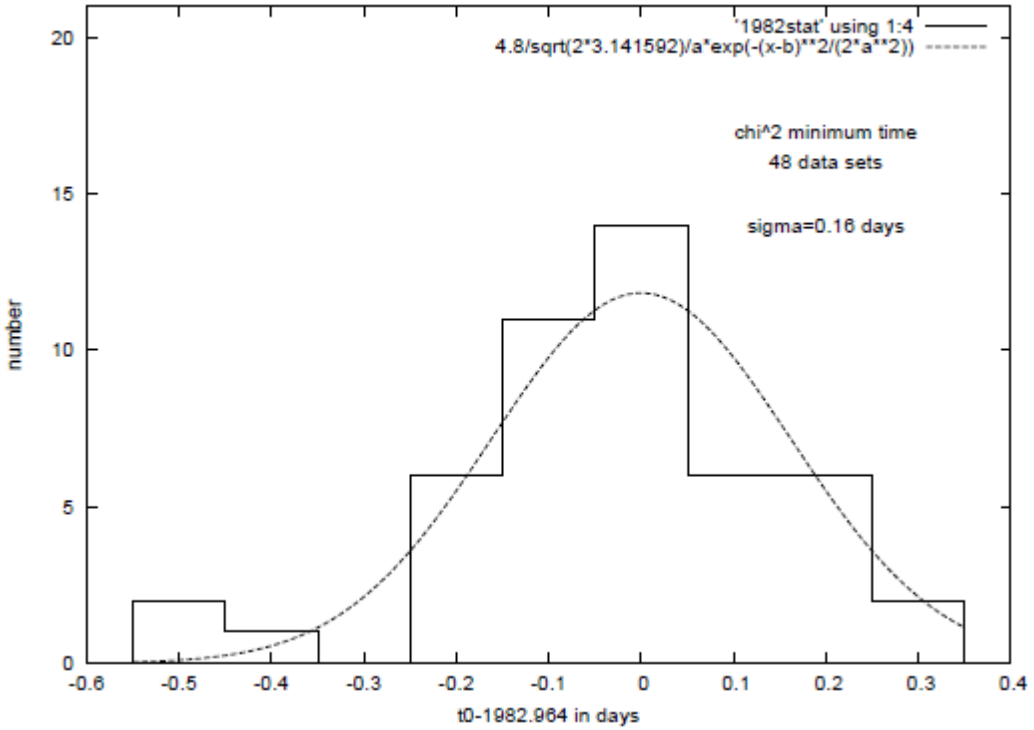
'1982stat' using 1:4
4.8/sqrt(2*3.141592)/a*exp(-(x-b)**2/(2*a**2))
chi^2 minimum time
48 data sets
sigma=0.16 days
number
t0-1982.964 in days
20
15
10
5
0
-0.6
-0.5
-0.4
-0.3
-0.2
-0.1
0
0.1
0.2
0.3
0.4

1995.8426

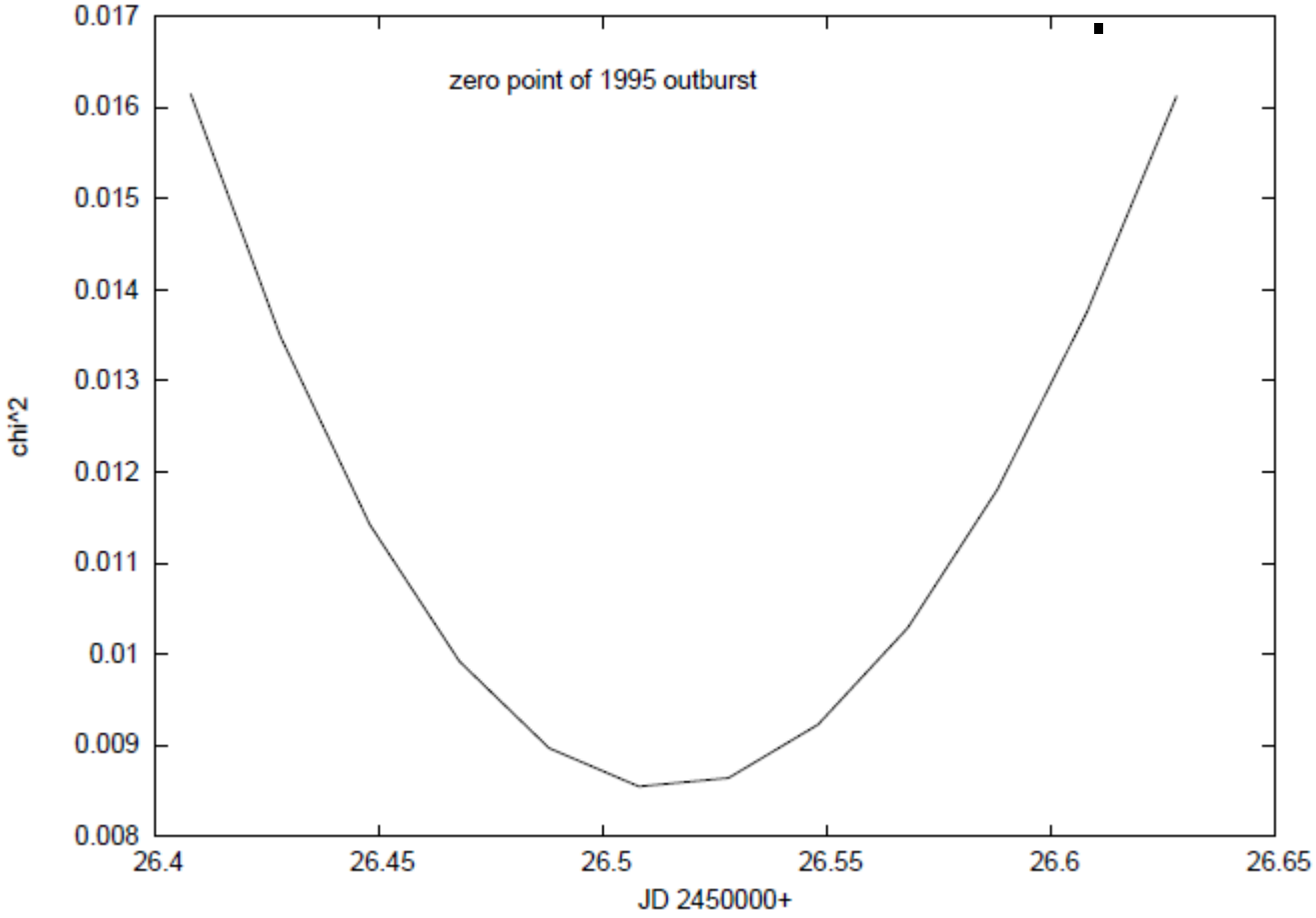
zero point of 1995 outburst
chi^2
0.017
0.016
0.015
0.014
0.013
0.012
0.011
0.01
0.009
0.008
26.4
26.45
26.5
26.55
26.6
26.65
JD 2450000+

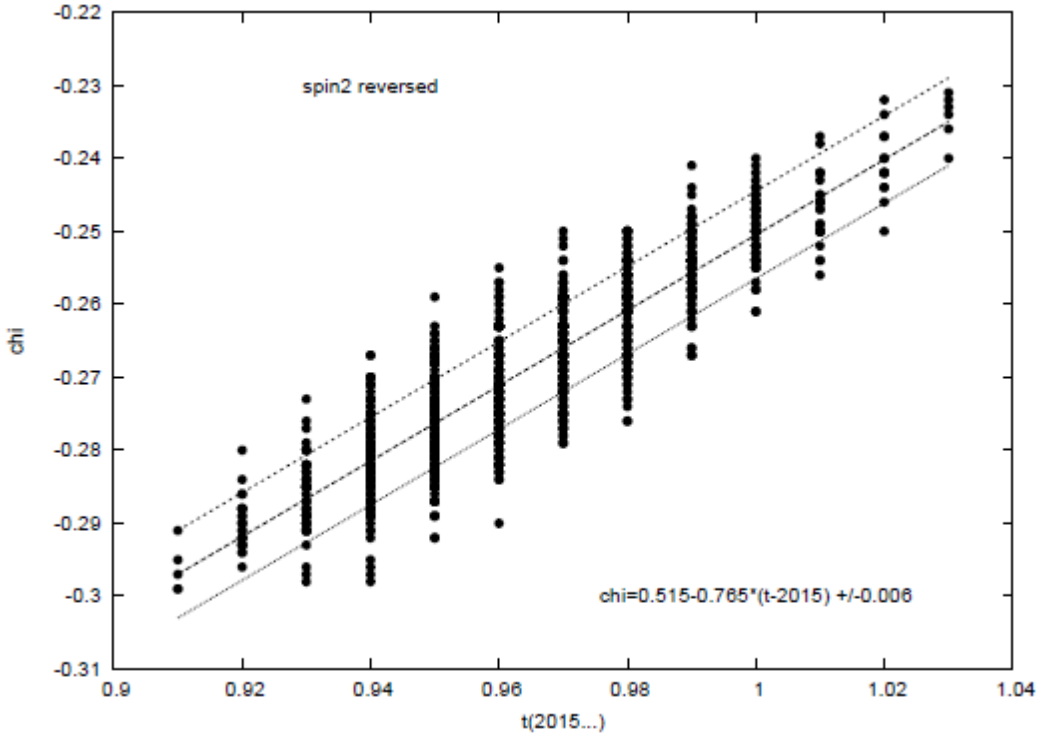
spin2 reversed
chi=0.515-0.765*(t-2015) +/-0.006
chi
t(2015...)
-0.22
-0.23
-0.24
-0.25
-0.26
-0.27
-0.28
-0.29
-0.3
-0.31
0.9
0.92
0.94
0.96
0.98
1
1.02
1.04

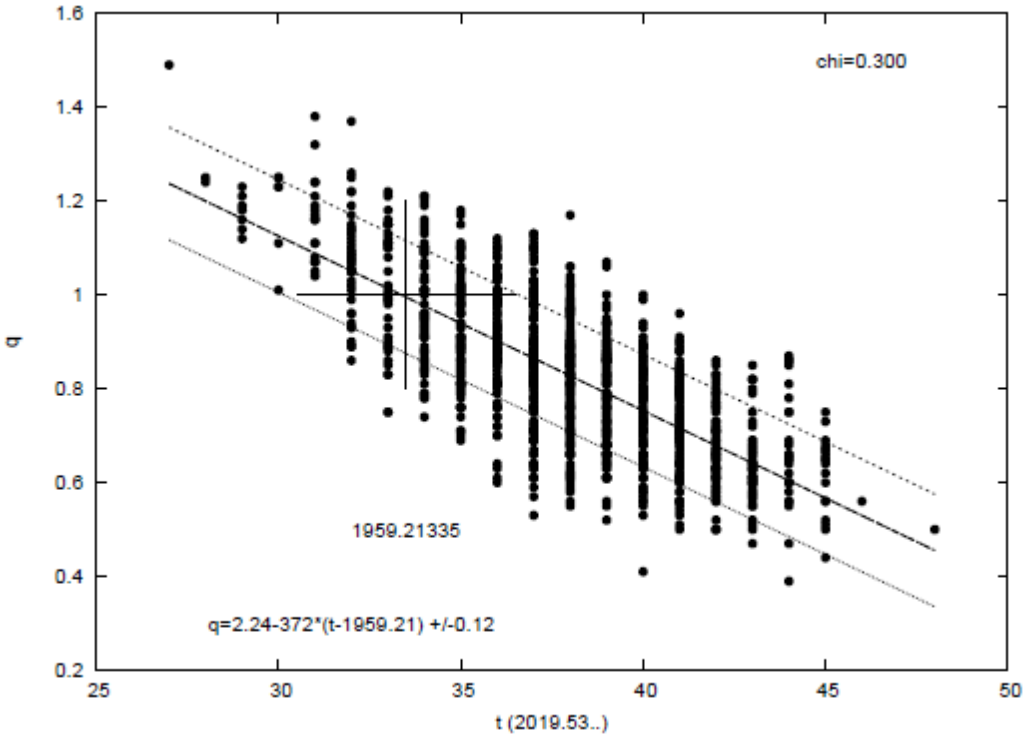
chi=0.300
1959.21335
q=2.24-372*(t-1959.21) +/-0.12
q
t (2019.53..)
1.6
1.4
1.2
1
0.8
0.6
0.4
0.2
25
30
35
40
45
50

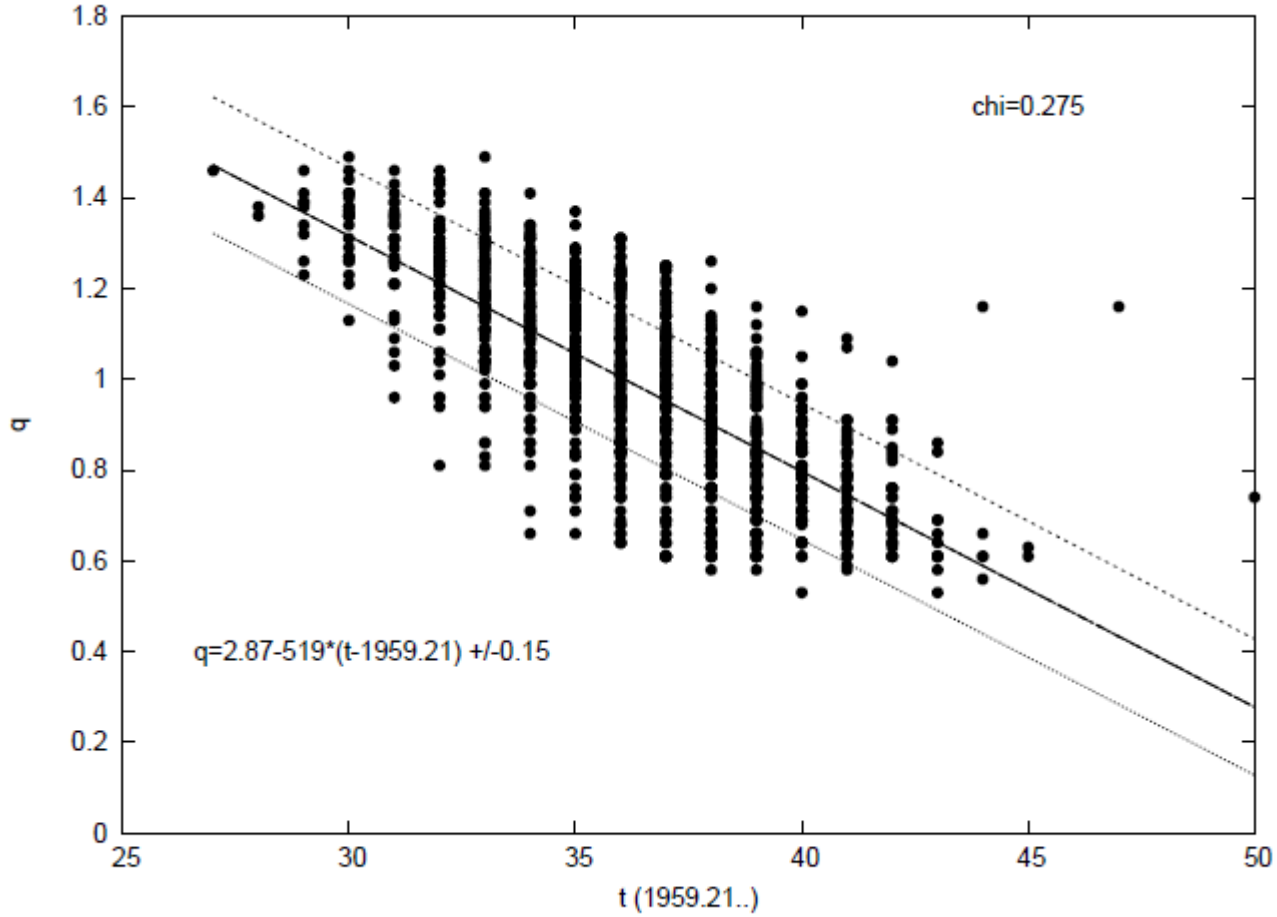
chi=0.275
q=2.87-519*(t-1959.21) +/-0.15
q
t (1959.21..)
1.8
1.6
1.4
1.2
1
0.8
0.6
0.4
0.2
0
25
30
35
40
45
50

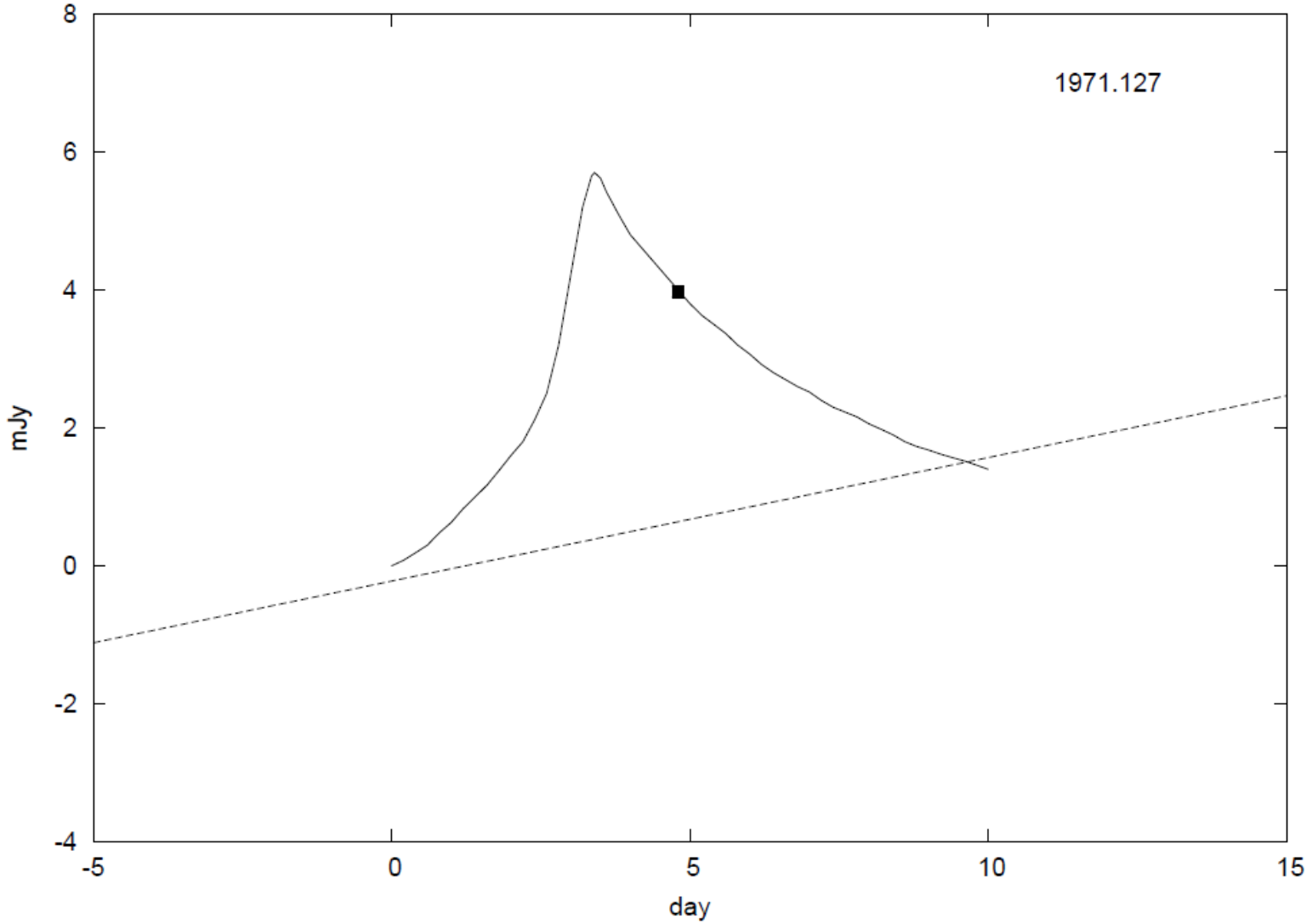

Fig. 2.— Observations of the brightness of OJ287 at the expected 1971 outburst time. The solid

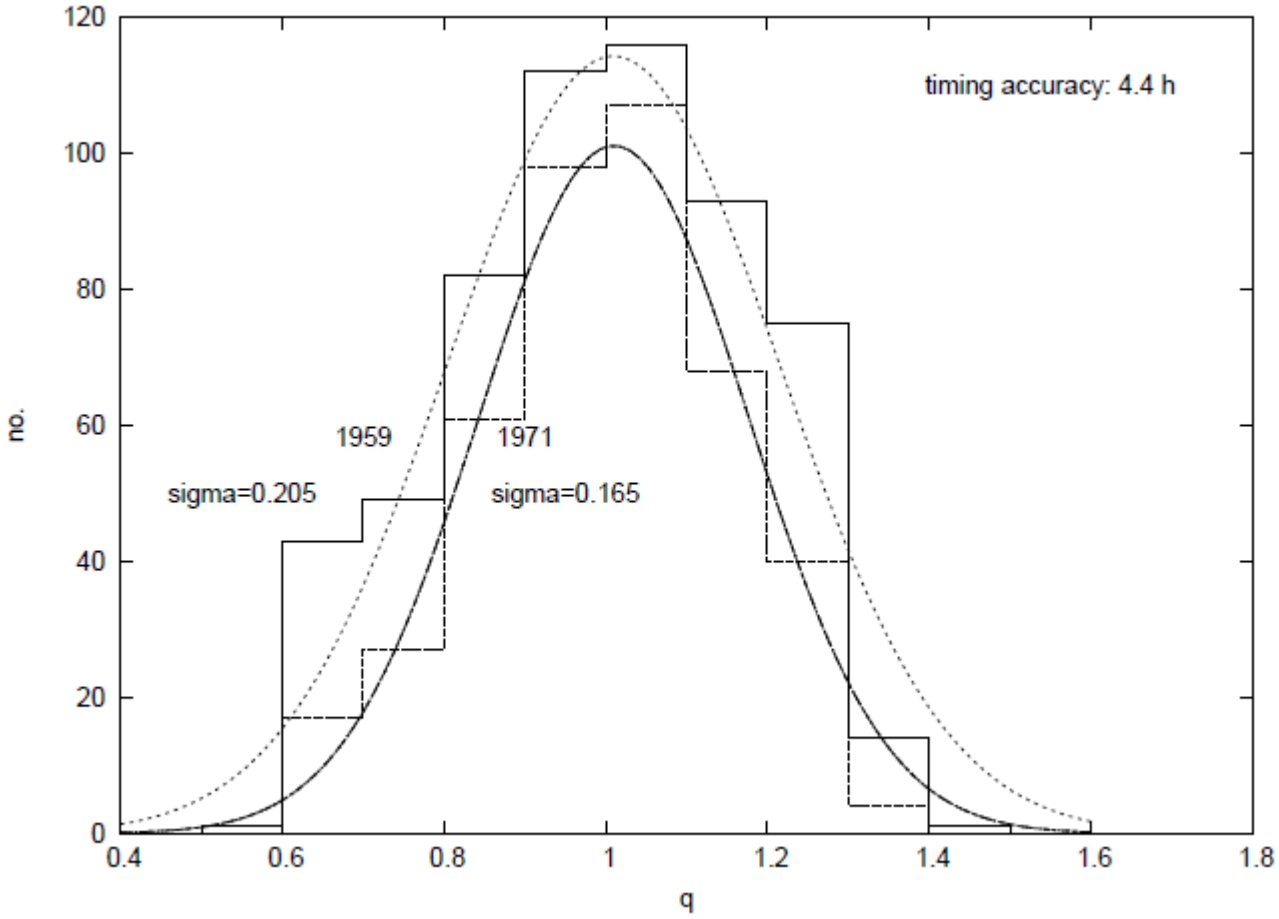
timing accuracy: 4.4 h
1959
sigma=0.205
1971
sigma=0.165
no.
q
0
20
40
60
80
100
120
0.4
0.6
0.8
1
1.2
1.4
1.6
1.8

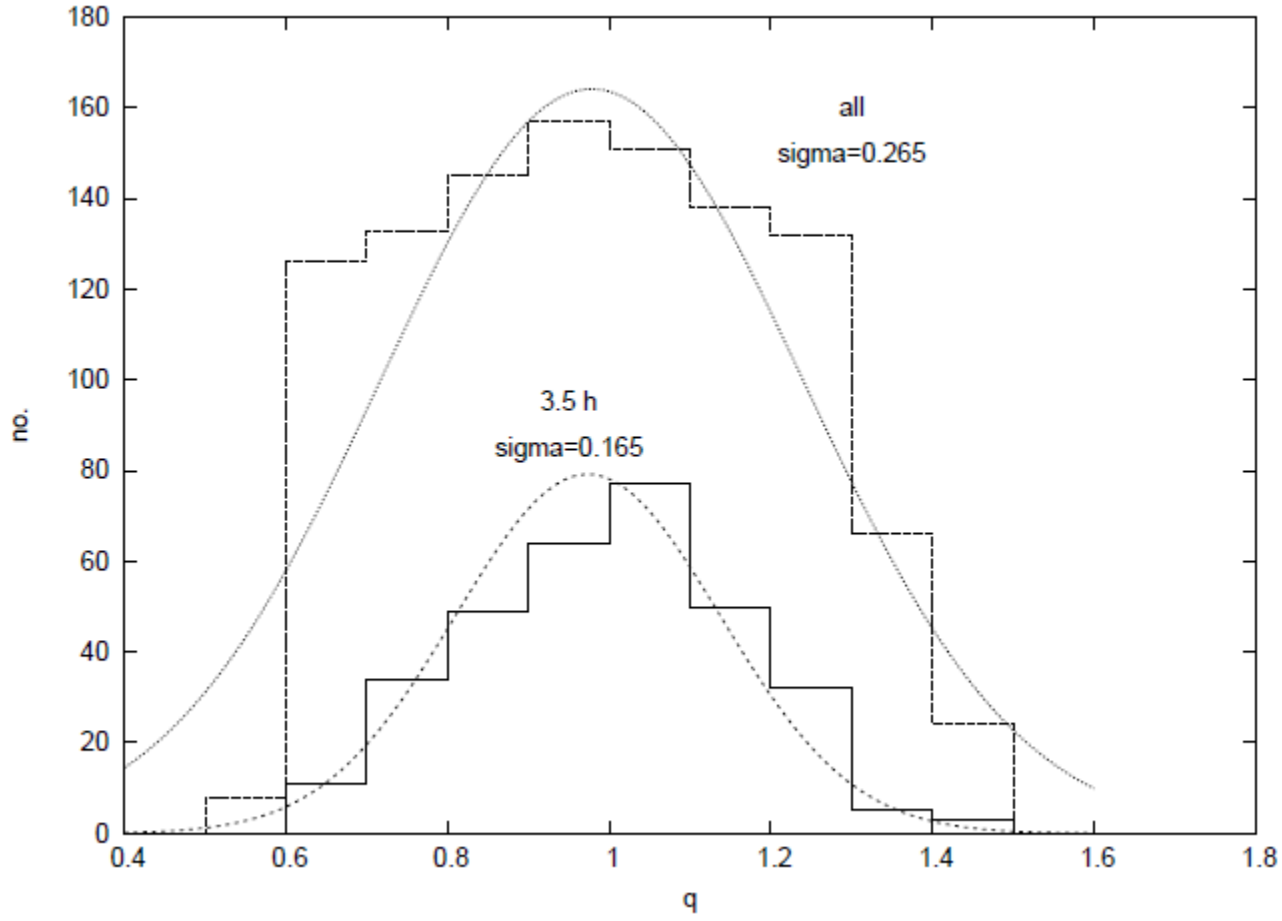
all
sigma=0.265
3.5 h
sigma=0.165
no.
q
0
20
40
60
80
100
120
140
160
180
0.4
0.6
0.8
1
1.2
1.4
1.6
1.8

On the possibility of testing black hole no-hair theorem during the present decade with OJ287

M. J.Valtonen[1,2], S. Mikkola[1], H. J.Lehto[1], A. Gopakumar [3], R. Hudec [4,5]
and
J. Polednikova[4,5]

Space-based photometry is required in 2019 July

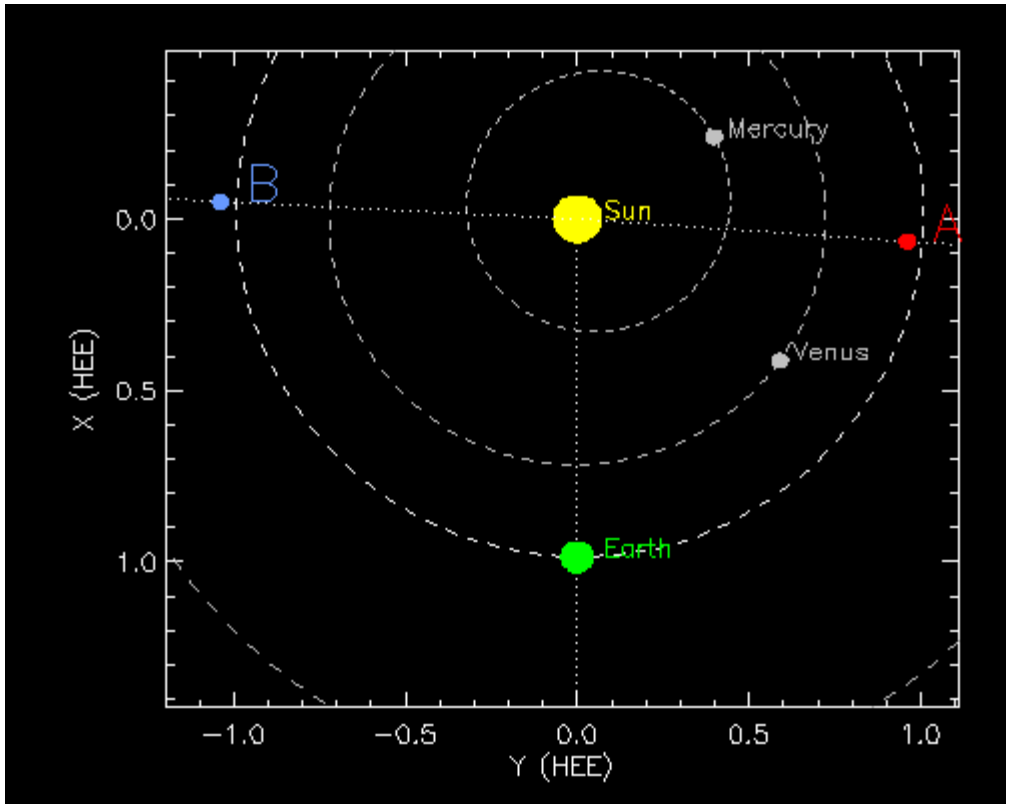

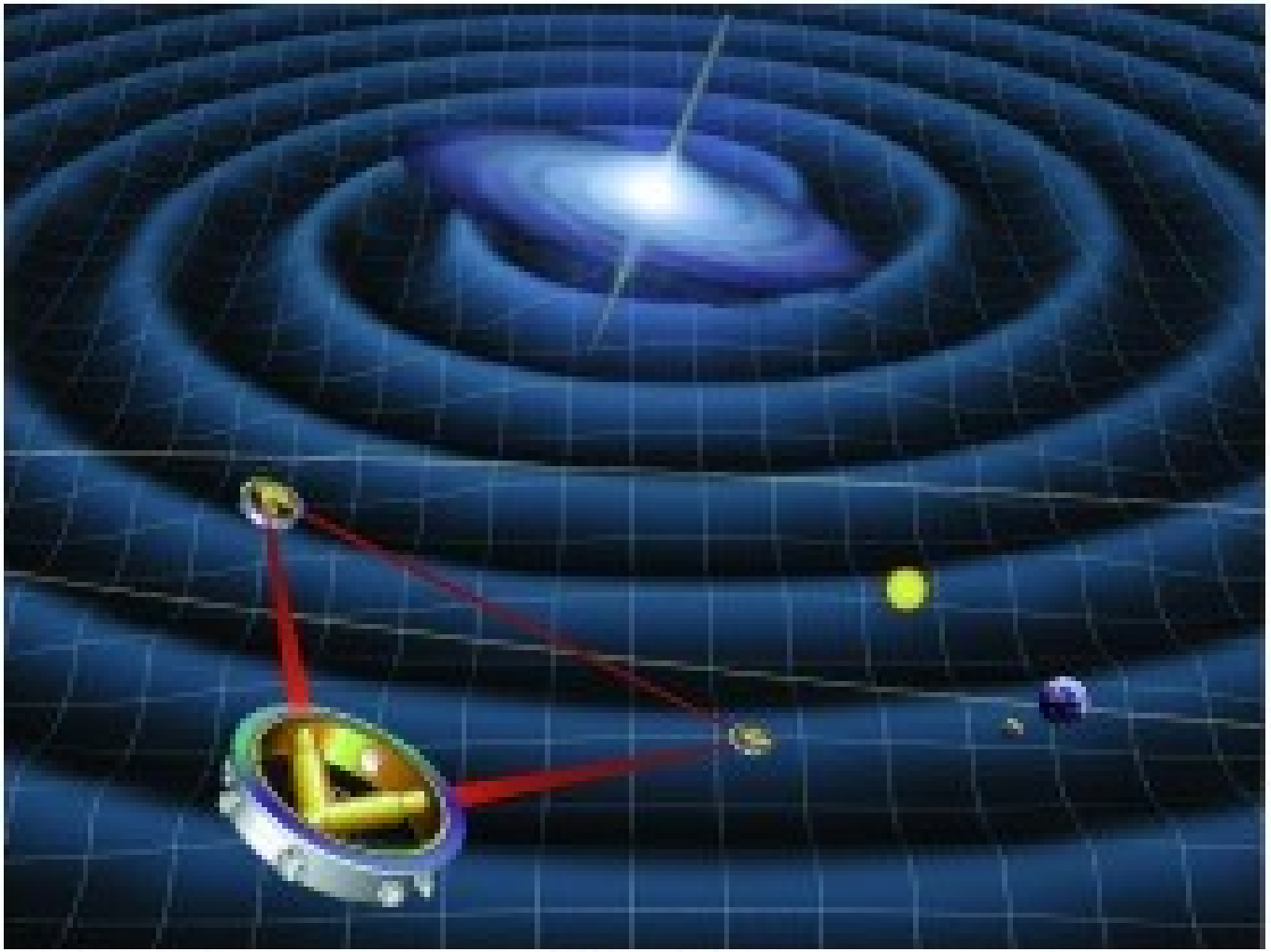

Artist's impression of the LISA spacecraft

Binary model

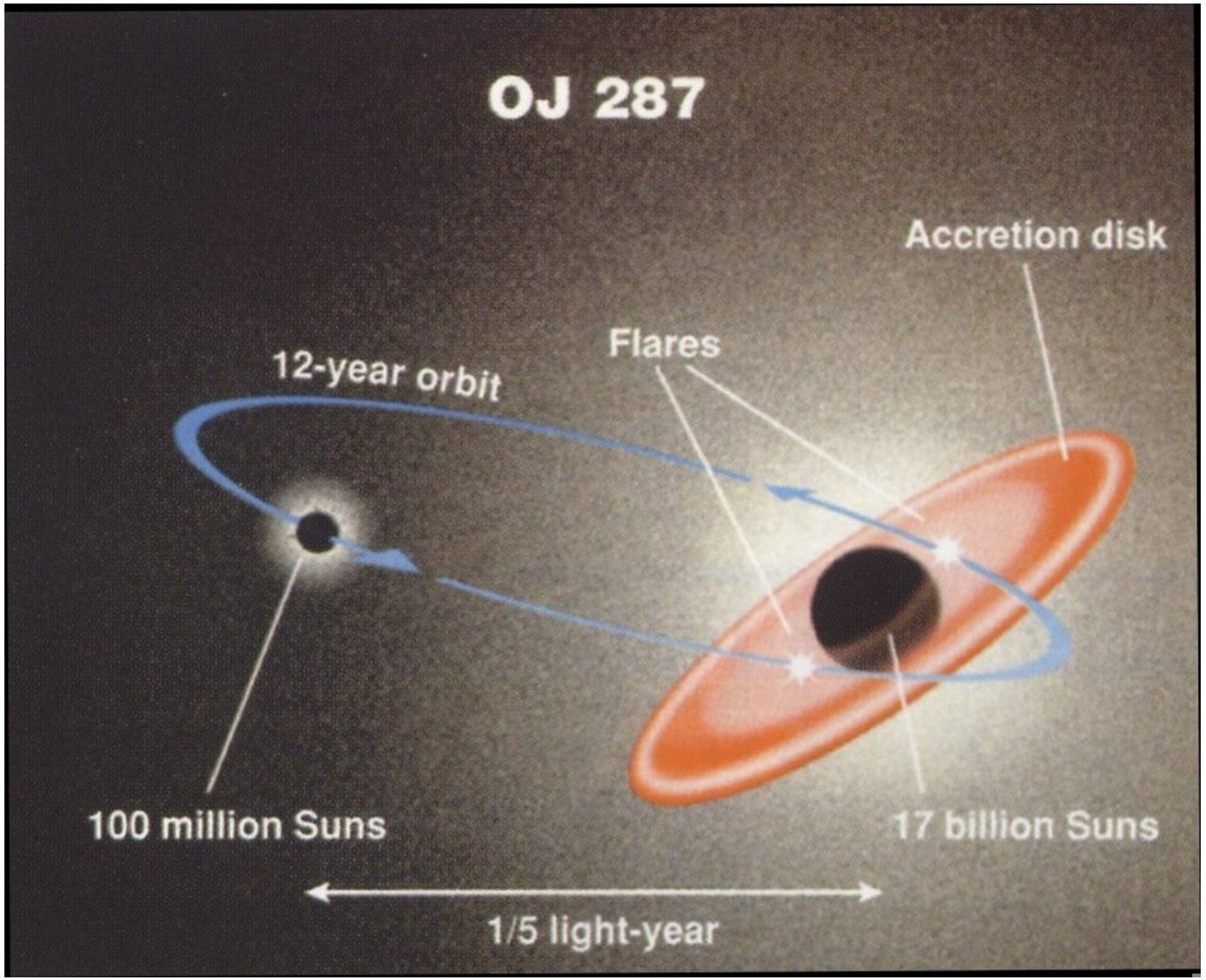

The multi–spectral–range behavior of OJ 287 in 2005–2010

I. Agudo[1], S. G. Jorstad[1], A. P. Marscher[1], V. M. Larionov[2,3], J. L. Gómez[4], H. Wiesemeyer[5], C. Thum[6], M. Gurwell[7], J. Heidt[8], and F. D. D'Arcangelo[1,9]

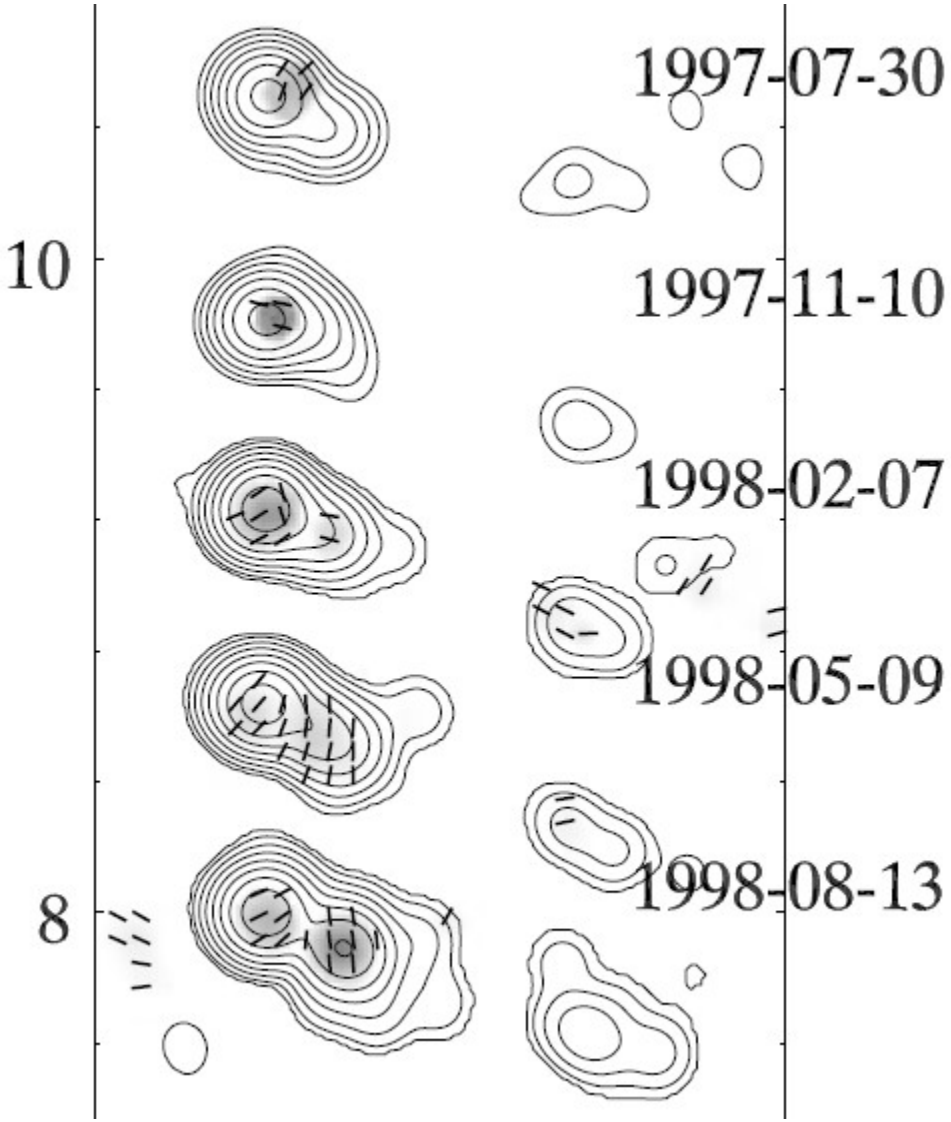

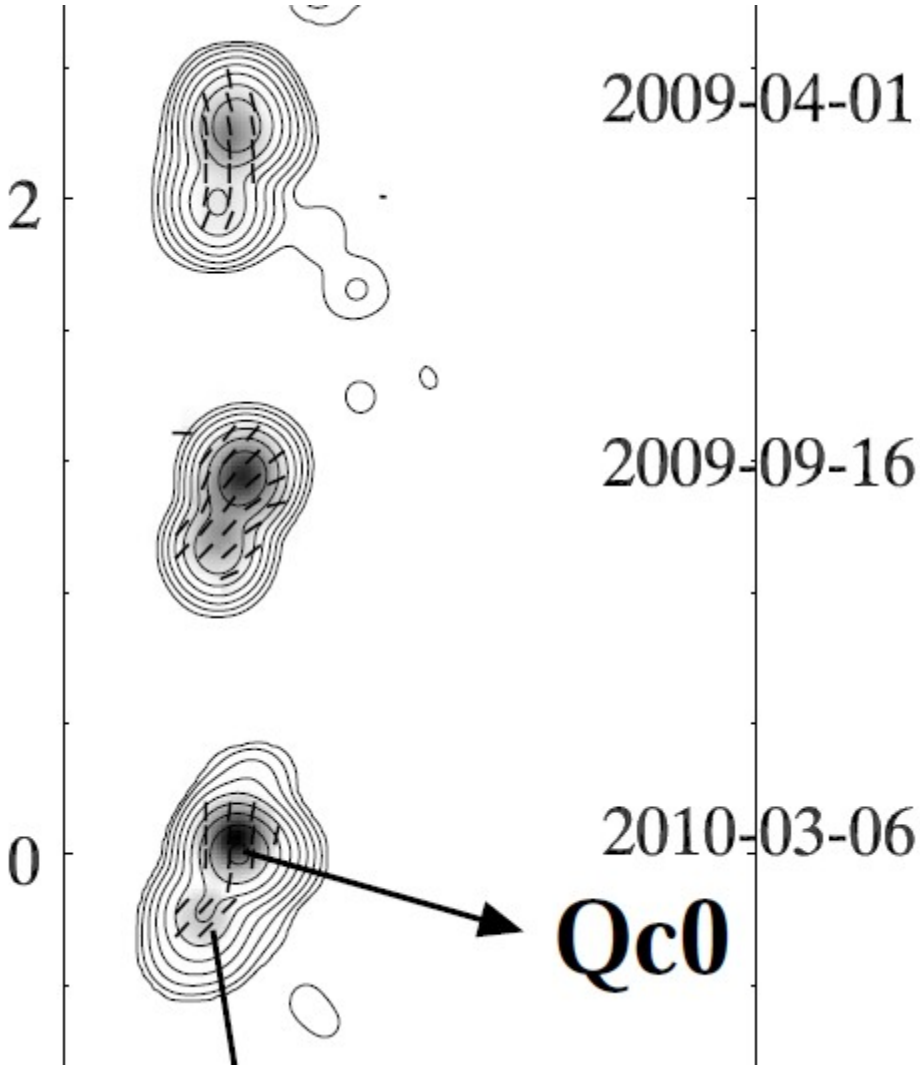
2009-04-01
2
2009-09-16
2010-03-06
0
Qc0

Romero, Abraham et al. 2000: Precessing jet

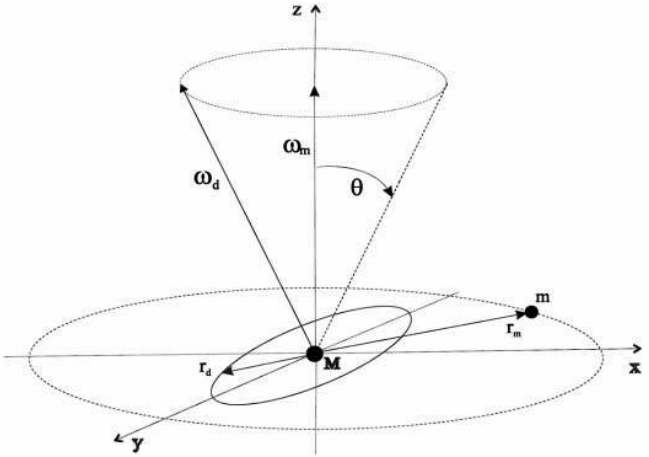

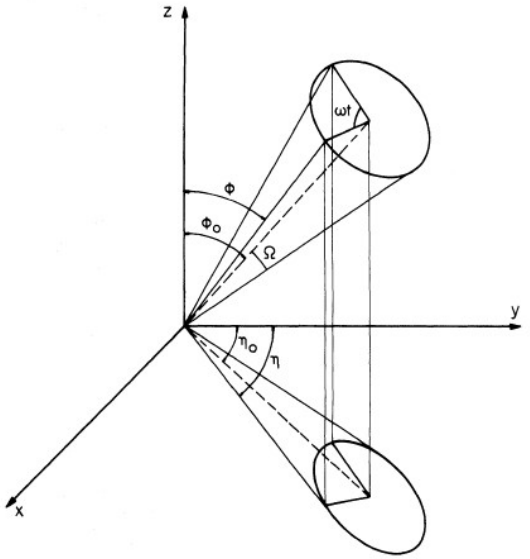

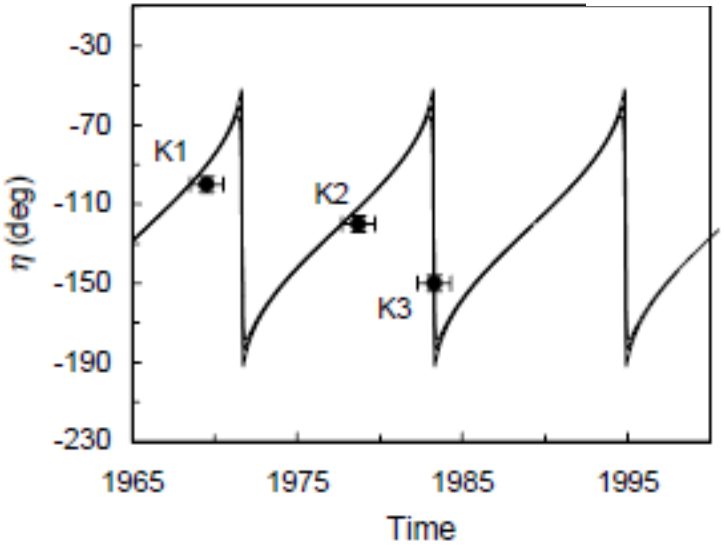

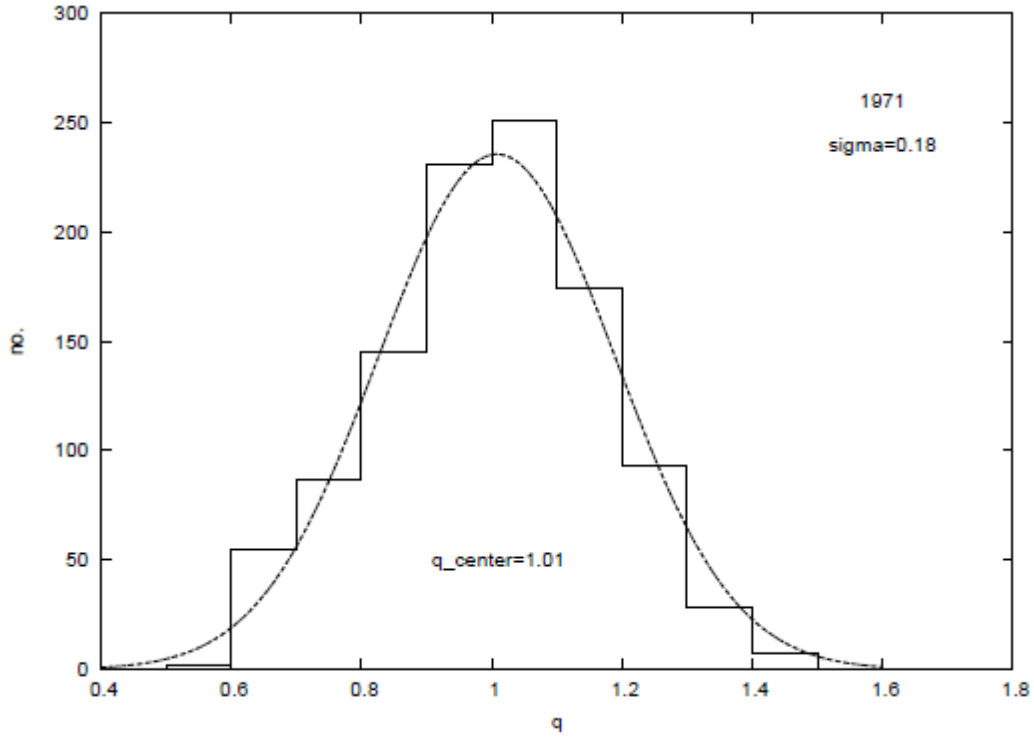
1971
sigma=0.18
q_center=1.01
no.
q
300
250
200
150
100
50
0
0.4
0.6
0.8
1
1.2
1.4
1.6
1.8

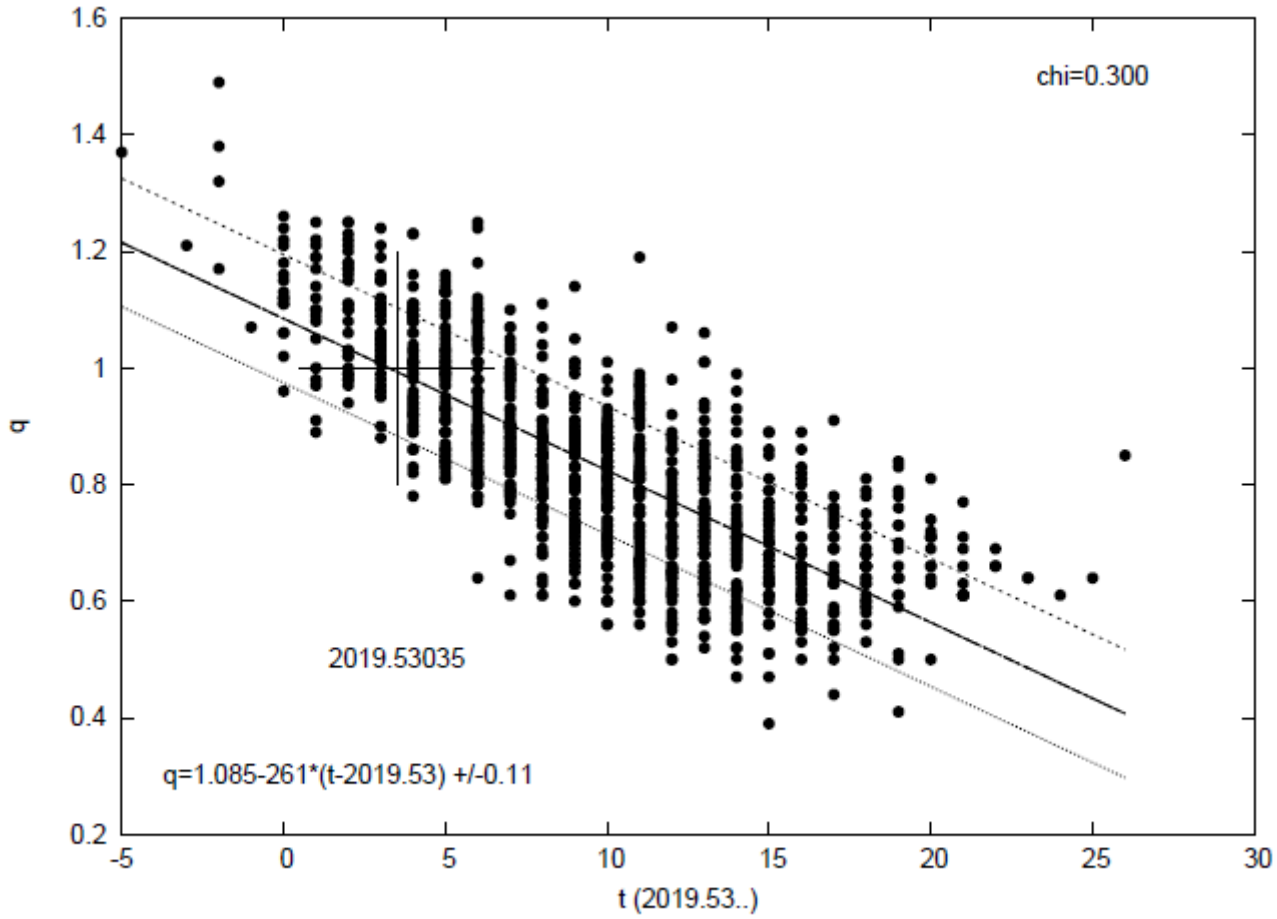
chi=0.300
2019.53035
q=1.085-261*(t-2019.53) +/-0.11
q
t (2019.53..)
1.6
1.4
1.2
1
0.8
0.6
0.4
0.2
-5
0
5
10
15
20
25
30

Tateyama & Kingham 2004: Precessing helical jet

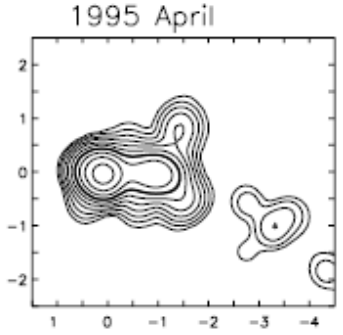

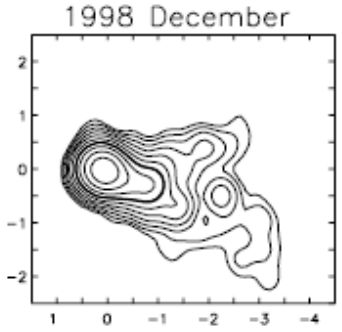

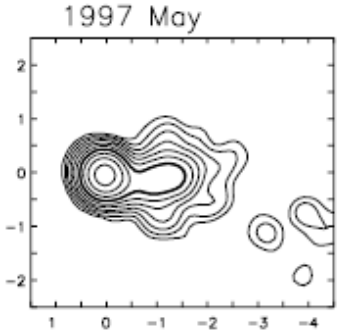

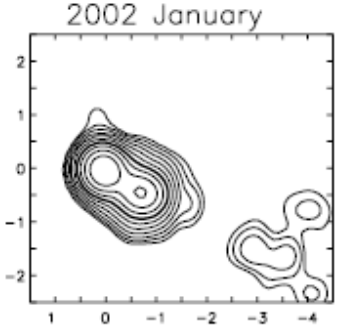

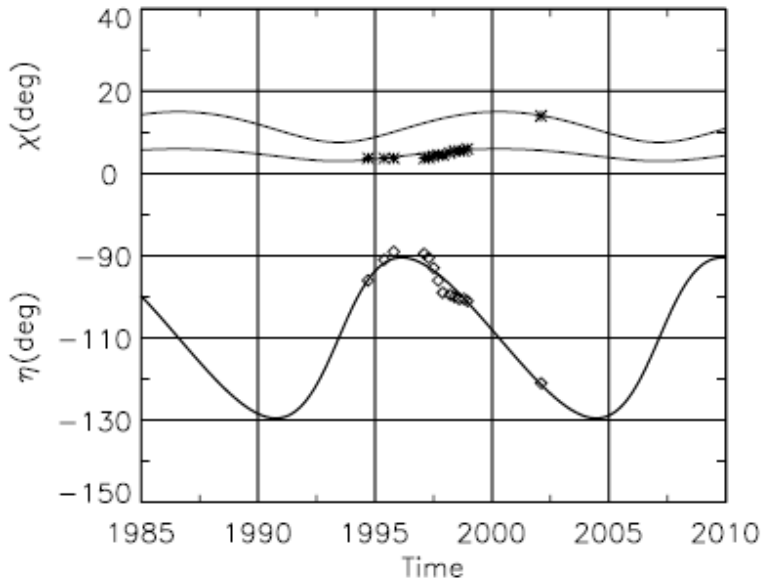

Jet direction: black hole spin or accretion disk axis?

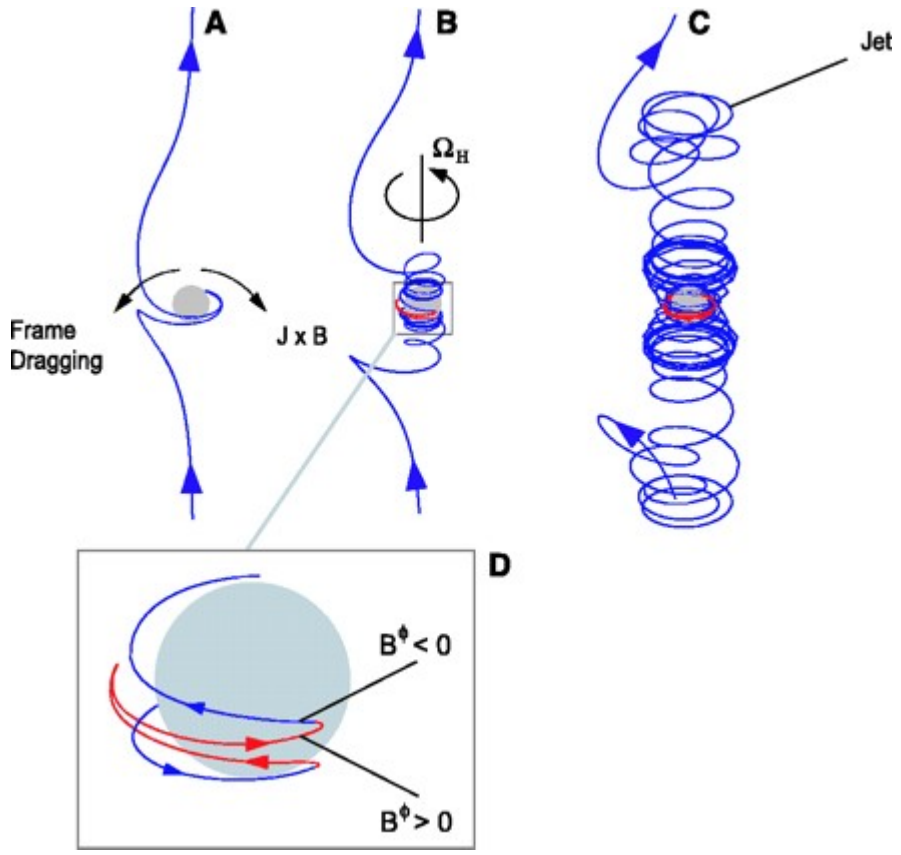

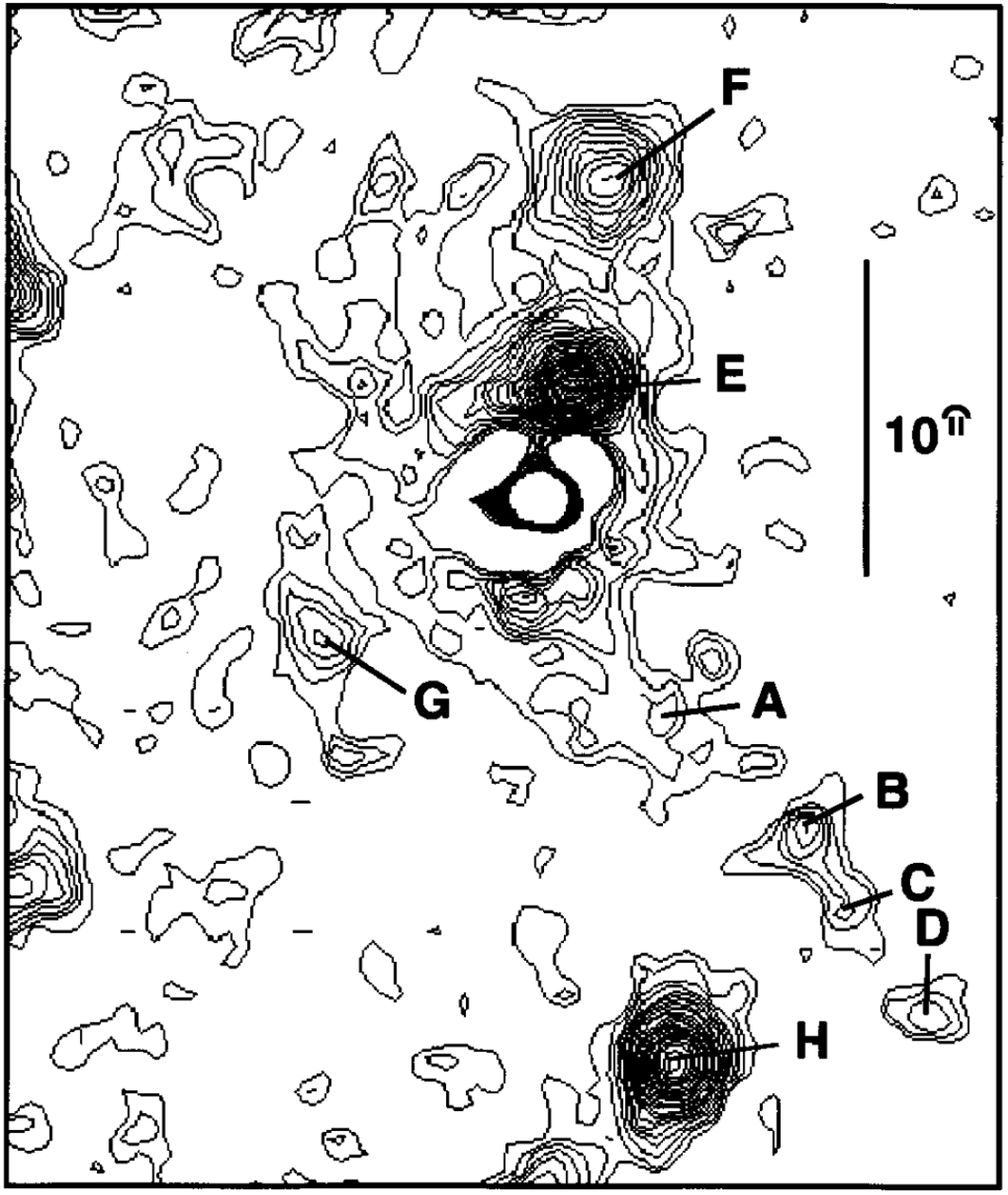
F
E
10″
G
A
B
C
D
H

The Astrophysical Journal, 729:33 (6pp), 2011 March 1 doi:10.1088/0004-637X/7

TESTING THE 1995 BINARY BLACK HOLE MODEL OF OJ287

M. J. Valtonen[1,2], H. J. Lehto[1], L. O. Takalo[1], and A. Sillanpää[1]
[1] Tuorla Observatory, Department of Physics and Astronomy, University of Turku, 21500 Piikkiö, Finland
[2] Helsinki Institute of Physics, FIN-00014 University of Helsinki, Finland
Received 2010 March 4; accepted 2010 December 31; published 2011 February 7

ABSTRACT

In 1995, a binary black hole model was proposed for the quasar OJ287, where the smaller secondary black hole impacts the accretion disk of the primary black hole twice during its 12 yr orbit and causes a double peak of optical outbursts. The model predicted four major outbursts and one minor outburst during the period 1996–2010. All five have now been observed. In this paper, we ask how accurate the predictions were. We use the latest optical observations from Tuorla Observatory and the KVA telescope at La Palma together with previously published data to construct a light curve for this period. We average the data in 0.04 yr bins, and subtract the observed flux from the 1995 model flux at each bin. We find that the residuals are small: they are well described by random noise of amplitude 1.4 mJy. This level is small compared with the amplitudes of the major outbursts, 5–7 mJy. Ignoring the noise, the binary model explains the optical data remarkably well.

Eccentric evolution of supermassive black hole binaries

Masaki Iwasawa[1,2] , Sangyong An[3] , Tatsushi Matsubayashi[4] ,
Yoko Funato[5] , Junichiro Makino[2]

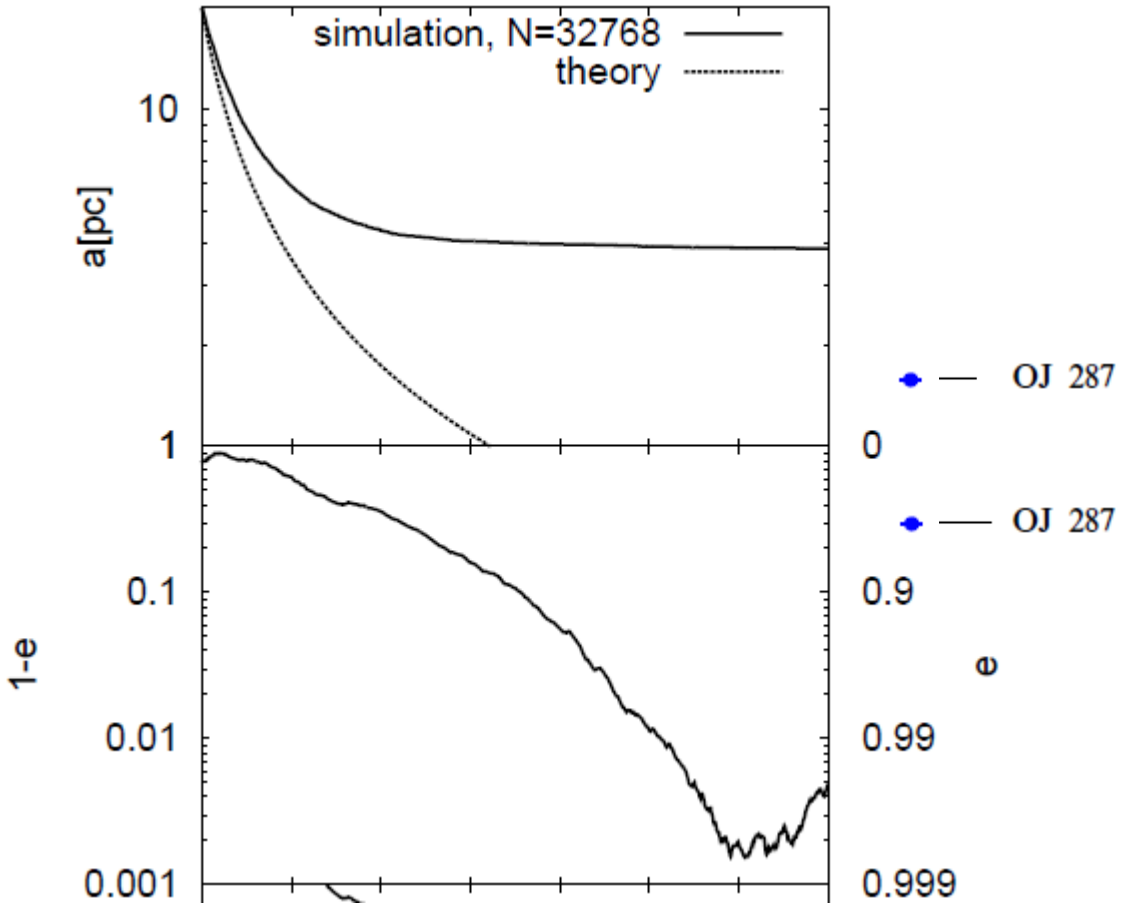

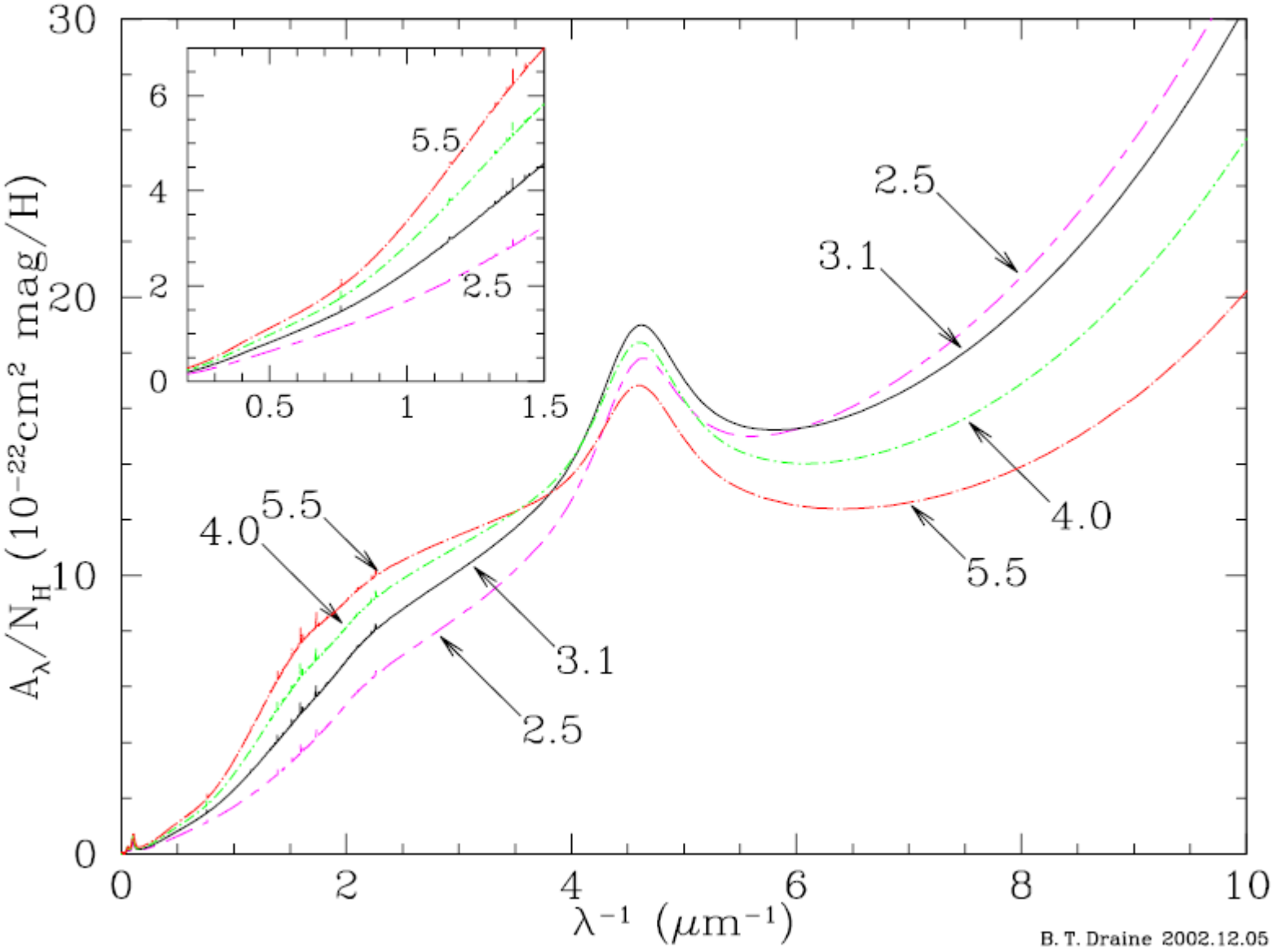
30
20
10
0
0
2
4
6
8
10
A_λ/N_H (10^{-22}cm^2 mag/H)
λ^{-1} (μm^{-1})
2.5
3.1
4.0
5.5
5.5
4.0
3.1
2.5
6
4
2
0
0.5
1
1.5
5.5
2.5
B. T. Draine 2002.12.05

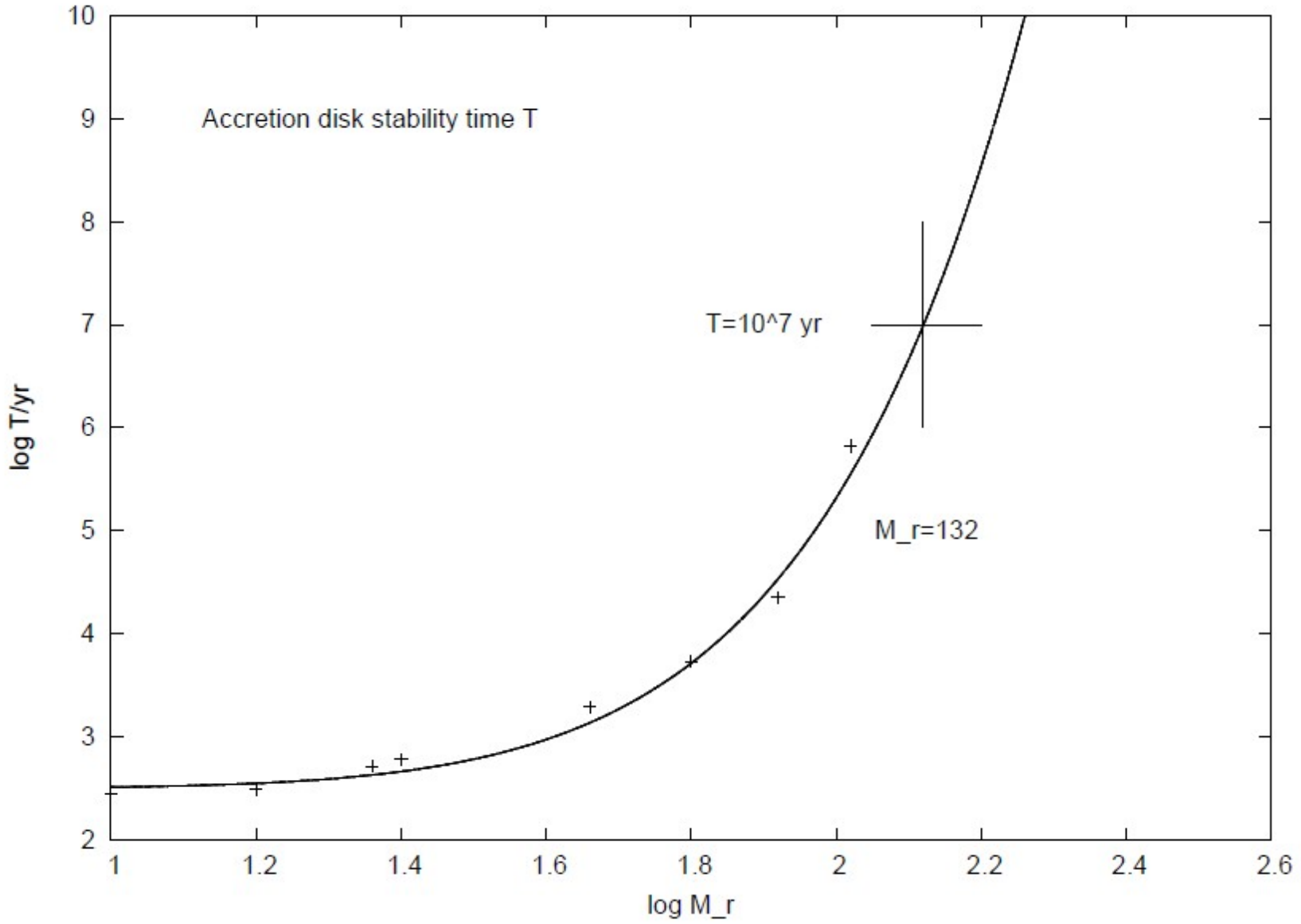
Accretion disk stability time T
T=10^7 yr
M_r=132
log T/yr
log M_r
10
9
8
7
6
5
4
3
2
1
1.2
1.4
1.6
1.8
2
2.2
2.4
2.6

The Megaparsec-Scale X-ray Jet of the BL Lac Object OJ287

Alan P. Marscher[1] and Svetlana G. Jorstad[1,2]

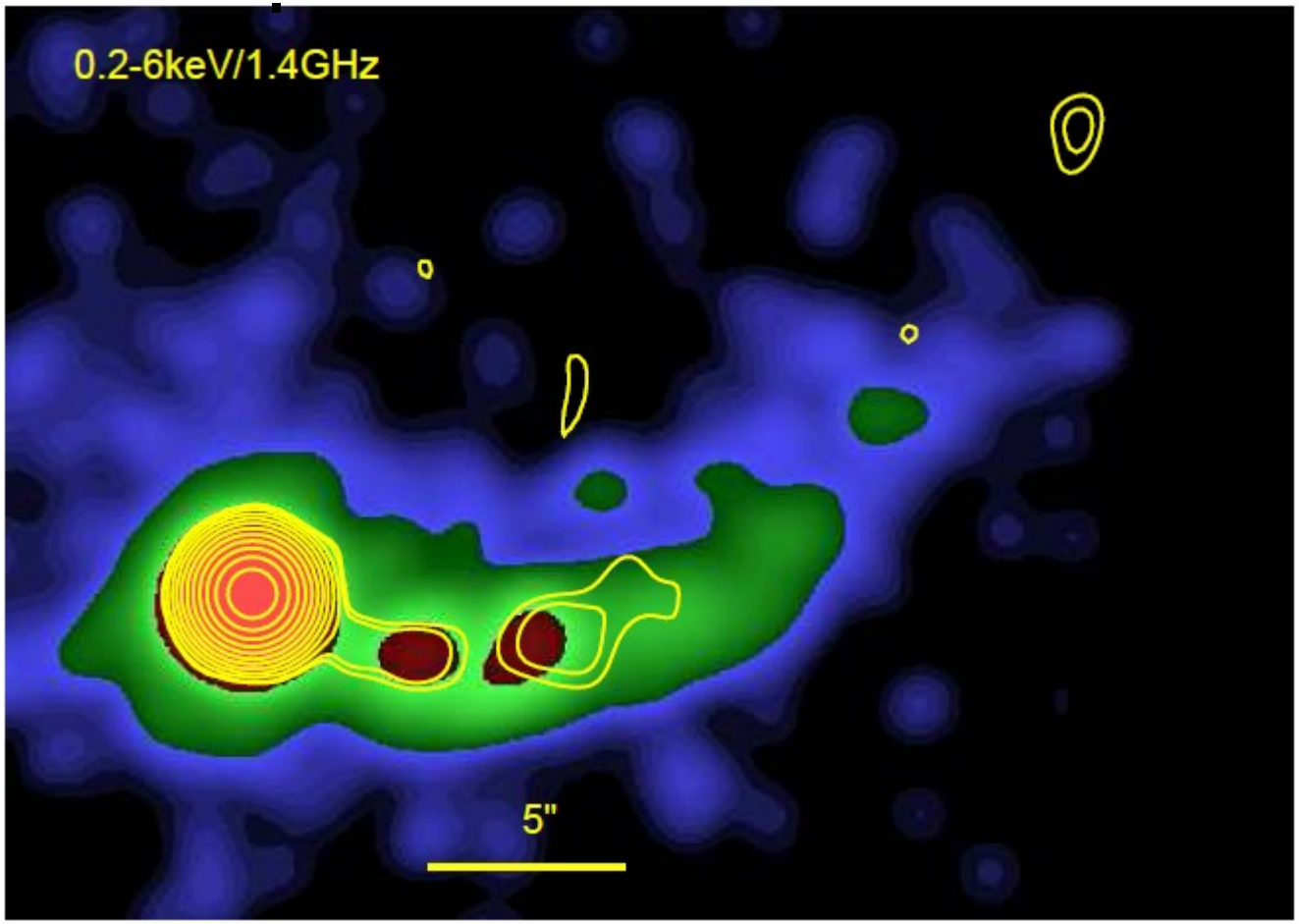

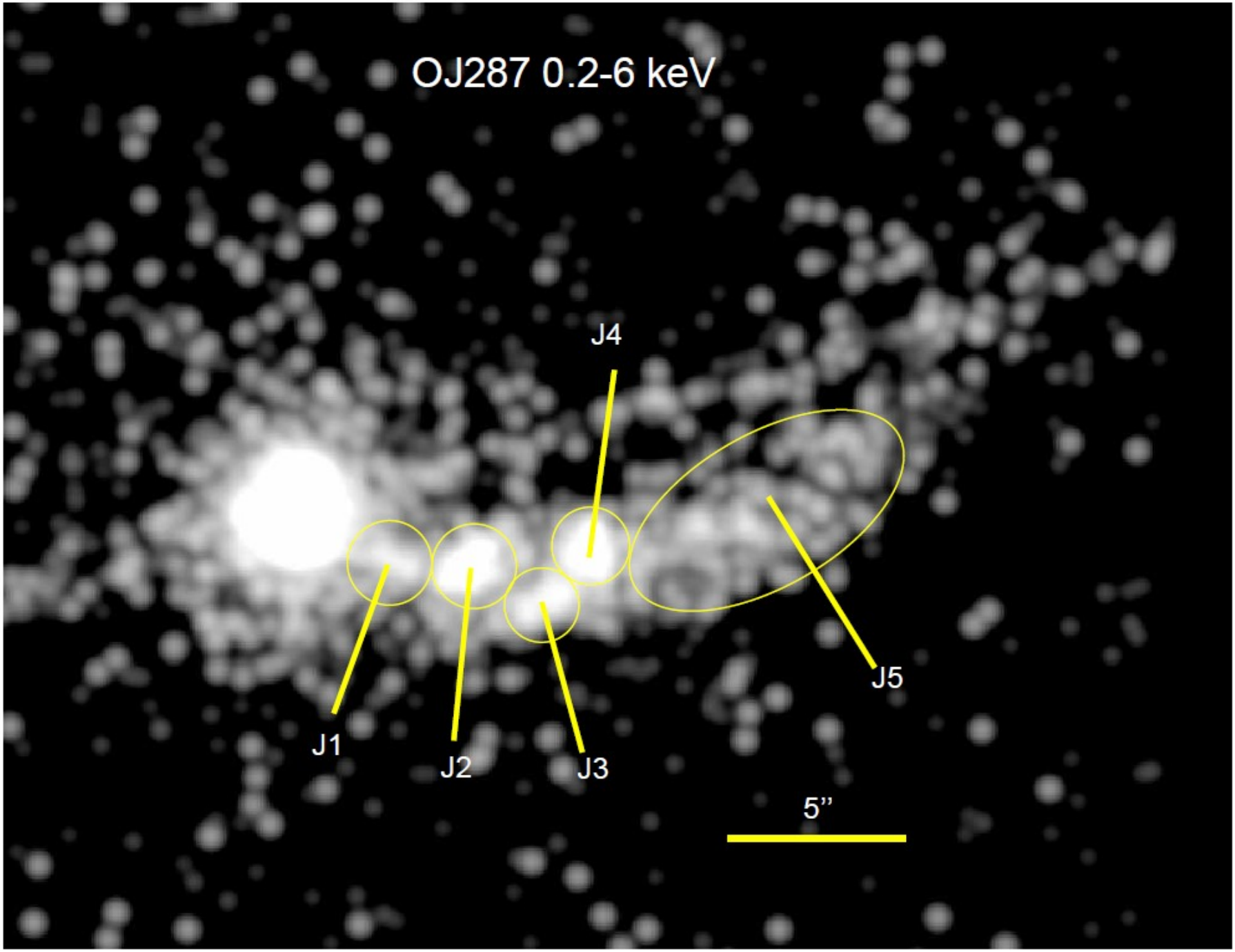
OJ287 0.2-6 keV
J4
J5
J1
J2
J3
5”

OJ287 light variations
Binary black hole model:
Sillanpää et al 1988

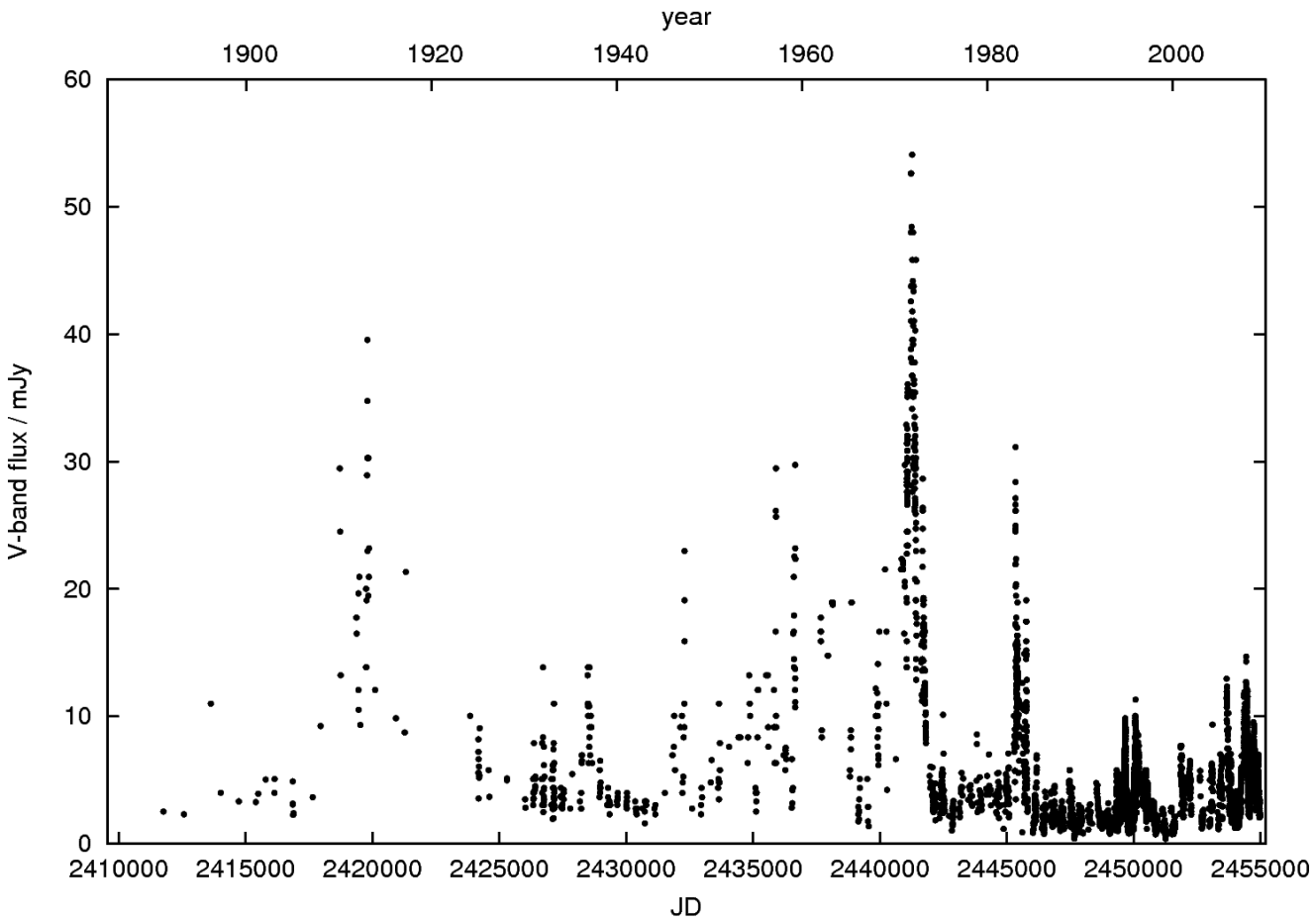

BLACK-HOLE MASS AND GROWTH RATE AT $Z \simeq 4.8$: A SHORT EPISODE OF FAST GROWTH FOLLOWED BY SHORT DUTY CYCLE ACTIVITY

BENNY TRAKHTENBROT[1], HAGAI NETZER[1], PAULINA LIRA[2] AND OHAD SHEMMER[3]

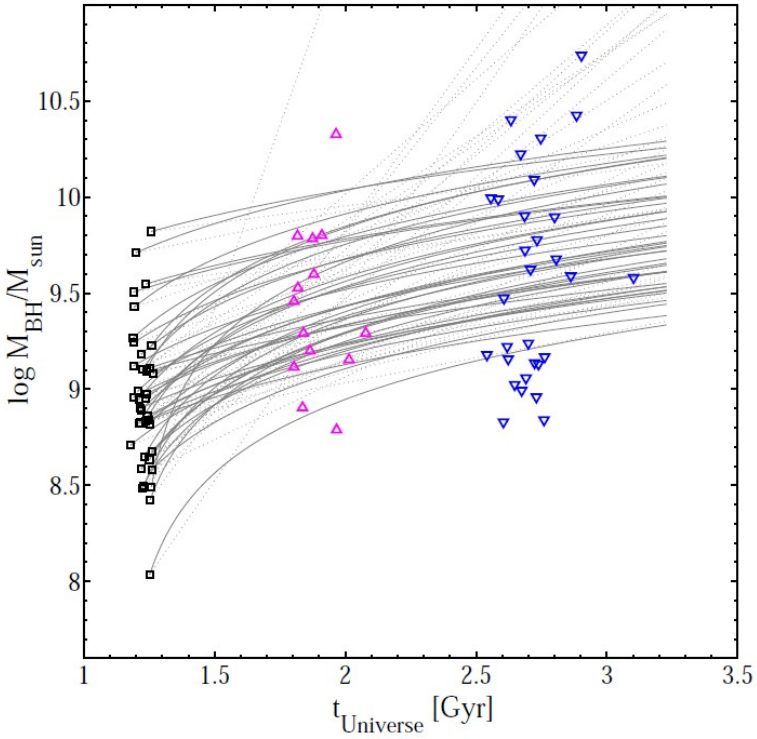

Figure 8. Evolution scenarios for the $z \simeq 4.8$ SMBHs with various duty cycles. Symbols are identical to those in Fig. 4. Solid lines describe $M_{\rm BH}$ growth under the assumption of constant $L_{\rm bol}$ and a duty cycle of 20%. Dotted lines represent the constant $L/L_{\rm Edd}$ scenario and a duty cycle of 10%.

Jets at All Scales
Proceedings IAU Symposium No. 275, 2010
G.E. Romero, R. Sunyaev, & T. Belloni, eds.

DOI: 00.0000/X000000000000000X

Jet-disk connection in OJ287

Mauri J. Valtonen[1,2], Tuomas Savolainen[3] and Kaj Wiik[2]

[1]Helsinki Institute of Physics, FIN-00014 University of Helsinki, Finland
email: mvaltonen2001@yahoo.com

[2]Dept. of Physics & Astronomy, Tuorla Observatory, University of Turku, 21500 Piikkiö, Finland
email: kaj.wiik@utu.fi

[3]Max-Planck-Institut für Radioastronomie, Auf dem Hügel 69, D-53121 Bonn, Germany
email: tsavolainen@mpifr-bonn.mpg.de

Optical polarization angle in OJ287 and the binary black hole model

Mauri J. Valtonen[1] and Carolin Villforth[2,3⋆]
[1] *Helsinki Institute of Physics, FIN-00014 University of Helsinki, Finland*
[2] *Tuorla Observatory, Department of Physics and Astronomy, University of Turku, Väisäläntie 20, FI-21500 Piikkiö, Finland*
[3] *Space Telescope Science Institute, 3700 San Martin Drive, 21218 Baltimore, Maryland, USA*

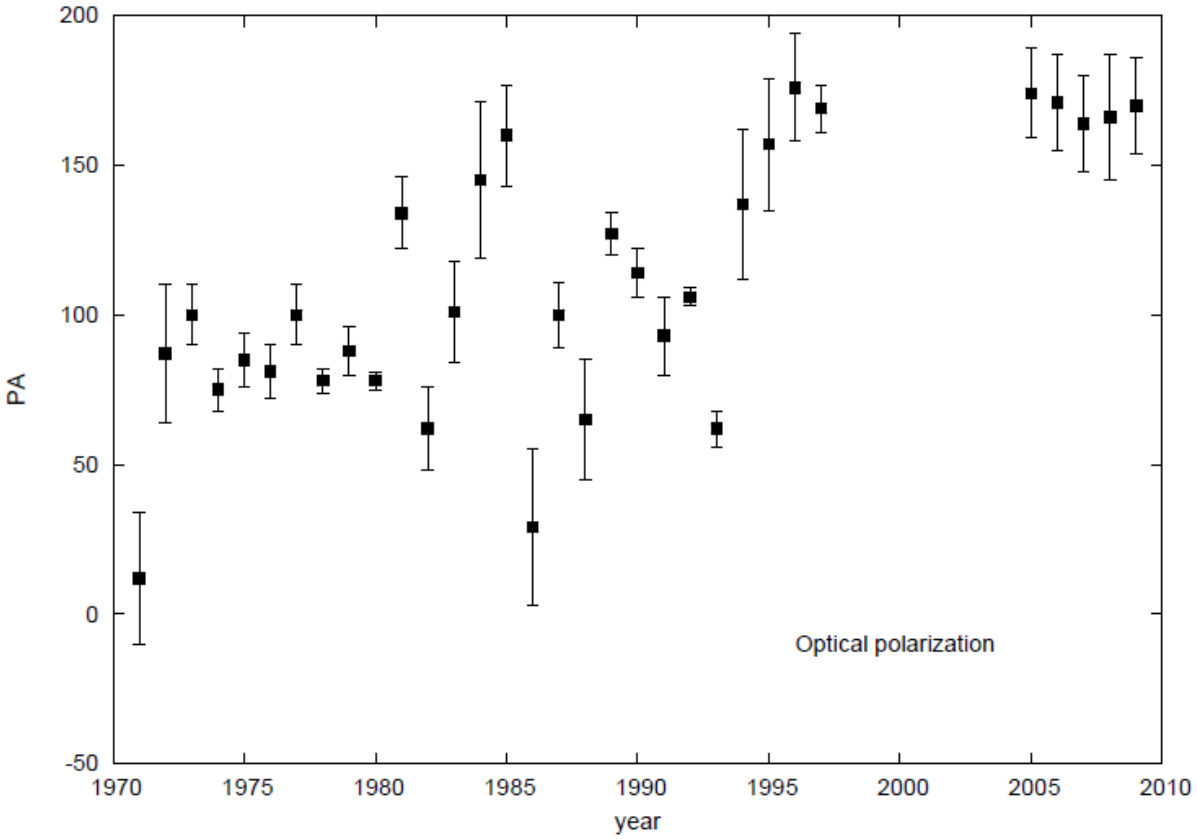

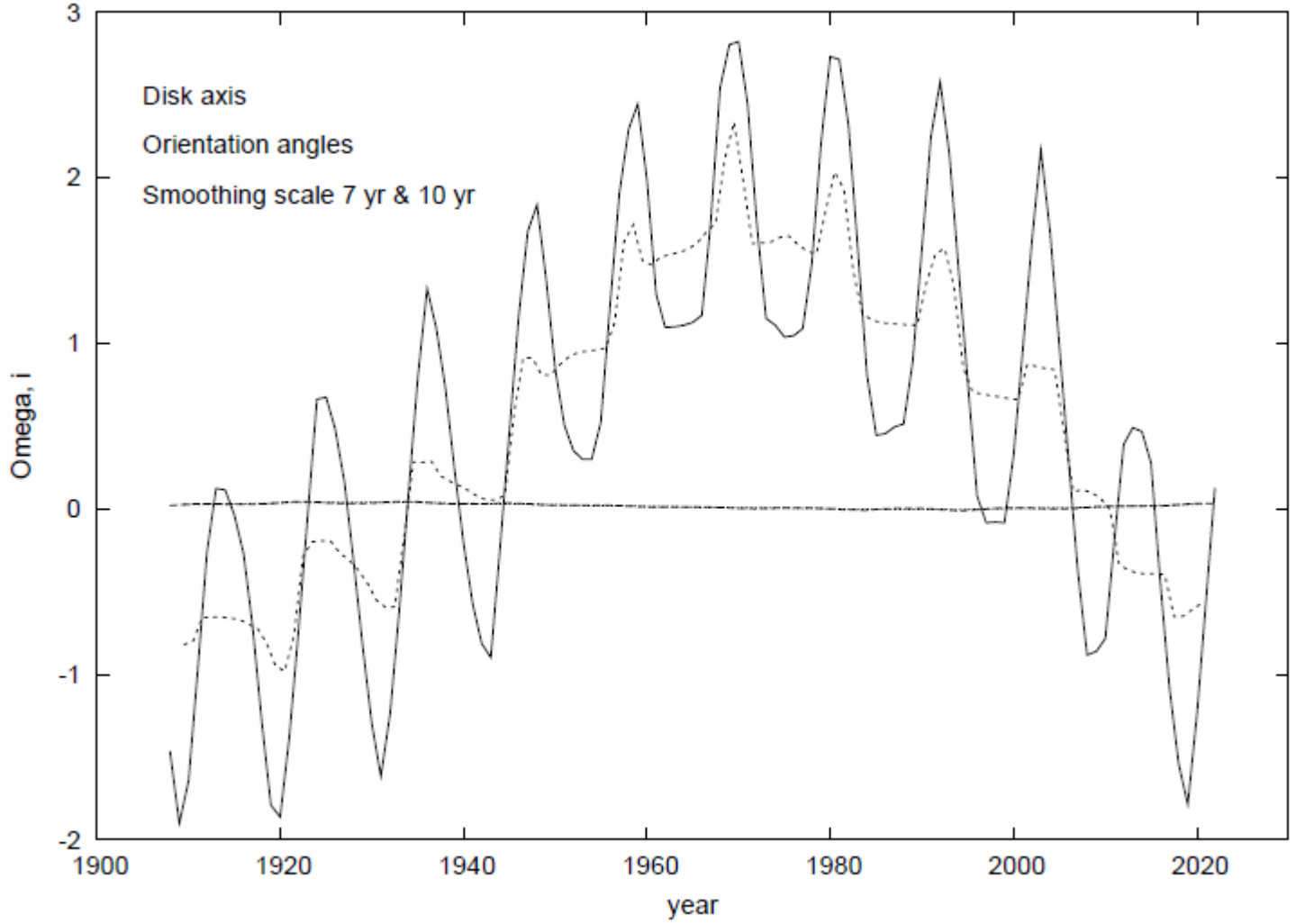

Figure 2. The evolution of the mean disk in the binary model.

Kozai cycle

$$\frac{di}{d\tau} = 0 \tag{1}$$

$$\frac{d\Omega}{d\tau} = -\frac{3}{4}\cos i \tag{2}$$

(Valtonen and Karttunen 2006) where τ is the normalized time coordinate,

$$\tau \sim \frac{P}{P_e}\frac{t}{P} \tag{3}$$

and t is time, and P and P_e are the inner and outer periods,

$P_e \sim 12$ yr, $P \sim P_e/5$, and $P_{Kozai} \sim 120$ yr

Jet perpendicular to disk: optical base flux determines viewing angle, Gamma

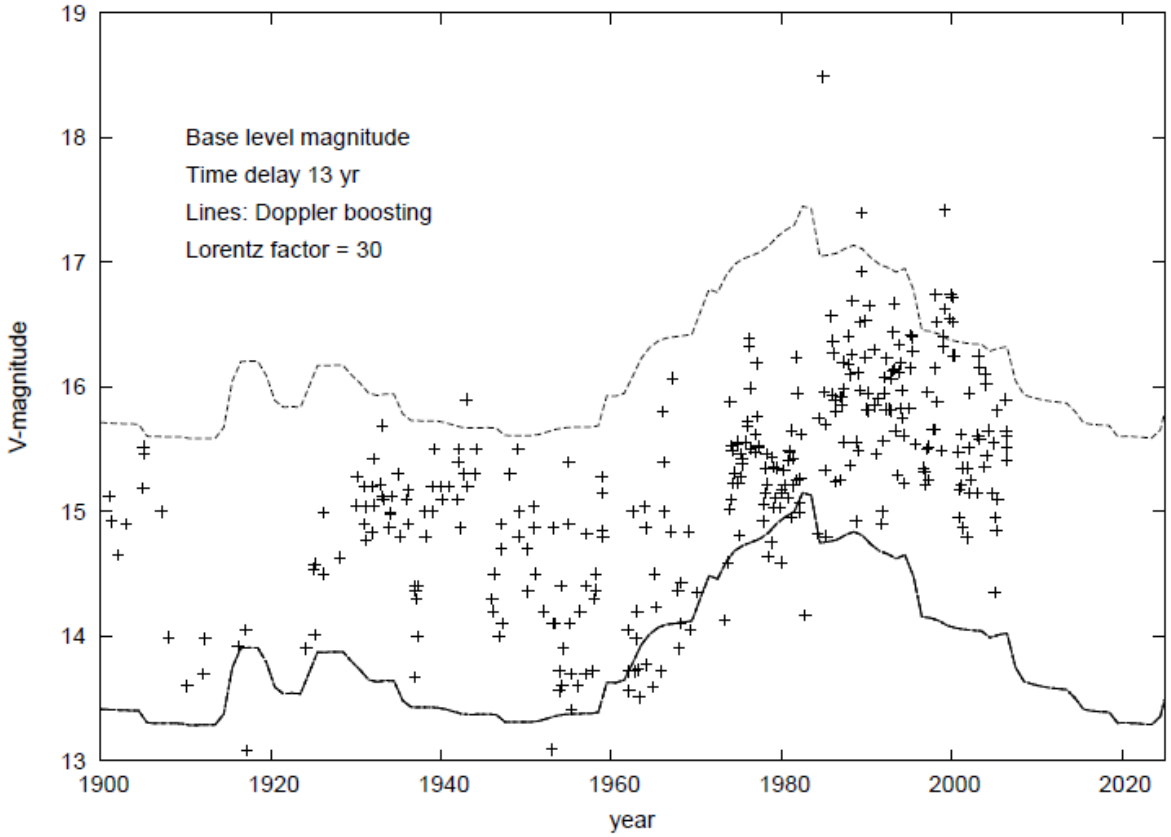

Figure 3. The variation of the base level brightness in OJ287.

Evolution of viewing angle

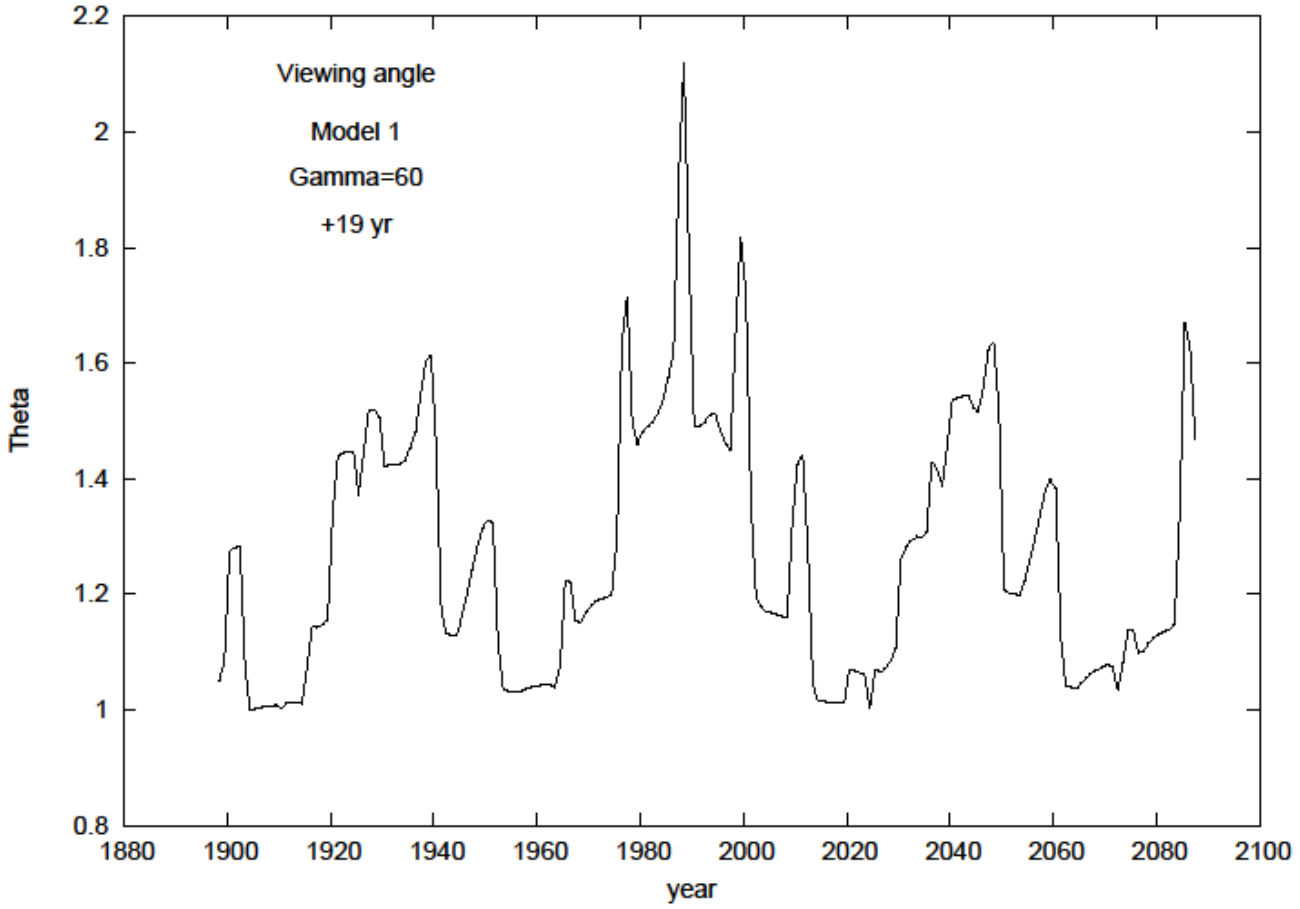

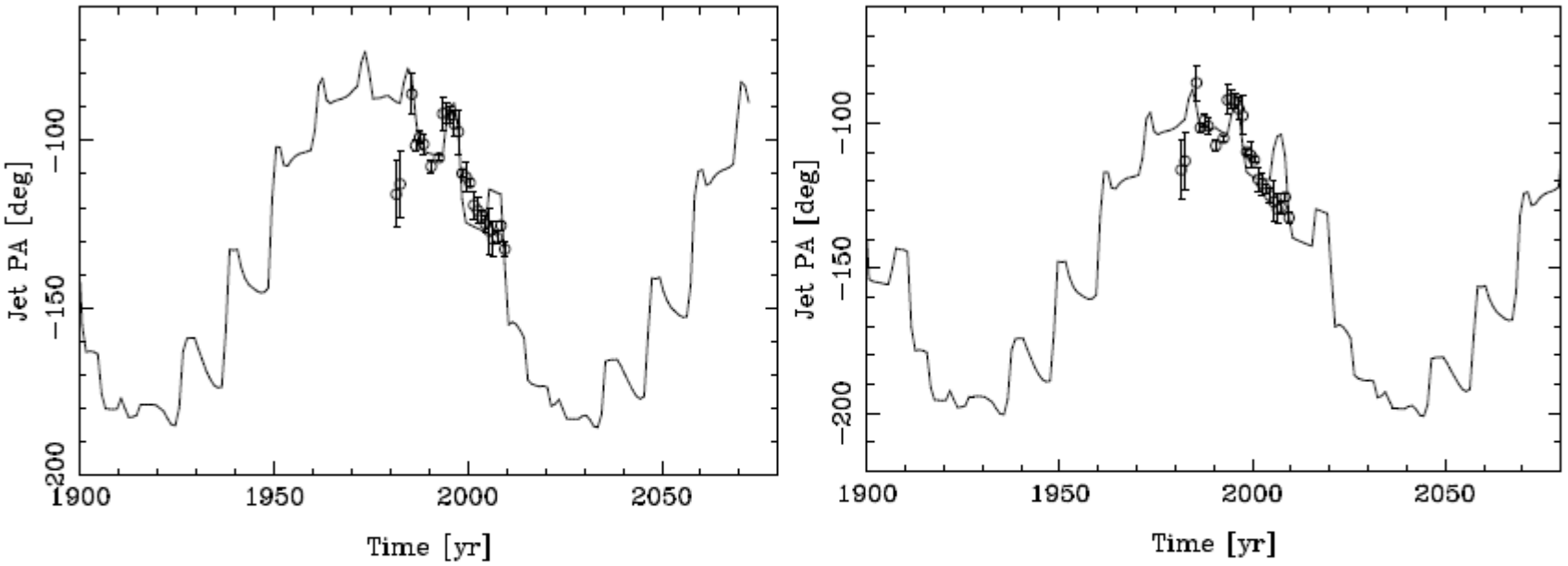

Figure 1. The line shows the variation of the jet angle as a function of time, based on the binary model of OJ 287. The viewing angle of the jet varies between 1 and 2 degrees. The circles represent the yearly average PA observed in the 2-6 cm wavelength range. The error bars represent the standard deviation of the PA when more than two observations per year were available. *Left:* A 4-year lag is introduced between changes in the accretion disk orientation and jet reorientation. *Right:* The same as the left-hand side, but the lag is 14 years.

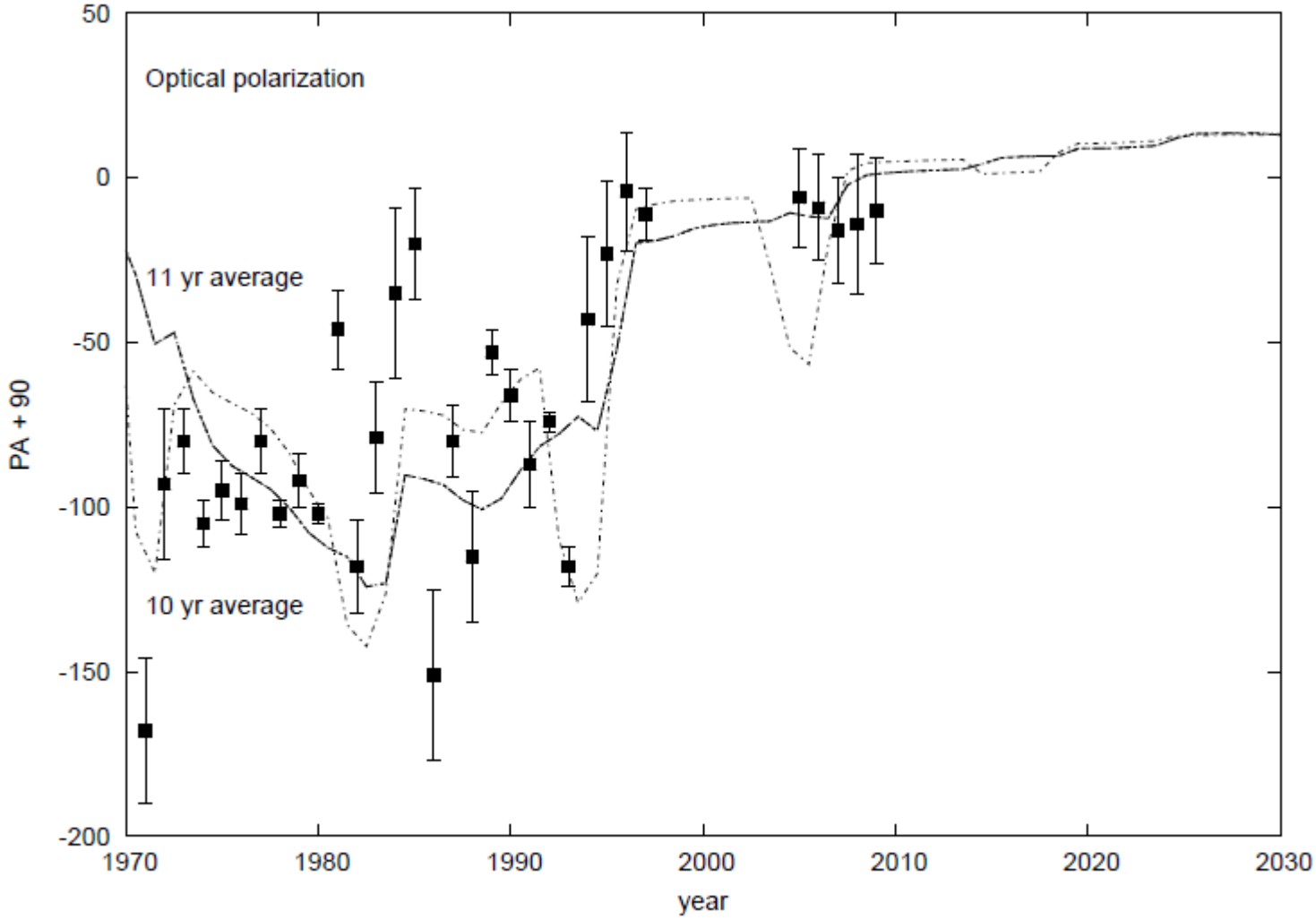

Figure 5. The evolution of the optical polarization angle com-

Projected spin angle vs. observations

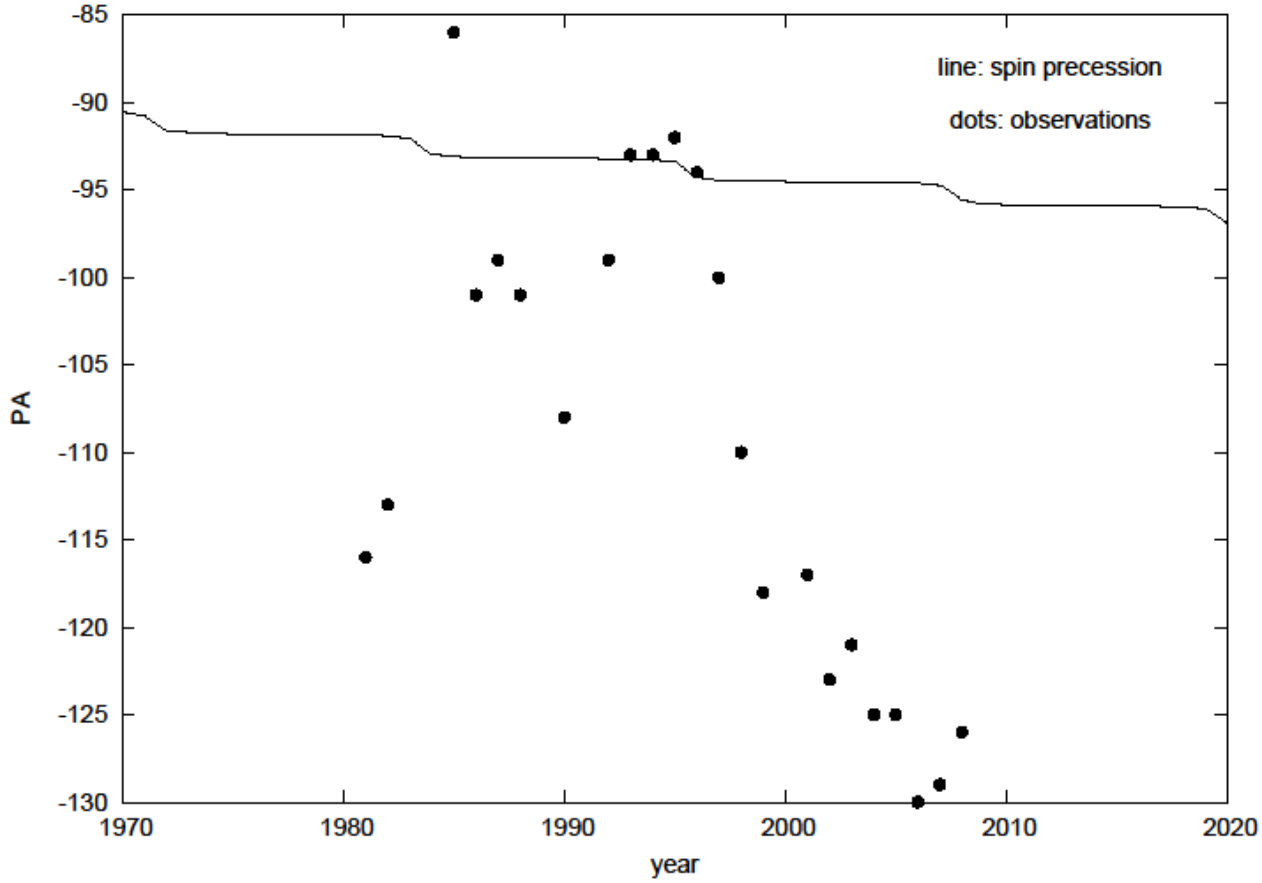

The Megaparsec-Scale X-ray Jet of the BL Lac Object OJ287

Alan P. Marscher[1] and Svetlana G. Jorstad[1,2]

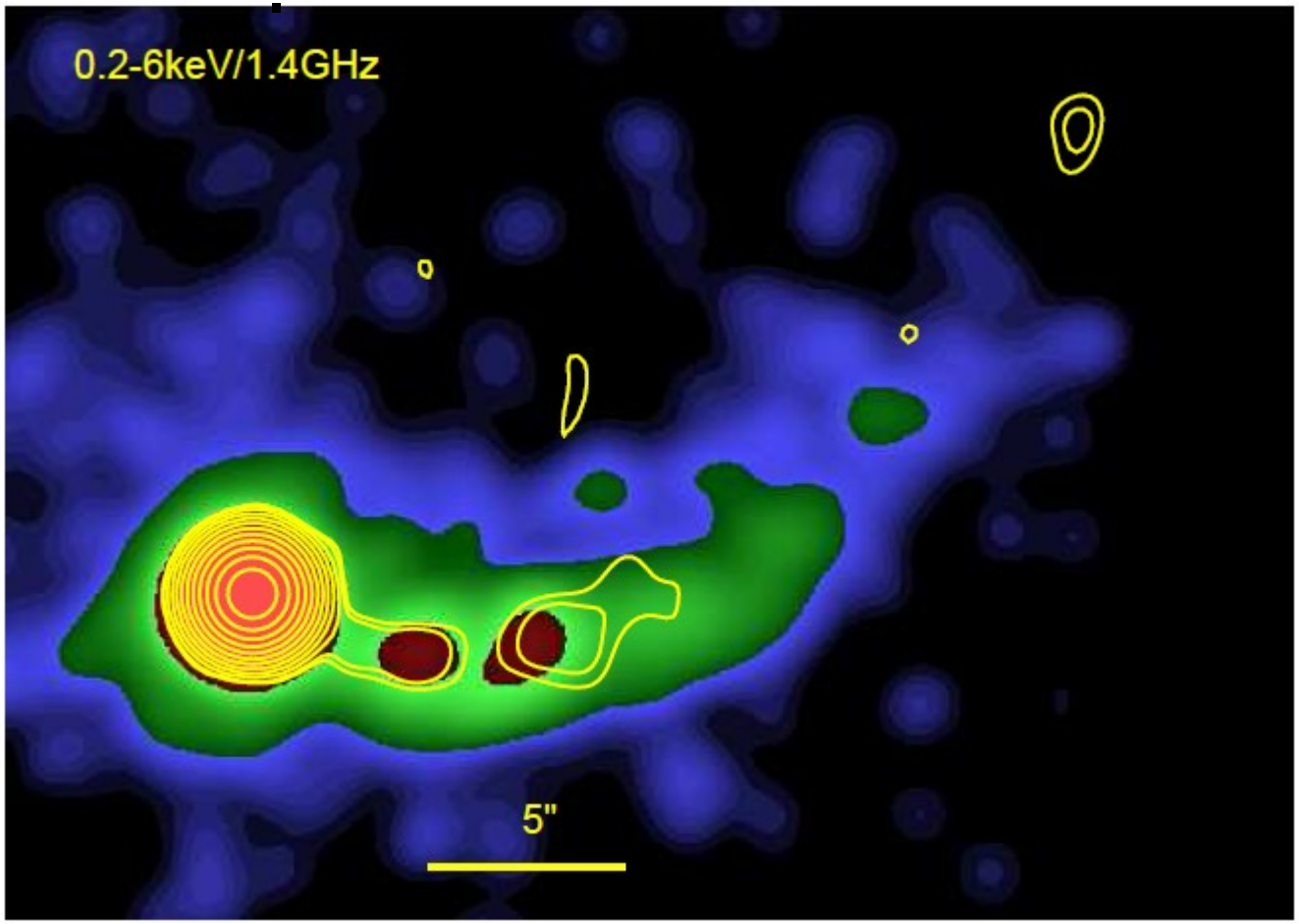

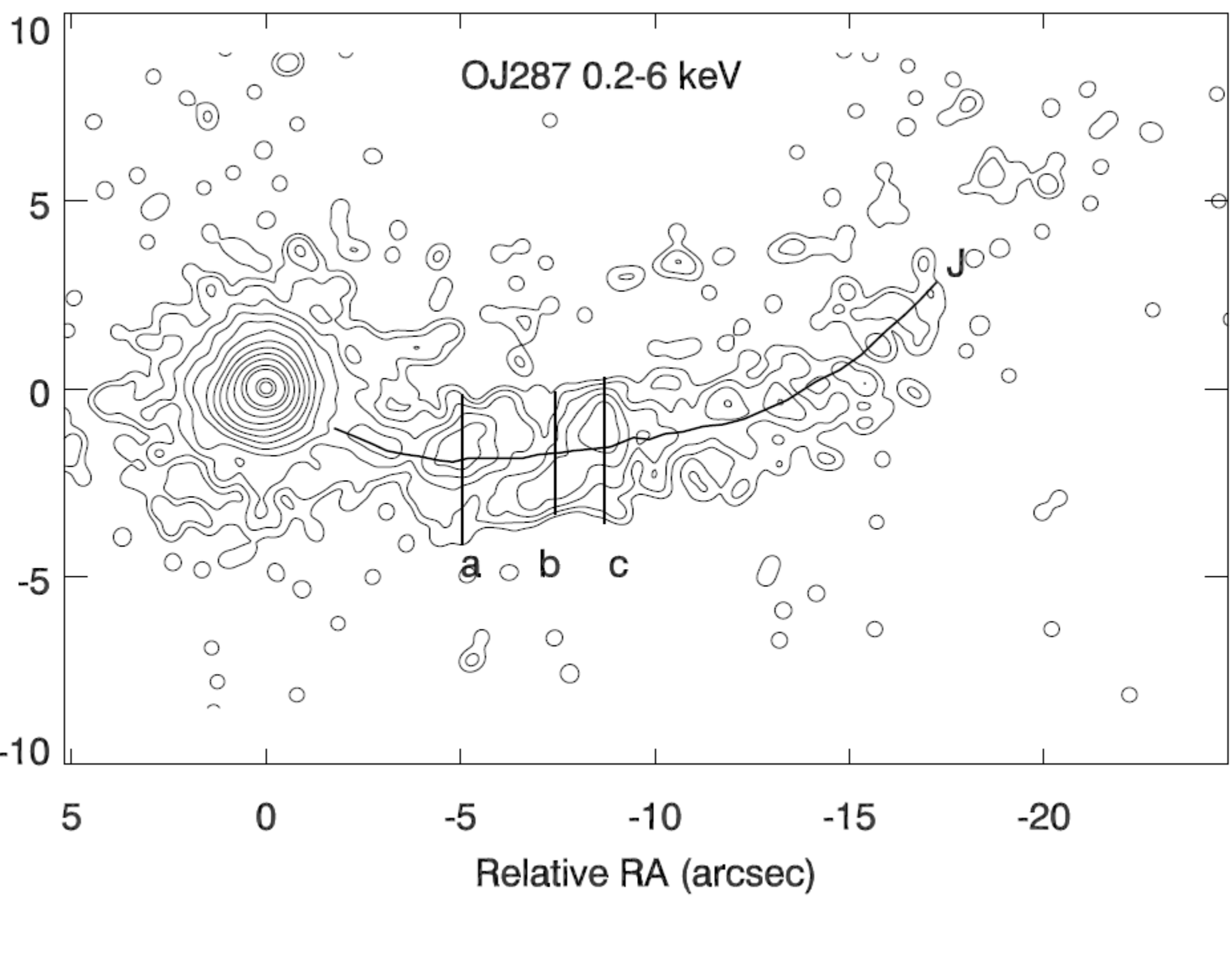
OJ287 0.2-6 keV
J
a
b
c
10
5
0
-5
-10
5
0
-5
-10
-15
-20
Relative RA (arcsec)

Conclusions

- Small scale jet direction given by the disk axis, not BH spin axis
- Spin rotation shows up in the wiggles of the large scale jet
- Overall jet curvature may be related black hole binary history
- There is a delay in reorientation between radio and optical jet regions
- Radio jet should stop rotation in the sky and start reversing at about 2030

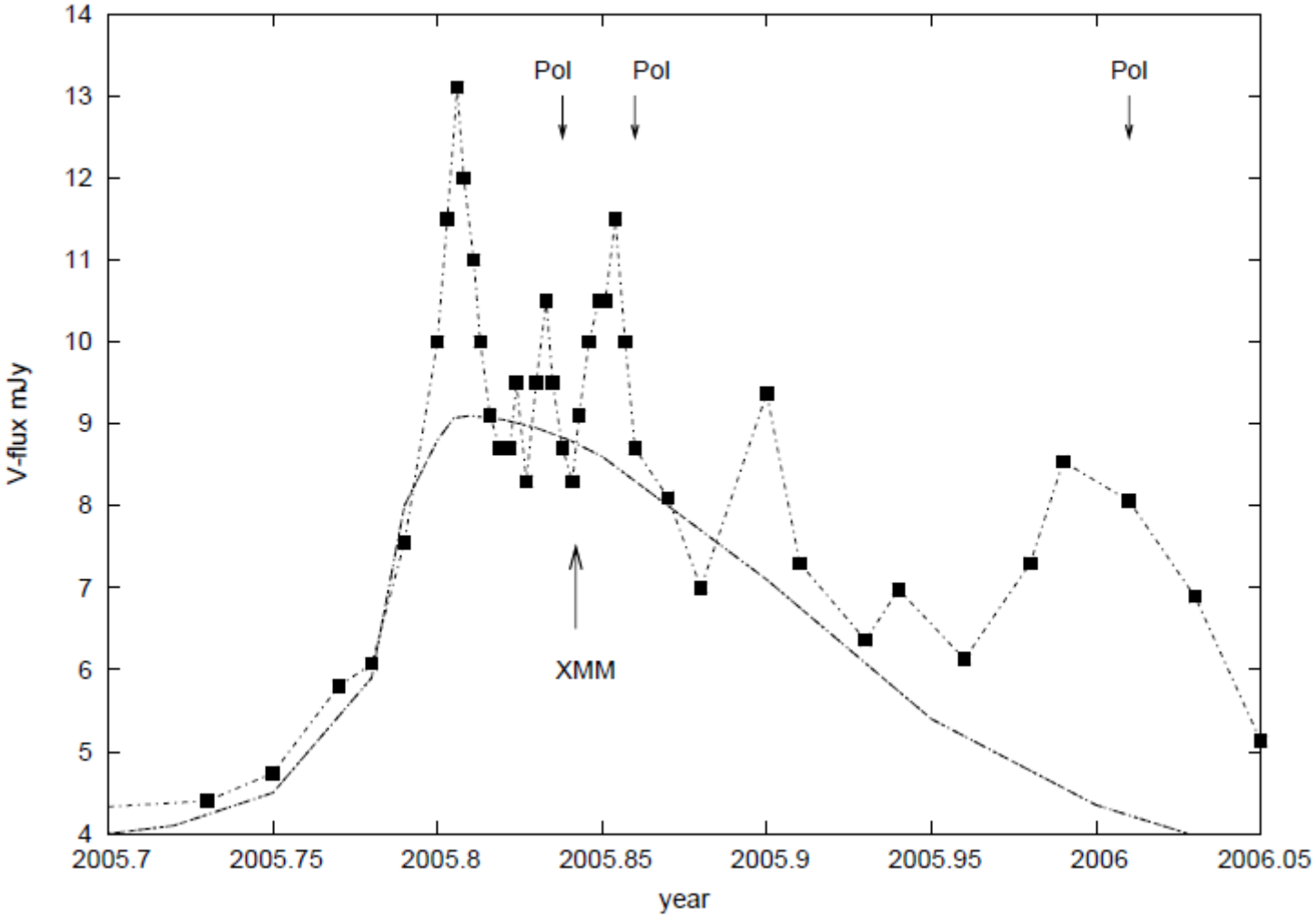
Pol
Pol
Pol
XMM
V-flux mJy
year
14
13
12
11
10
9
8
7
6
5
4
2005.7
2005.75
2005.8
2005.85
2005.9
2005.95
2006
2006.05

$$t_d = \quad 0.75$$

implies

α_g r $\dot{m}/\dot{m}_{\rm edd}$ =14

If ı $\dot{m}/\dot{m}_{\rm edd}$ =0.01

α_g =0.14

The 1995 model vs. Observations . A chi-square test (with 234 degrees of freedom) gives $\chi^2 = 205$, which corresponds to the probability $P = 0.9$ that the two distributions agree with each other. The corresponding correlation coefficient is 0.58.

CORRELATIONS: BEST OF 10^6 TRIALS

Correlated Quantities	χ^2	P(χ^2)	corr coeff
Obs vs. $\beta = 1$ model	310	6×10^{-4}	0.30
Obs vs. $\beta = 2$ model	305	10^{-3}	0.32
Obs vs. QPO model	290	7×10^{-3}	0.37
Obs vs. PO model	205	0.9	0.58

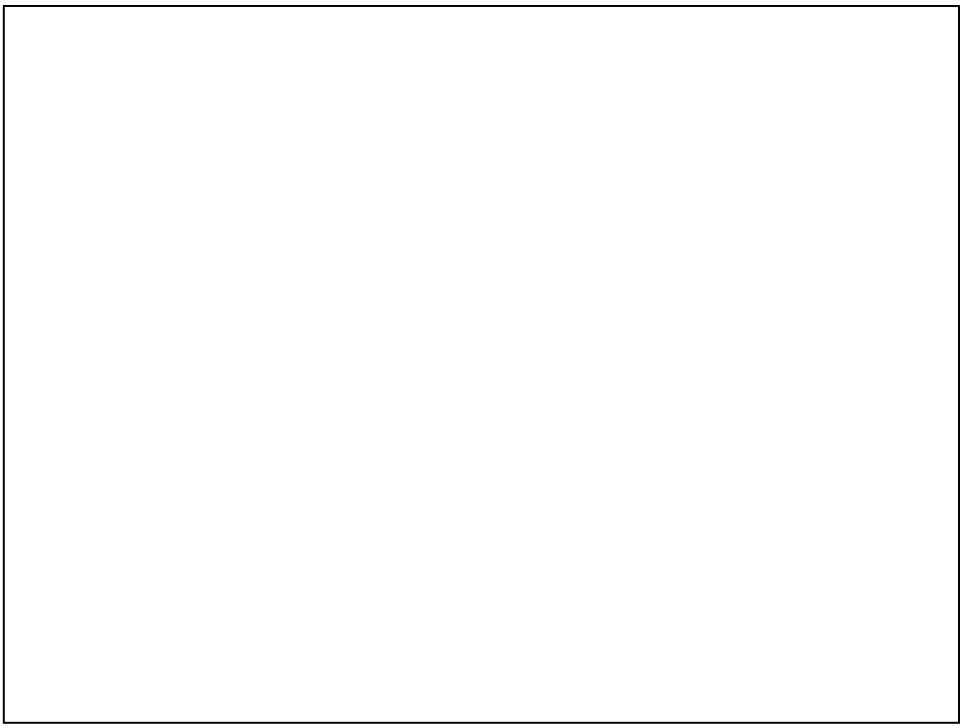

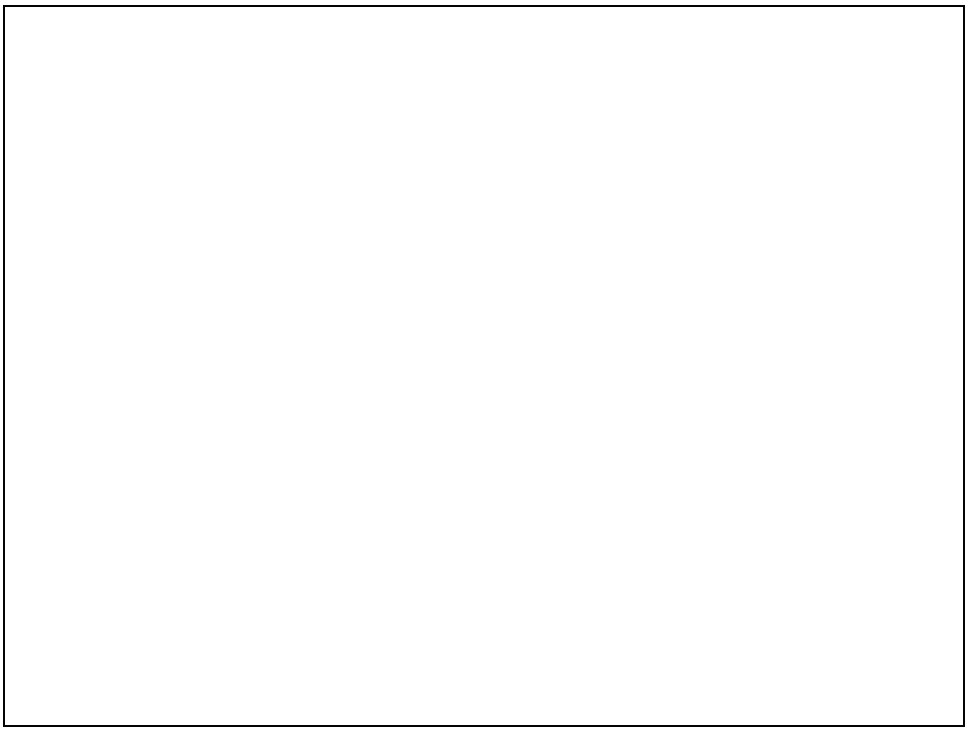

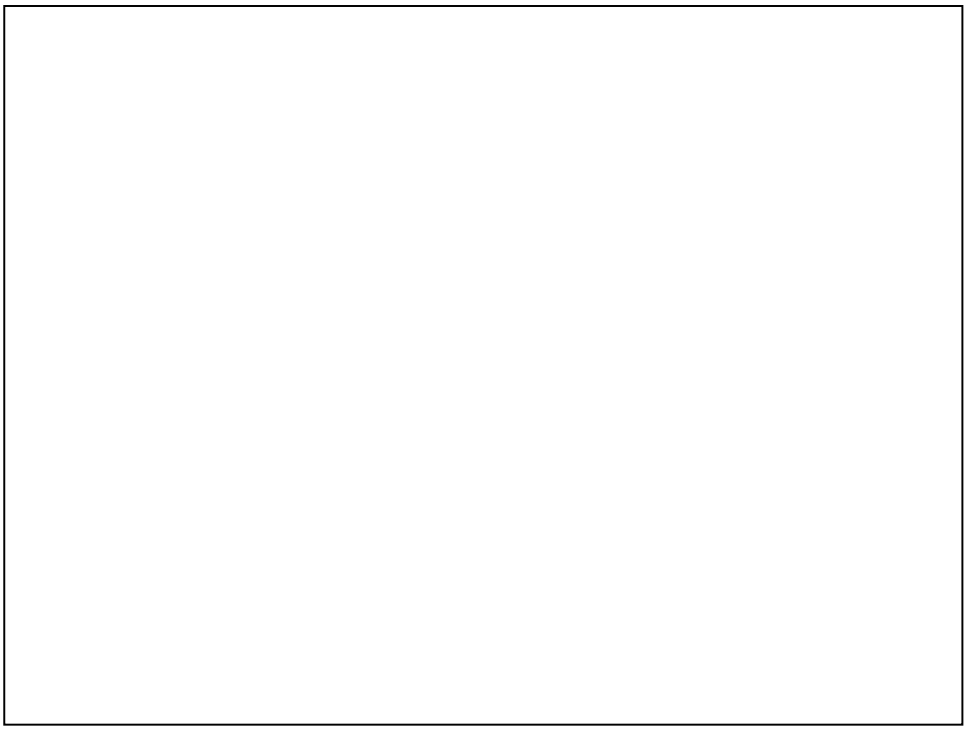

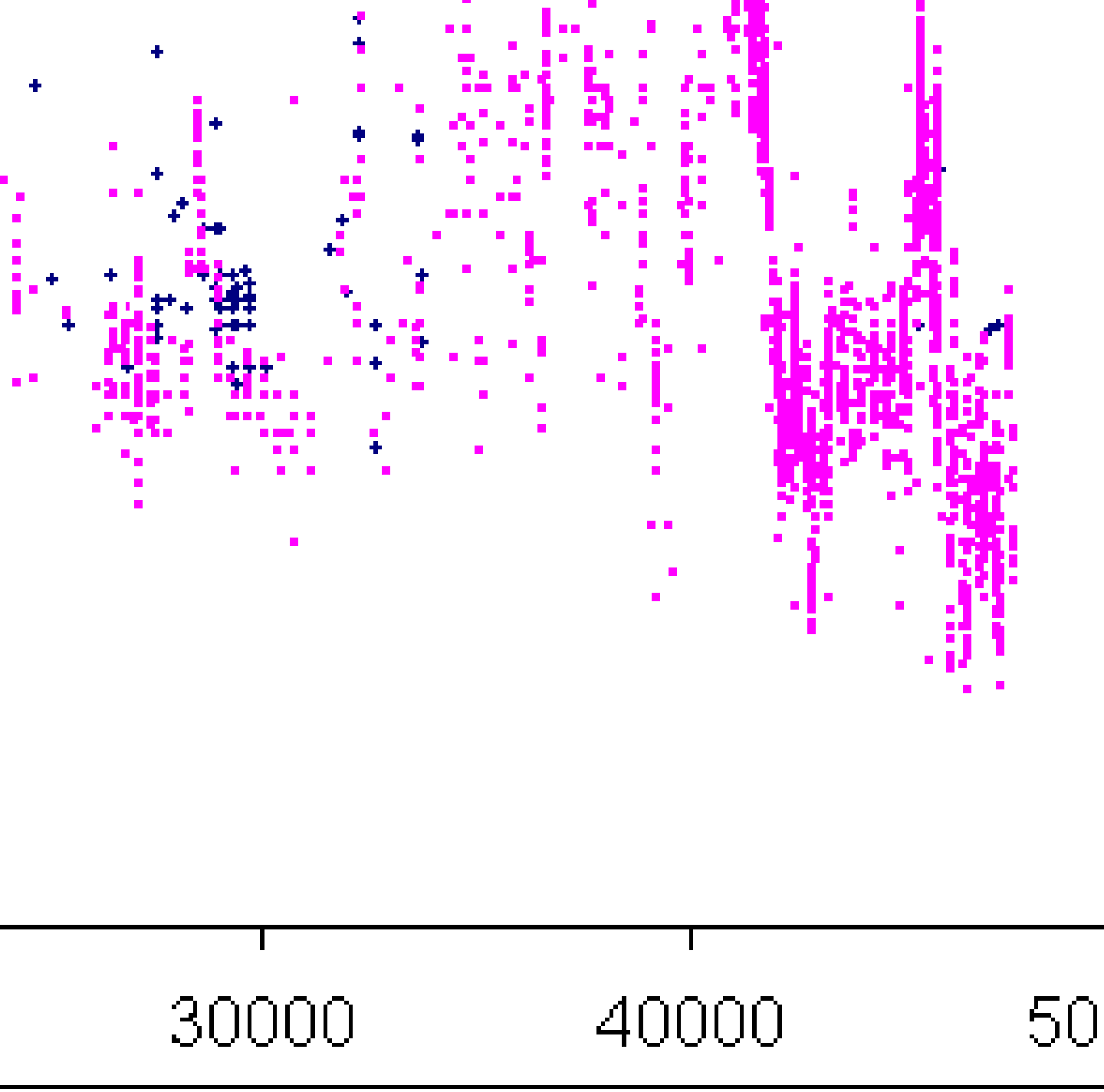
30000
40000
50

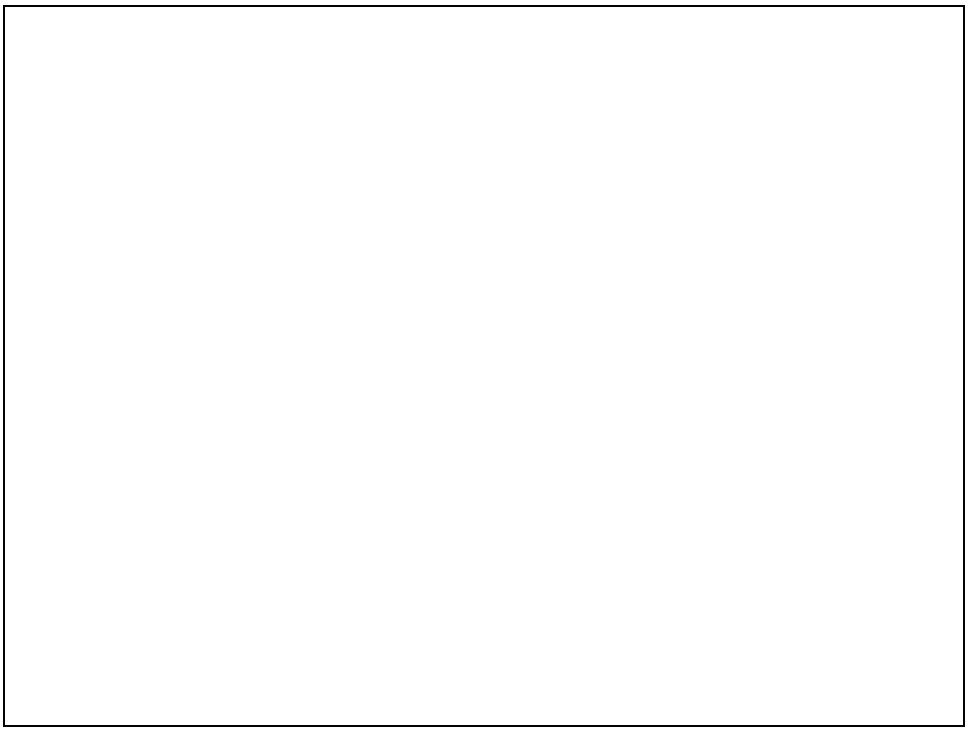

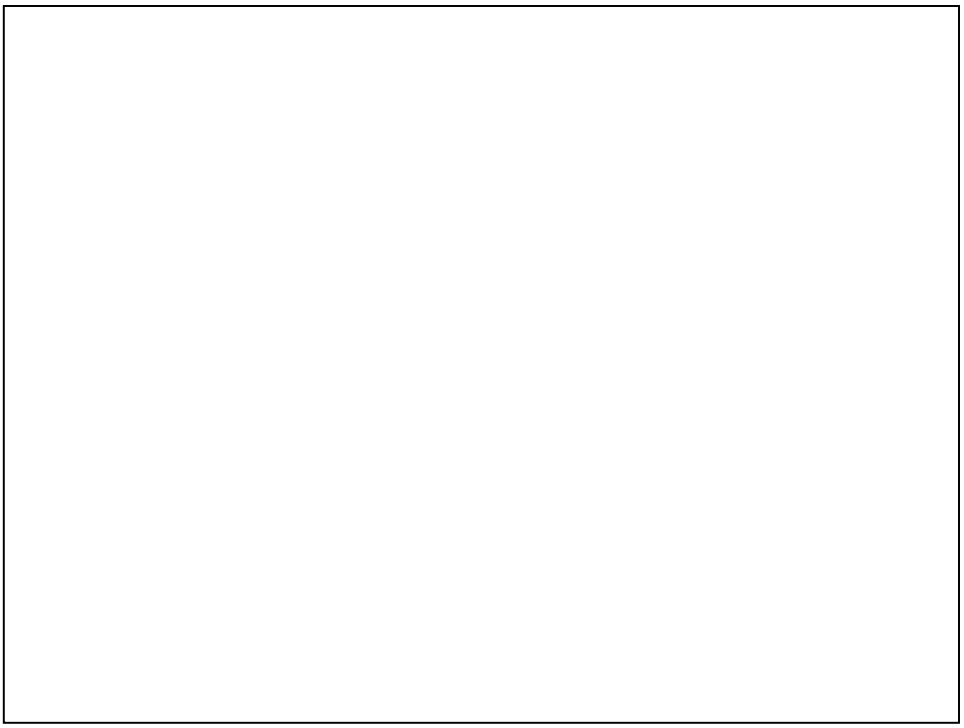

Nature Letter, 20 January 2011, 000, 000–000

Supermassive black holes do not correlate with dark matter halos of galaxies

John Kormendy[1,2,3] & Ralf Bender[2,3]

OJ 287

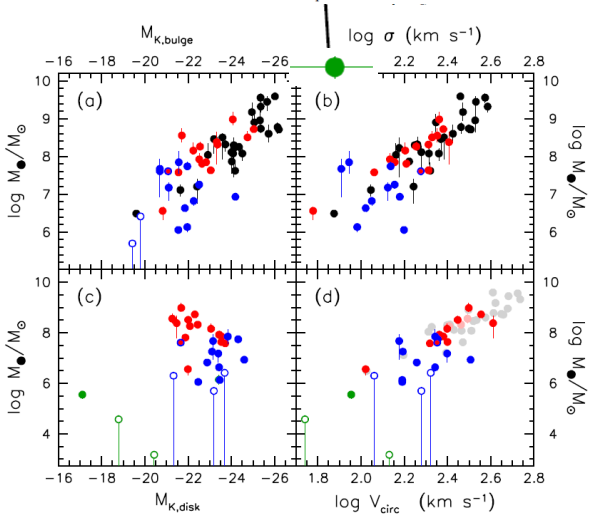

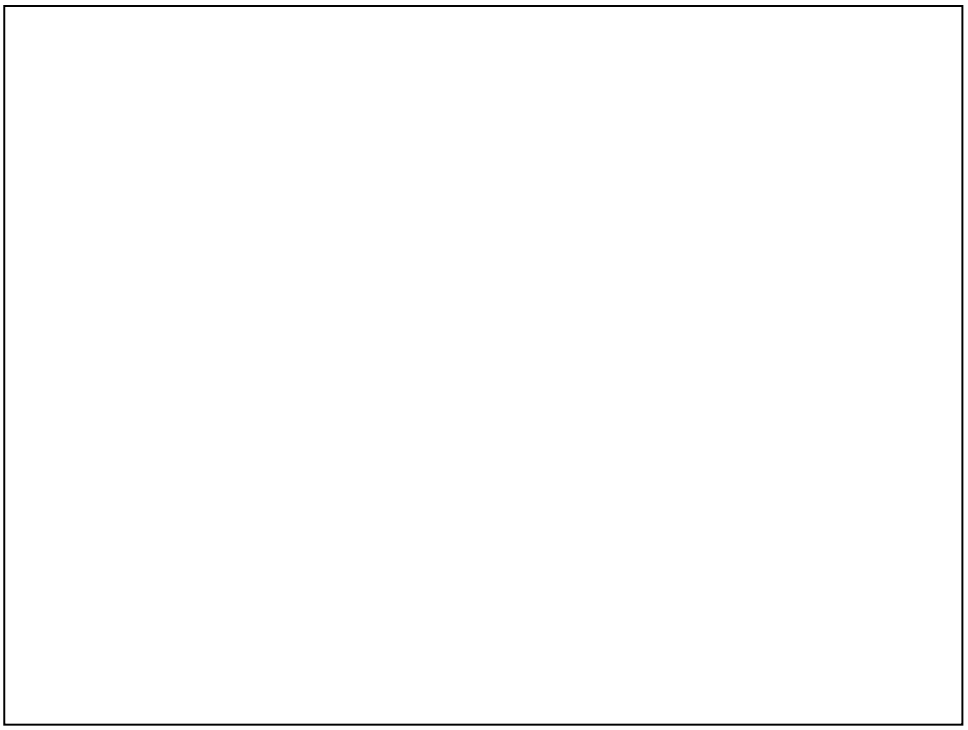

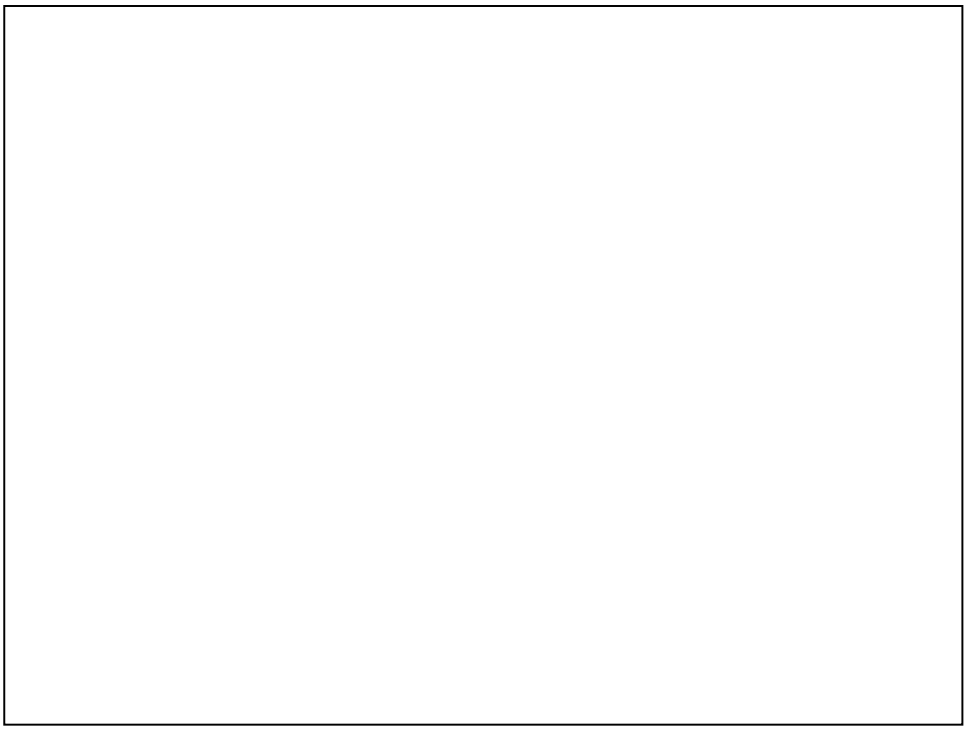

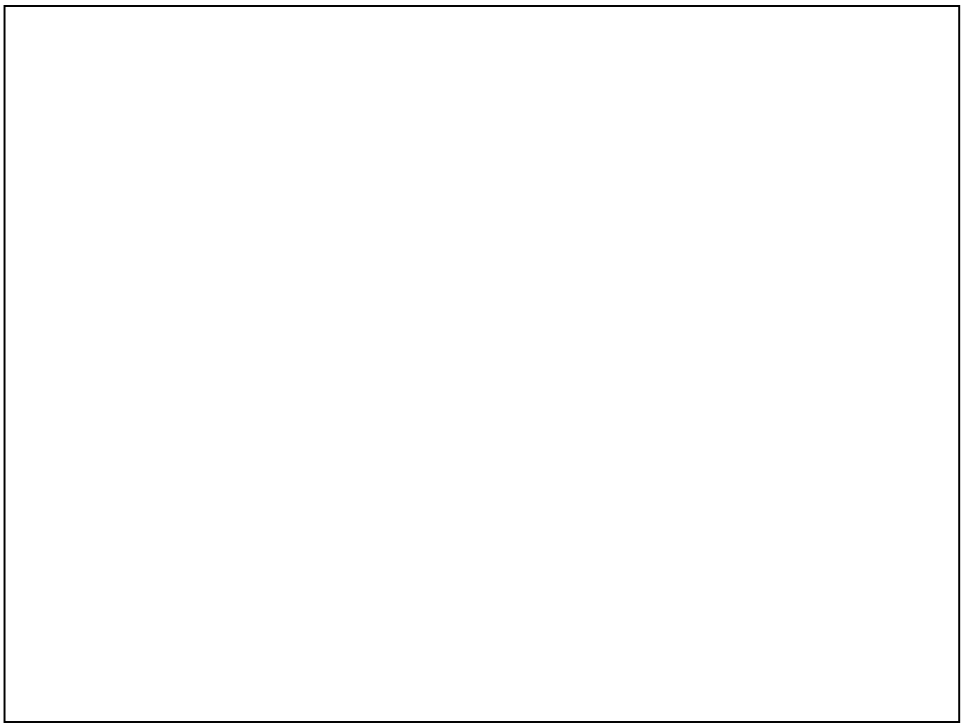

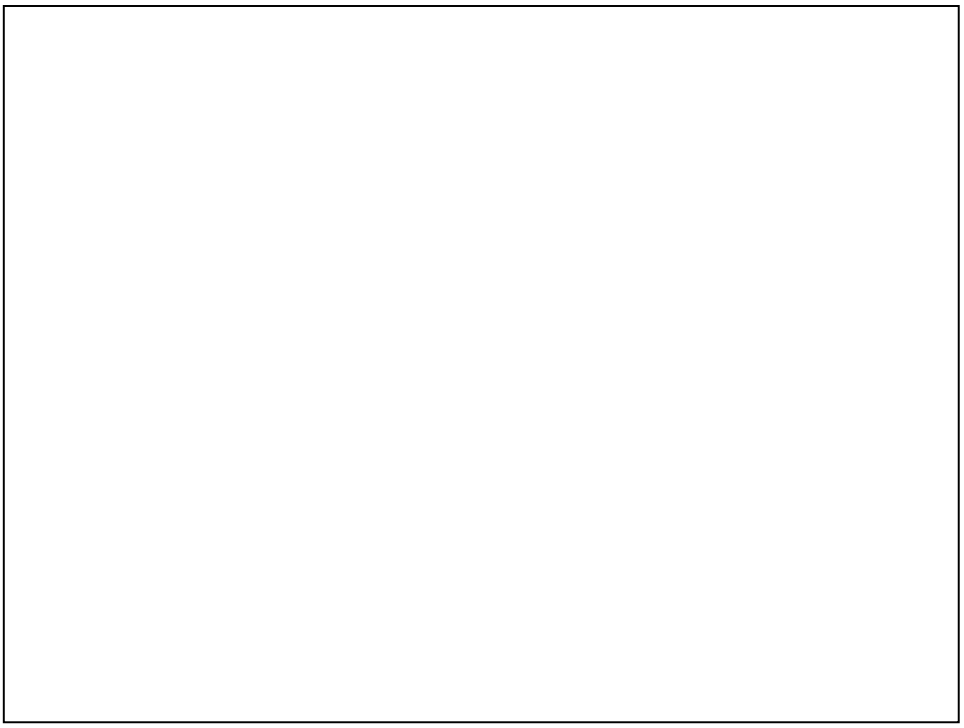

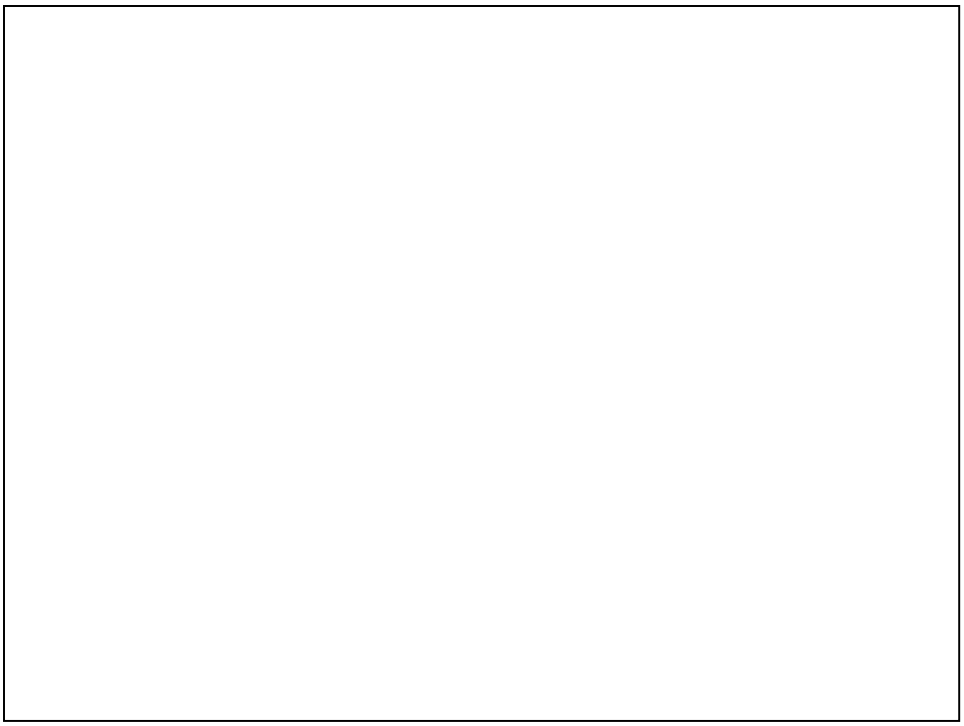

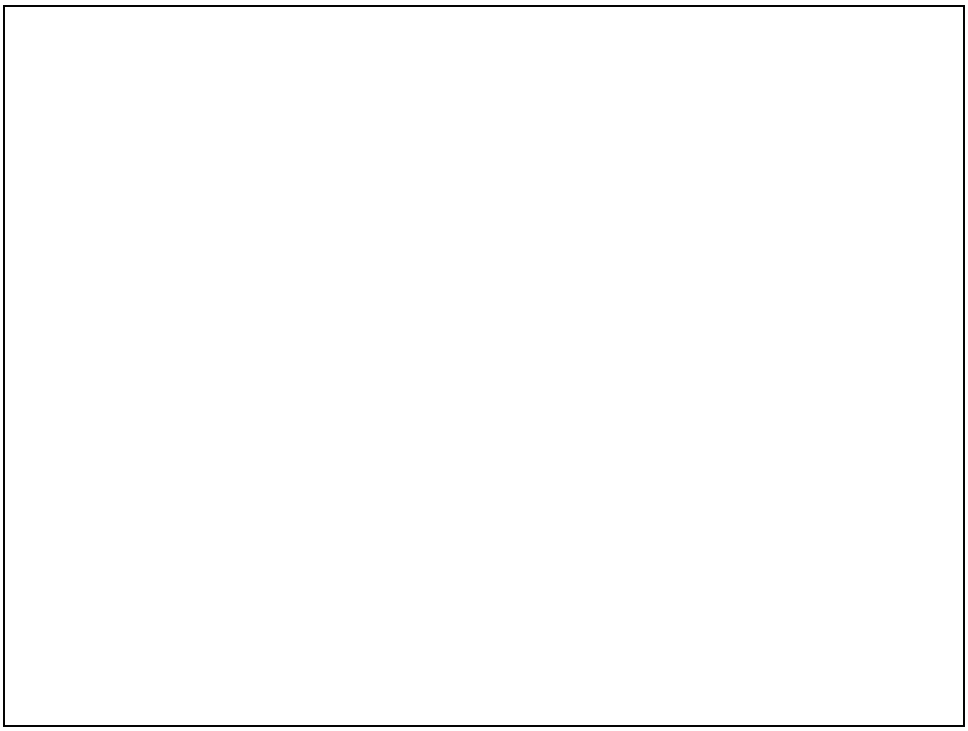

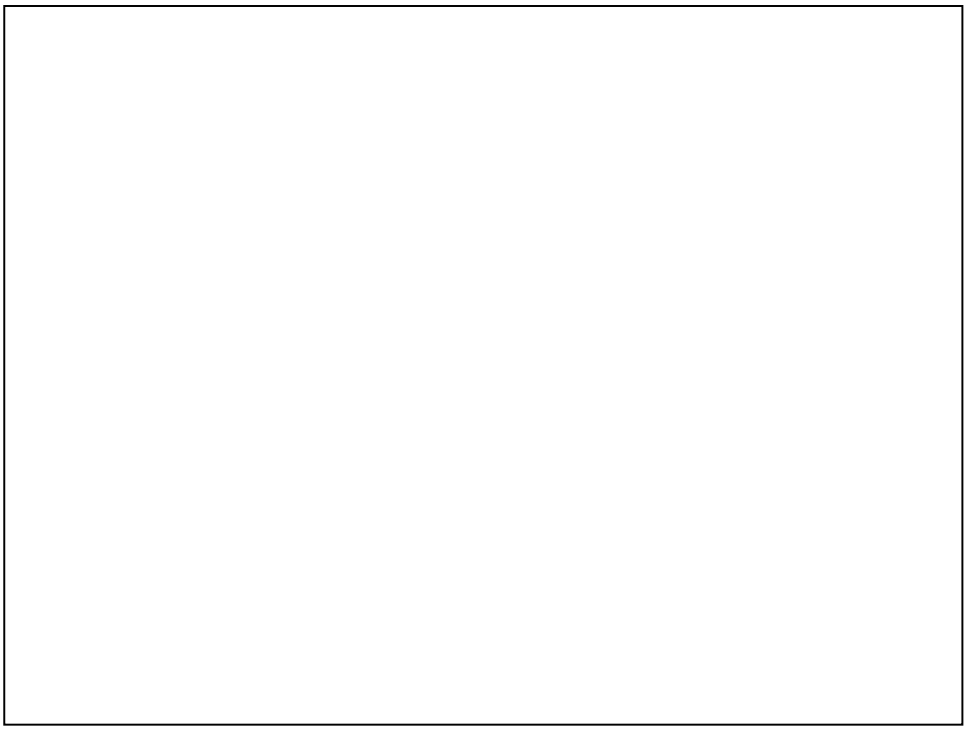

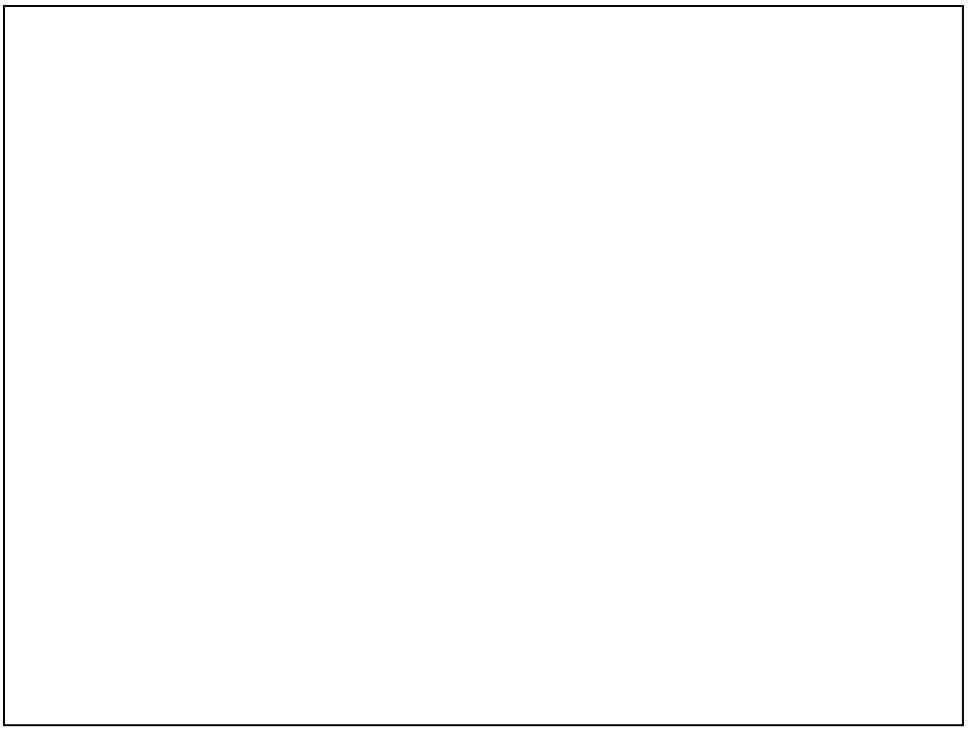

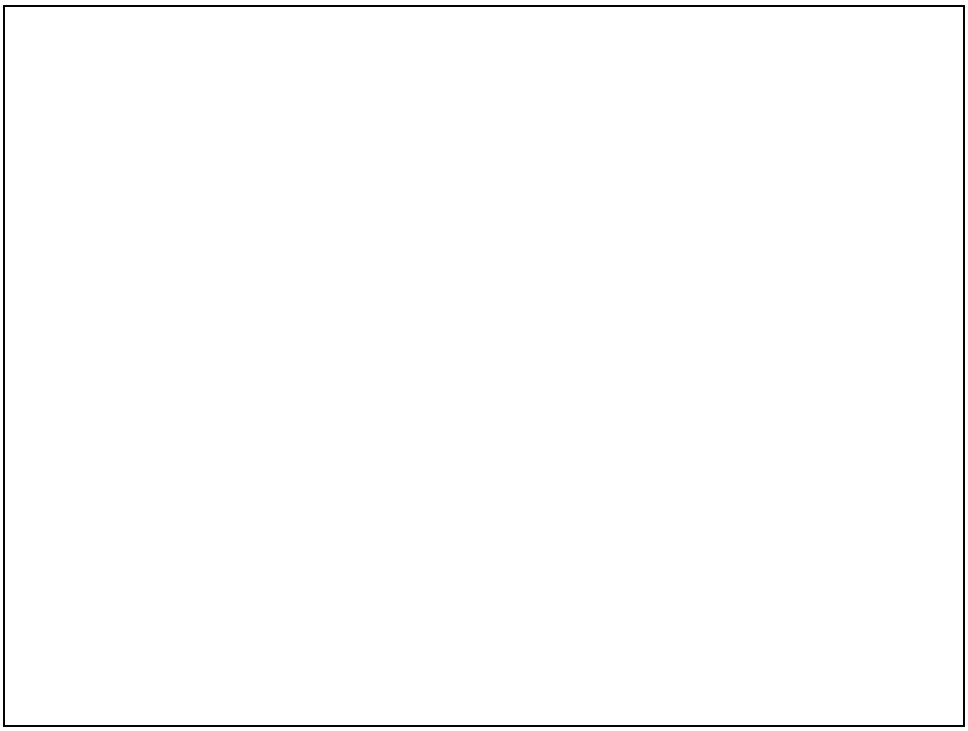

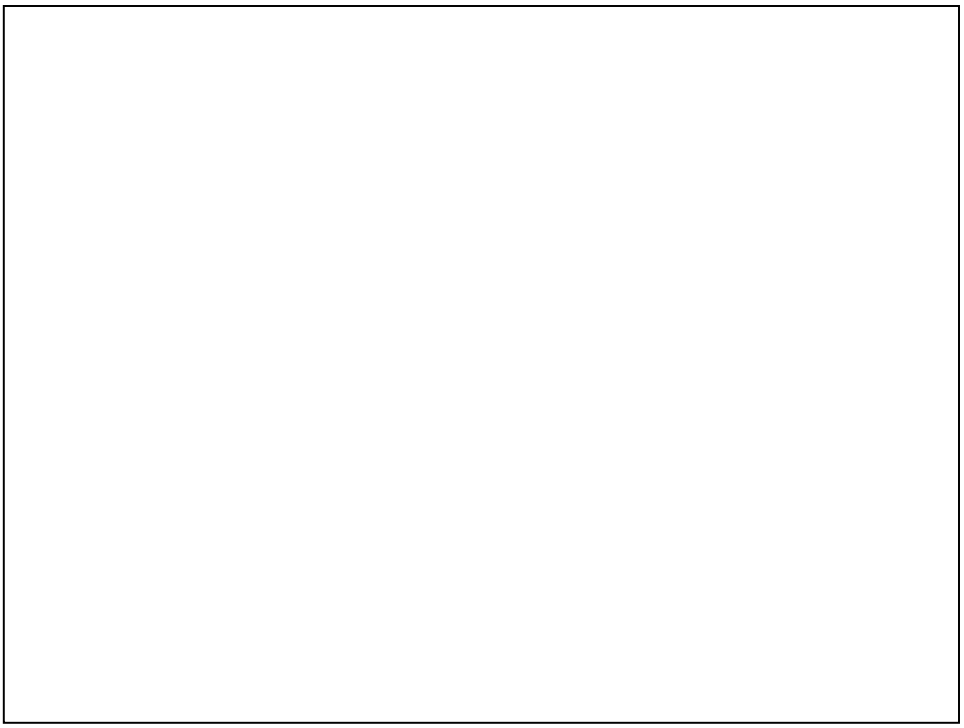

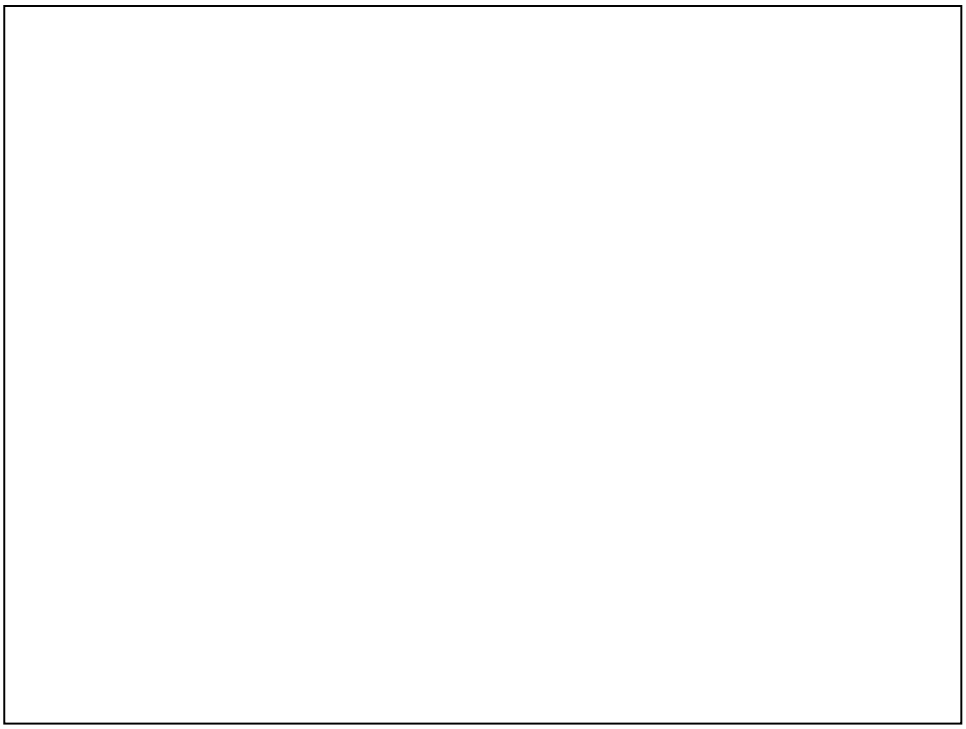

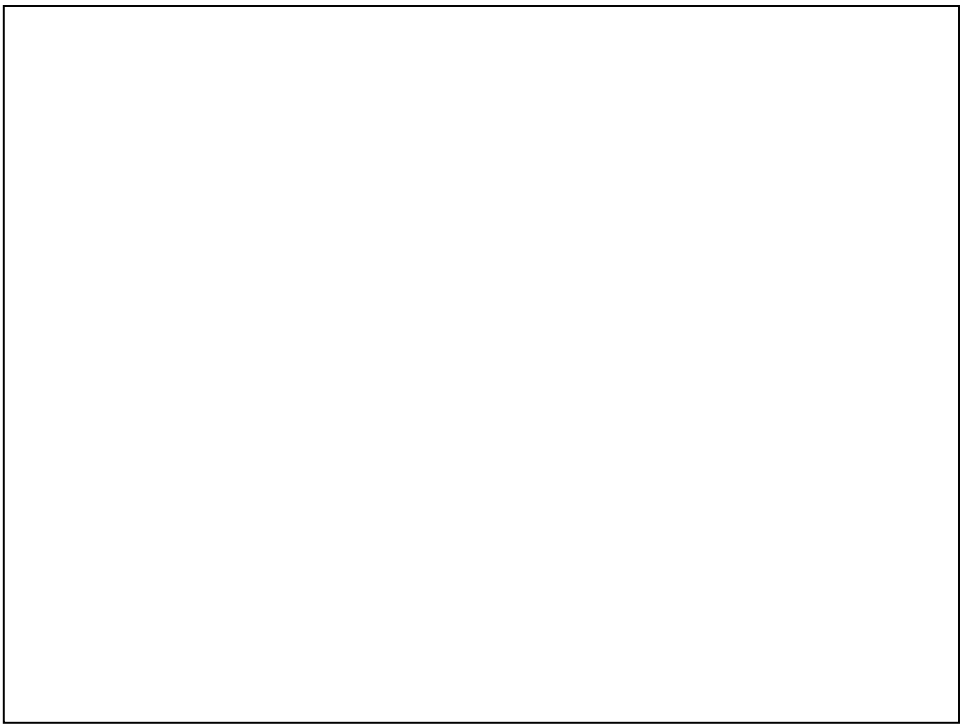

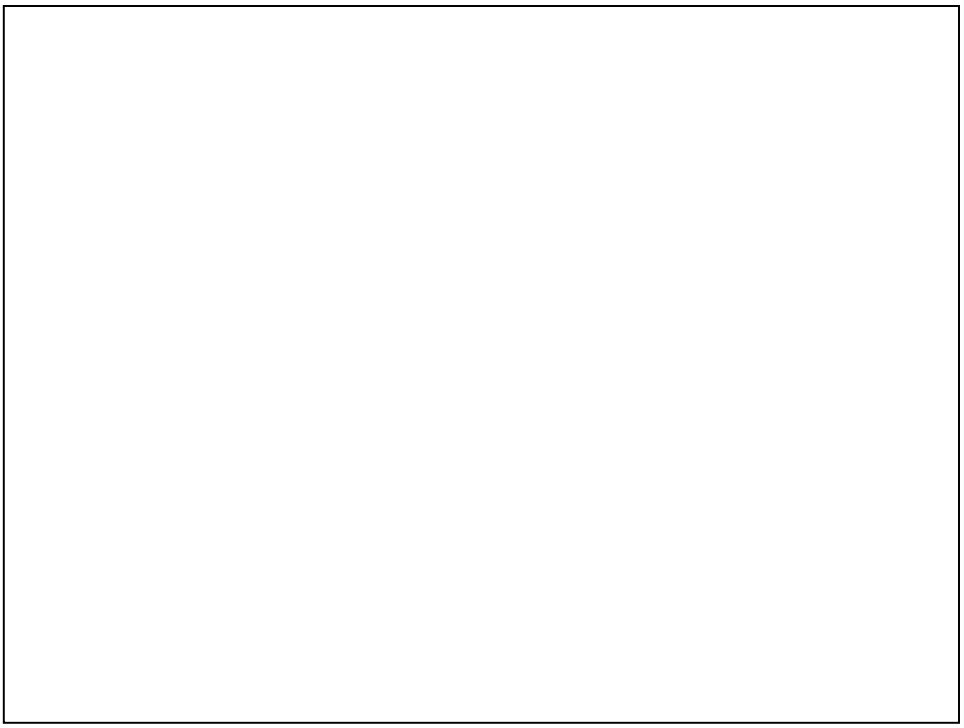

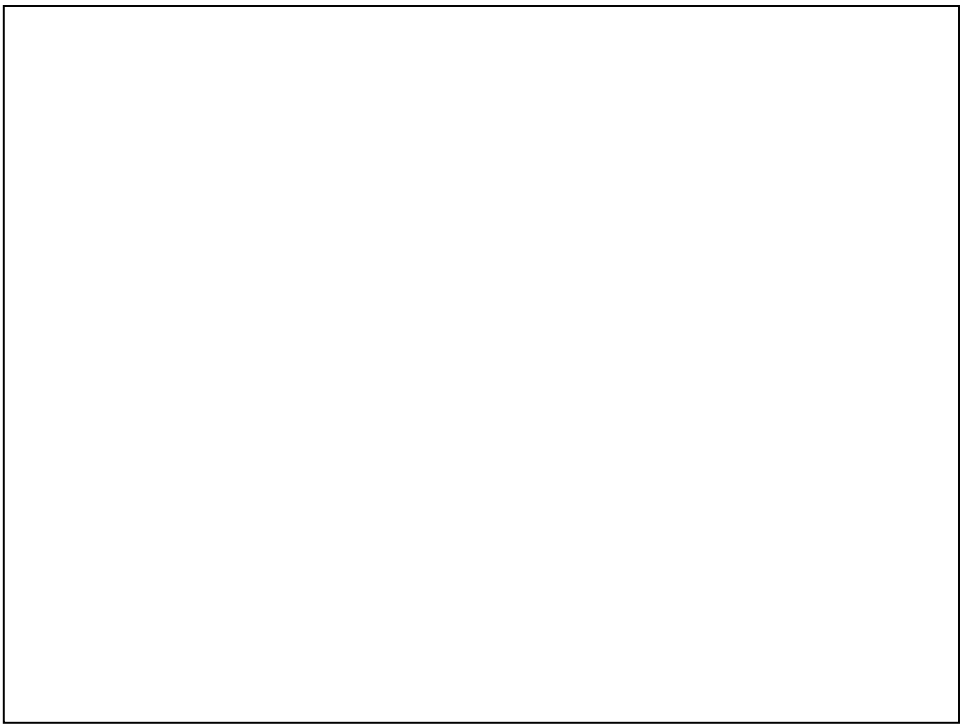

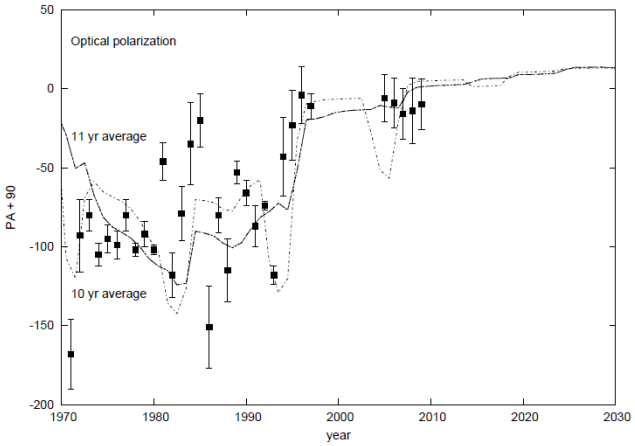

Figure 6. The evolution of the optical polarization angle compared with the model. The curves are for a 10 yr (dash-dot line) and for an 11 yr (dashed line) average. Observations refer to the values in Table 1 minus 180°. The theoretical lines are shifted by adding 90° since the electric vector does not project parallel to the jet axis.

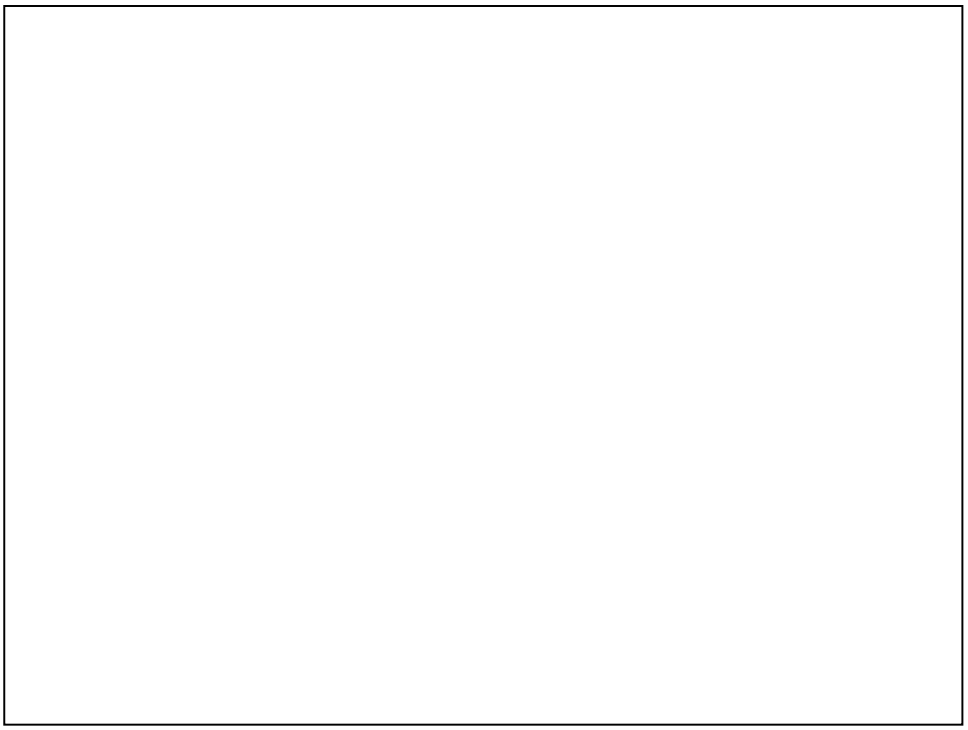

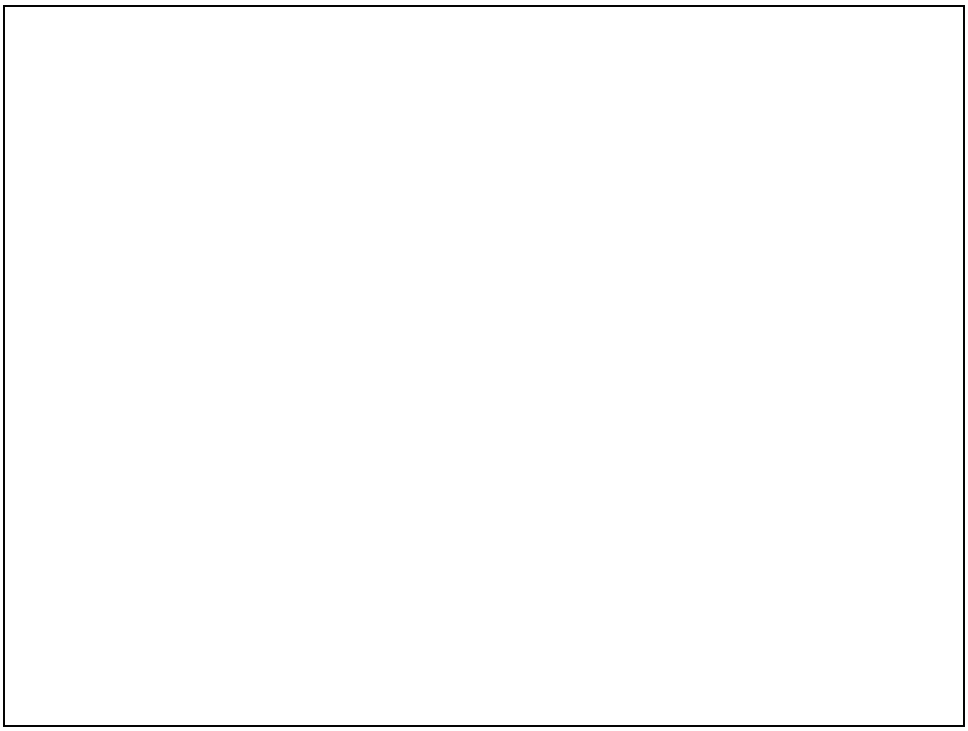

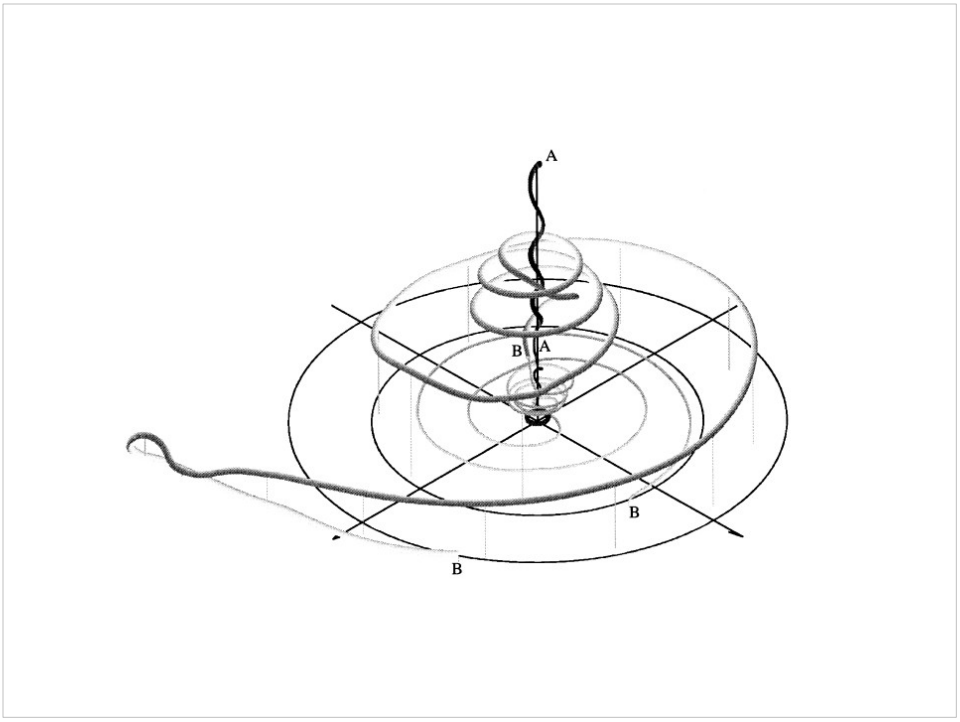
A
B
A
B
B

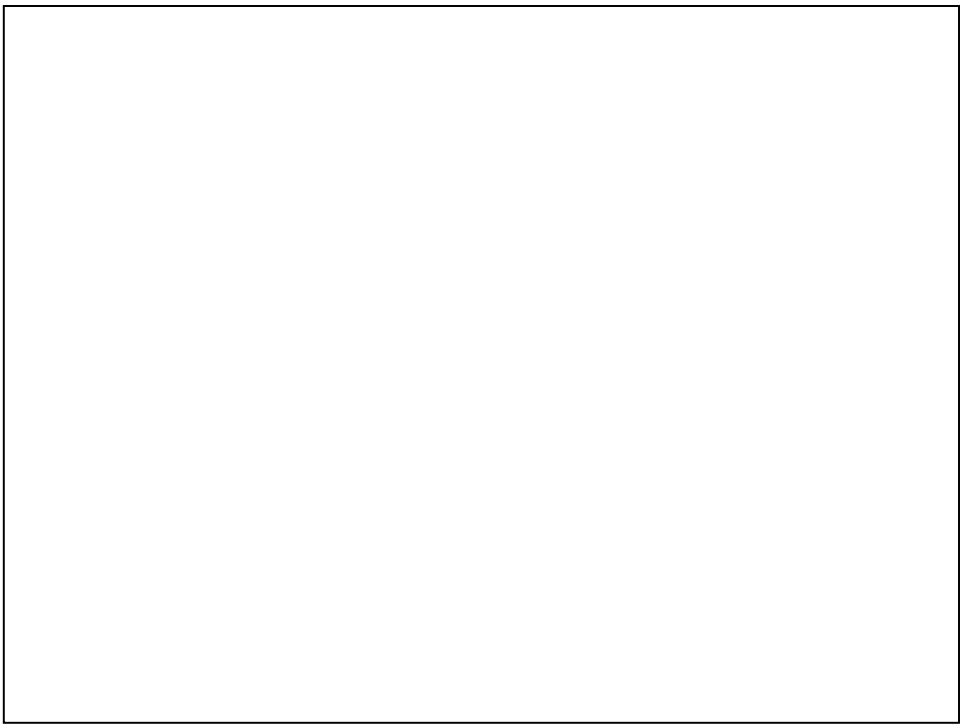

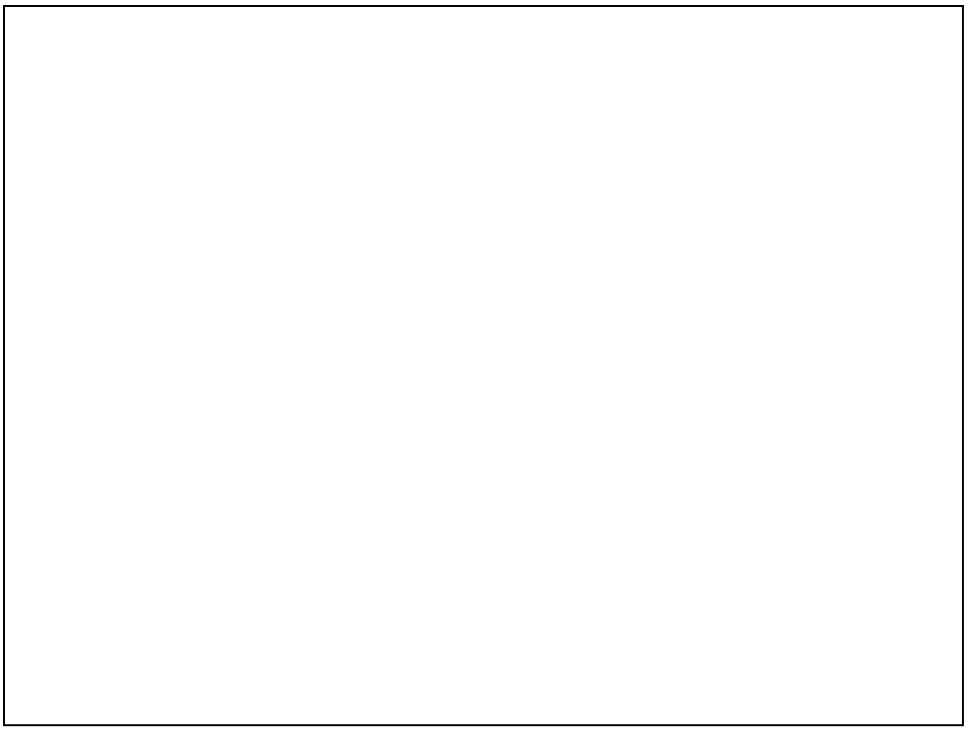

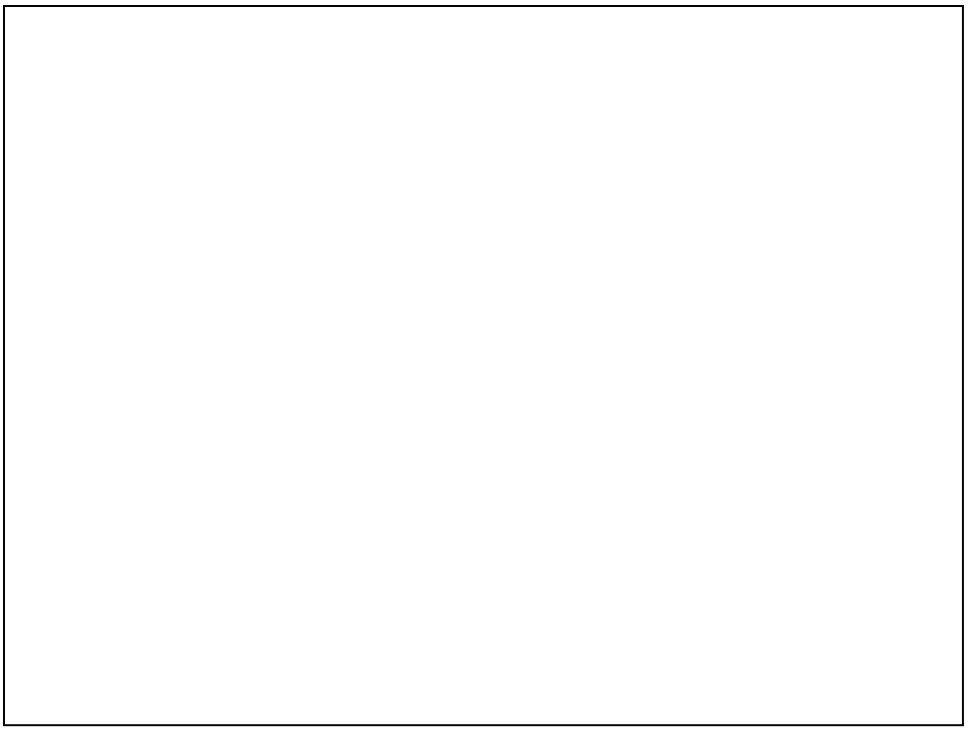

Next: 2015 – 2022 campaign

2015: accurate spin value

2019: test of no-hair –theorem

2022: confirmation of precession

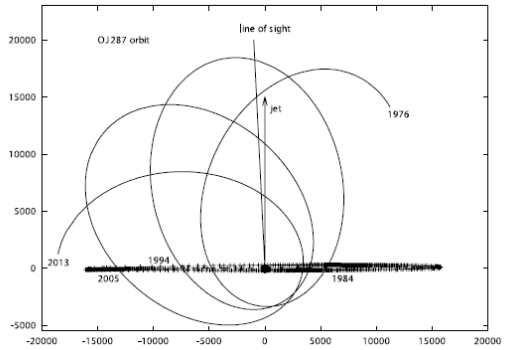

PN acceleration

.

$$\ddot{\boldsymbol{x}} \equiv \frac{d^2\boldsymbol{x}}{dt^2} = \ddot{\boldsymbol{x}}_0 + \ddot{\boldsymbol{x}}_{1\mathrm{PN}} + \ddot{\boldsymbol{x}}_{\mathrm{SO}} + \ddot{\boldsymbol{x}}_Q + \ddot{\boldsymbol{x}}_{2\mathrm{PN}} + \ddot{\boldsymbol{x}}_{2.5\mathrm{PN}},$$

$$\ddot{\boldsymbol{x}}_0 = -\frac{G\,m}{r^3}\,\boldsymbol{x}$$

$$\ddot{\boldsymbol{x}}_{1\mathrm{PN}} = -\frac{Gm}{c^2 r^2}\left\{\boldsymbol{n}\left[-2(2+\eta)\frac{Gm}{r} + (1+3\eta)v^2 - \frac{3}{2}\eta\dot{r}^2\right] - 2(2-\eta)\dot{r}\boldsymbol{v}\right\},$$

$$\begin{aligned}\ddot{\boldsymbol{x}}_{2\mathrm{PN}} = -\frac{G\,m}{c^4 r^2}\Bigg\{\boldsymbol{n}\Bigg[&\frac{3}{4}(12+29\eta)\left(\frac{G\,m}{r}\right)^2 \\ &+ \eta(3-4\eta)v^4 + \frac{15}{8}\eta(1-3\eta)\dot{r}^4 \\ &- \frac{3}{2}\eta(3-4\eta)v^2\dot{r}^2 - \frac{1}{2}\eta(13-4\eta)\left(\frac{G\,m}{r}\right)v^2 \\ &- (2+25\eta+2\eta^2)\left(\frac{G\,m}{r}\right)\dot{r}^2\Bigg] \\ &- \frac{1}{2}\dot{r}\boldsymbol{v}\Bigg[\eta(15+4\eta)v^2 - (4+41\eta+8\eta^2)\left(\frac{G\,m}{r}\right) \\ &-3\eta(3+2\eta)\dot{r}^2\Bigg]\Bigg\},\end{aligned}$$

Spin-orbit term

$$\ddot{\boldsymbol{x}}_{\mathrm{SO}} = \frac{G\,m}{r^2}\left(\frac{G\,m}{c^3\,r}\right)\left(\frac{1+\sqrt{1-4\,\eta}}{4}\right)$$
$$\times\,\chi\left\{\left[12\,\left[\boldsymbol{s}_1\cdot(\boldsymbol{n}\times\boldsymbol{v})\right]\right]\boldsymbol{n}\right.$$
$$+\left[\left(9+3\sqrt{1-4\,\eta}\right)\dot{r}\right](\boldsymbol{n}\times\boldsymbol{s}_1)$$
$$\left.-\left[7+\sqrt{1-4\,\eta}\right](\boldsymbol{v}\times\boldsymbol{s}_1)\right\},$$

$$\ddot{\boldsymbol{x}}_{2.5\mathrm{PN}} = \frac{8}{15}\frac{G^2 m^2 \eta}{c^5 r^3}\left\{\left[9v^2 + 17\frac{G\,m}{r}\right]\dot{r}\boldsymbol{n} - \left[3v^2 + 9\frac{G\,m}{r}\right]\boldsymbol{v}\right\},$$

$$\ddot{\mathbf{x}}_Q = q\,\chi^2\,\frac{3\,G^3\,m_1^2 m}{2\,c^4\,r^4}\left\{\left[5(\mathbf{n}\cdot\mathbf{s_1})^2 - \mathbf{1}\right]\mathbf{n} - \mathbf{2}(\mathbf{n}\cdot\mathbf{s_1})\mathbf{s_1}\right\}$$

no-hair theorem

quadrupole moment Q

$$Q = -q\frac{S^2}{Mc^2} \qquad \mathbf{S}_1 = G\,m_1^2\,\chi\,\mathbf{s}_1/c$$

unit vector $\mathbf{s}_1$

For black holes $q = 1$

for neutron stars $q > 2$

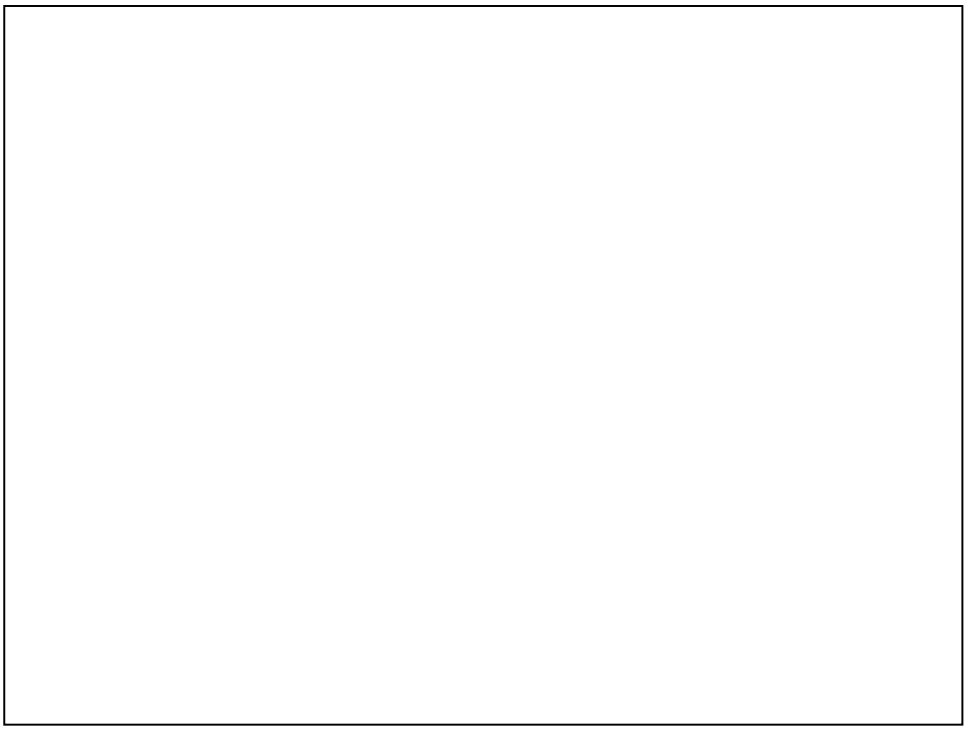

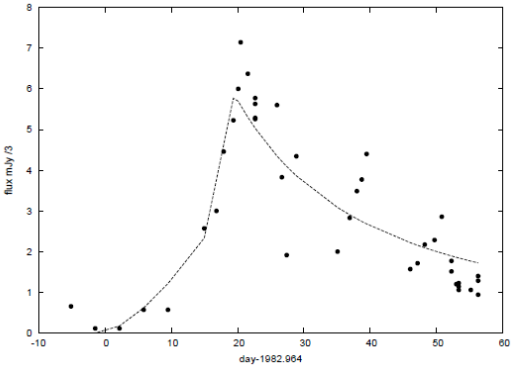
flux mJy /3
day-1982.964
0
1
2
3
4
5
6
7
8
-10
0
10
20
30
40
50
60

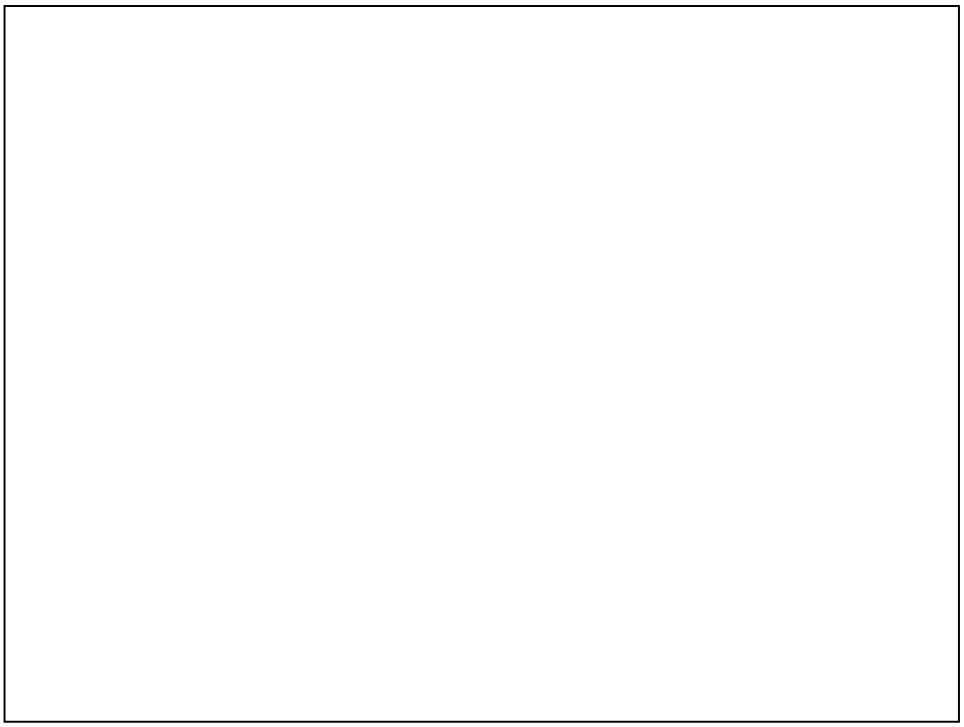

1995.8426

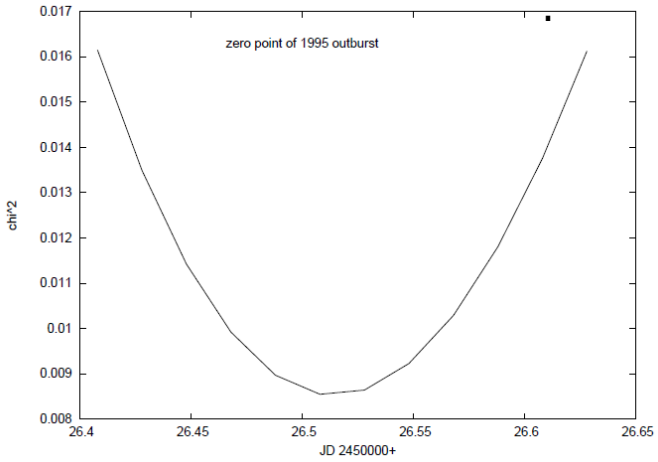
zero point of 1995 outburst
chi^2
0.017
0.016
0.015
0.014
0.013
0.012
0.011
0.01
0.009
0.008
26.4
26.45
26.5
26.55
26.6
26.65
JD 2450000+

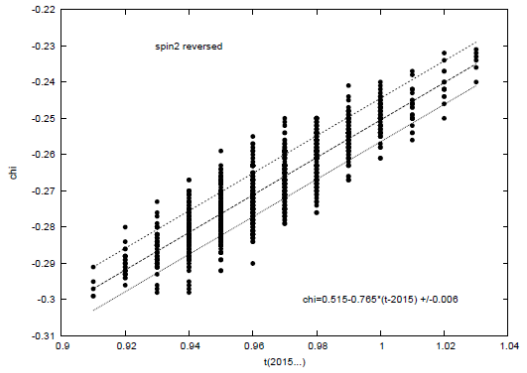
spin2 reversed
chi
t(2015...)
chi=0.515-0.765*(t-2015) +/-0.006
-0.22
-0.23
-0.24
-0.25
-0.26
-0.27
-0.28
-0.29
-0.3
-0.31
0.9
0.92
0.94
0.96
0.98
1
1.02
1.04

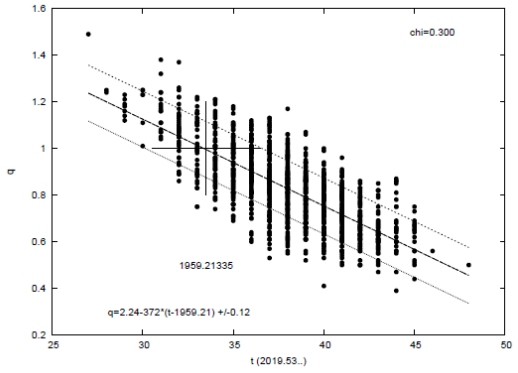
chi=0.300
1959.21335
q=2.24-372*(t-1959.21) +/-0.12
q
t (2019.53..)
1.6
1.4
1.2
1
0.8
0.6
0.4
0.2
25
30
35
40
45
50

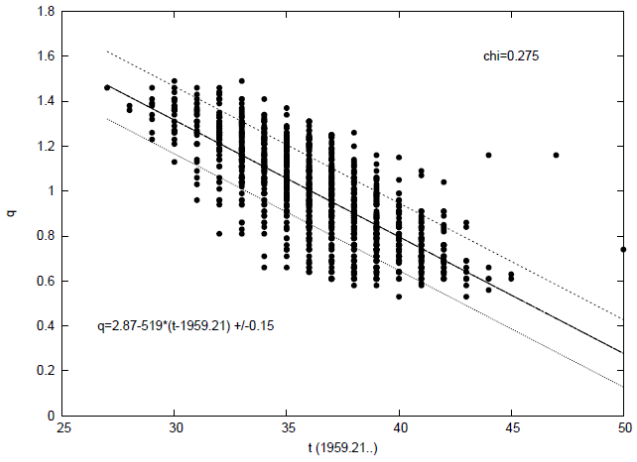
chi=0.275
q=2.87-519*(t-1959.21) +/-0.15
q
t (1959.21..)
1.8
1.6
1.4
1.2
1
0.8
0.6
0.4
0.2
0
25
30
35
40
45
50

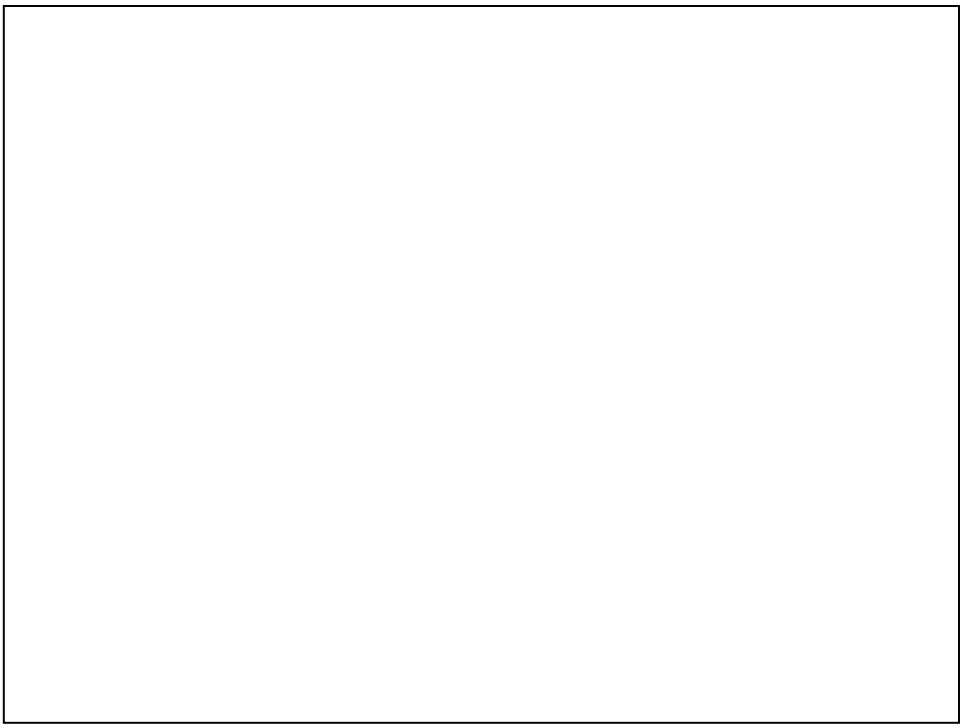

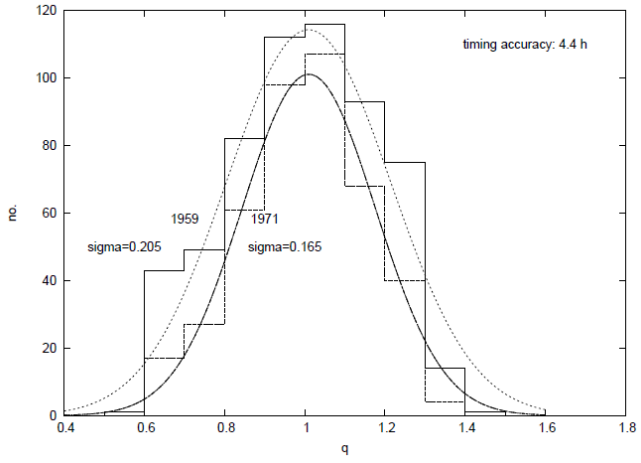
timing accuracy: 4.4 h
1959
1971
sigma=0.205
sigma=0.165
no.
q
0
20
40
60
80
100
120
0.4
0.6
0.8
1
1.2
1.4
1.6
1.8

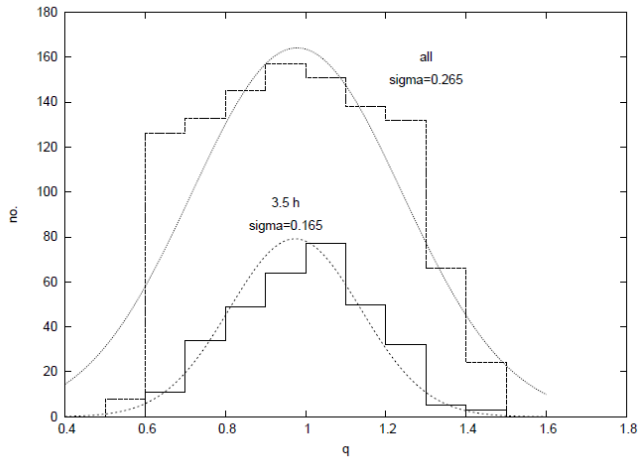
all
sigma=0.265
3.5 h
sigma=0.165
no.
q
0
20
40
60
80
100
120
140
160
180
0.4
0.6
0.8
1
1.2
1.4
1.6
1.8

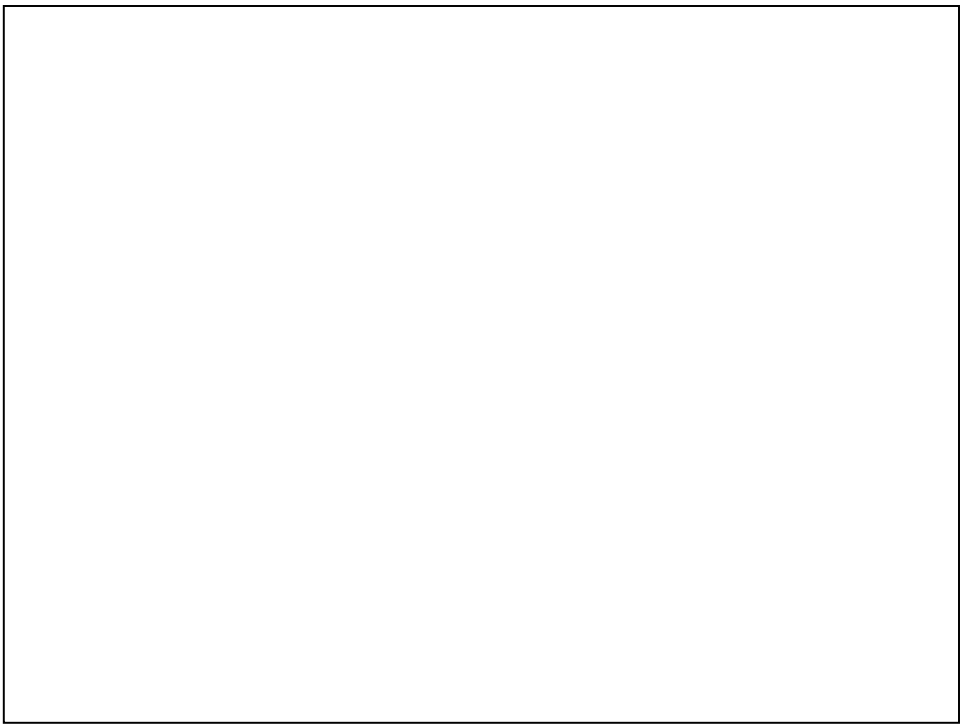

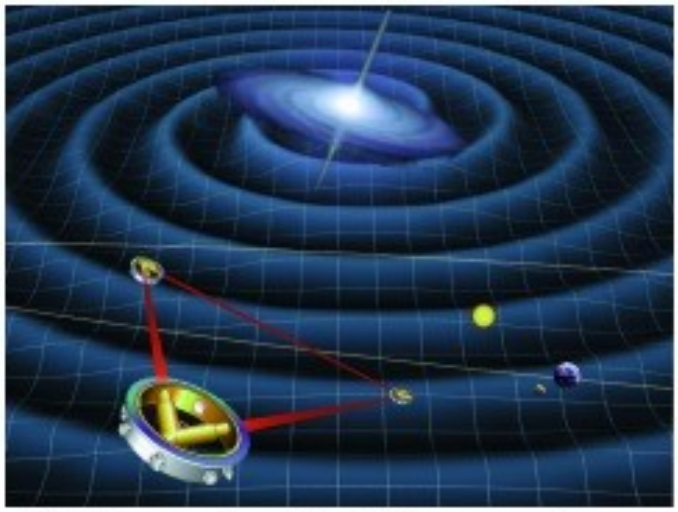

Artist's impression of the LISA spacecraft
© NASA (public domain)

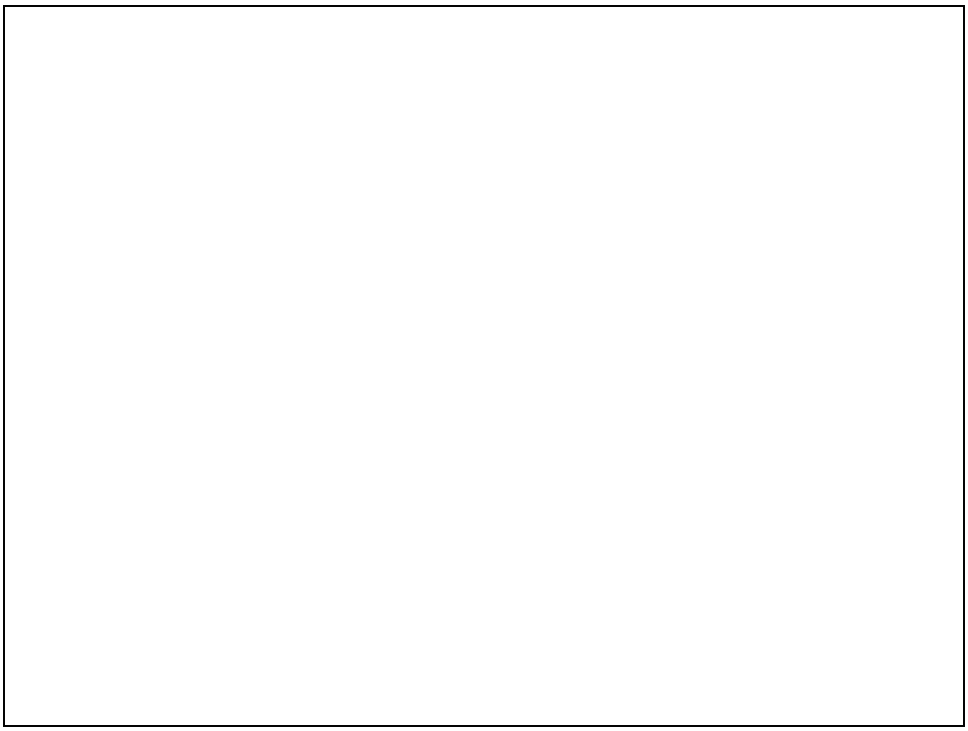

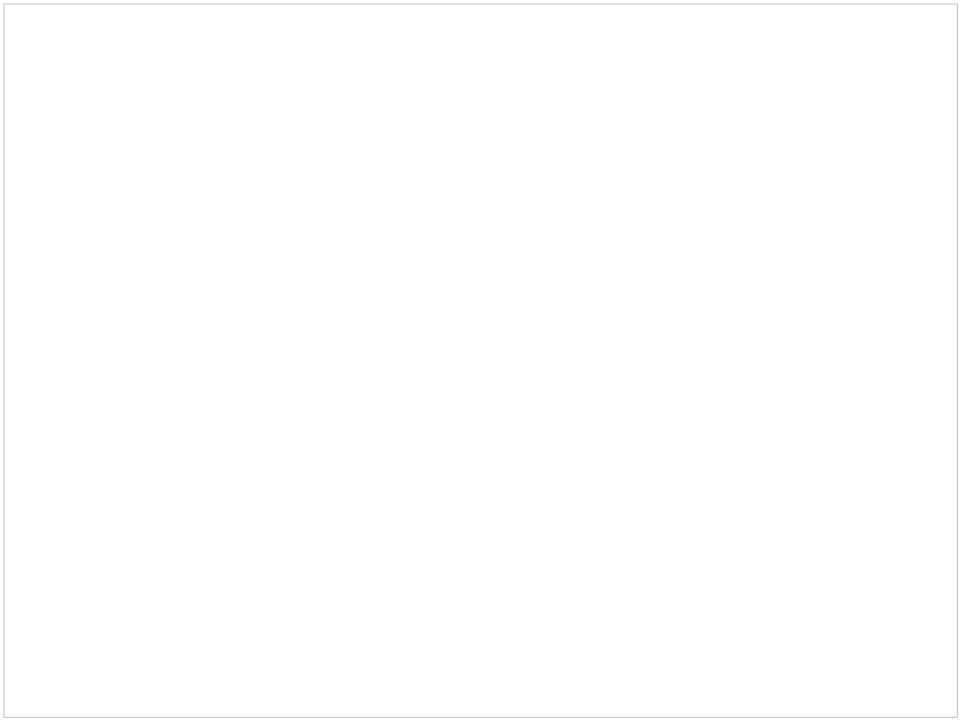

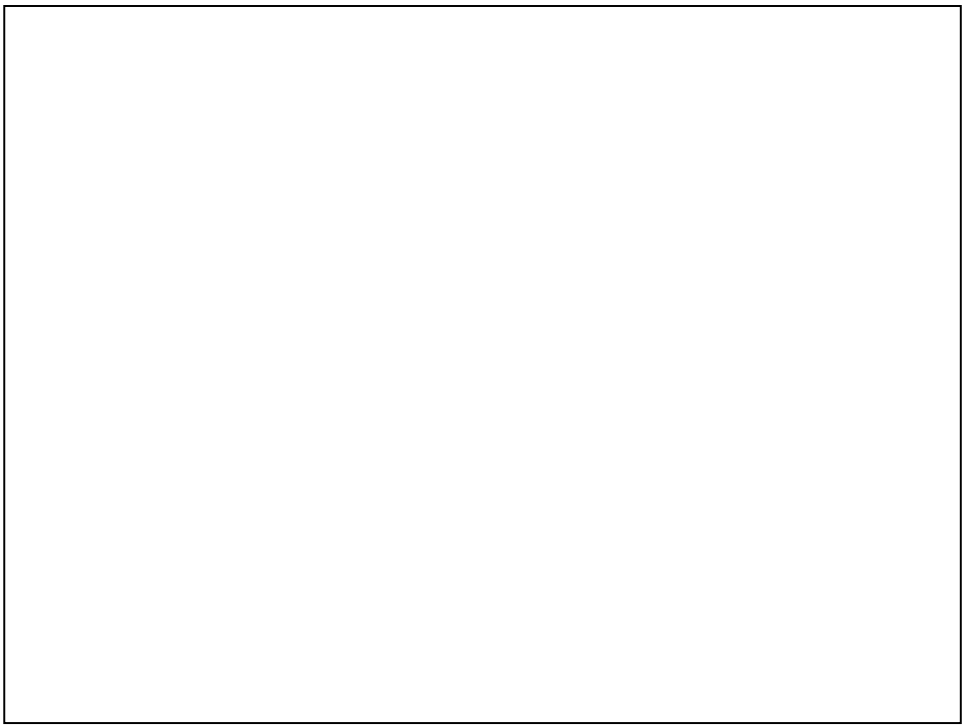

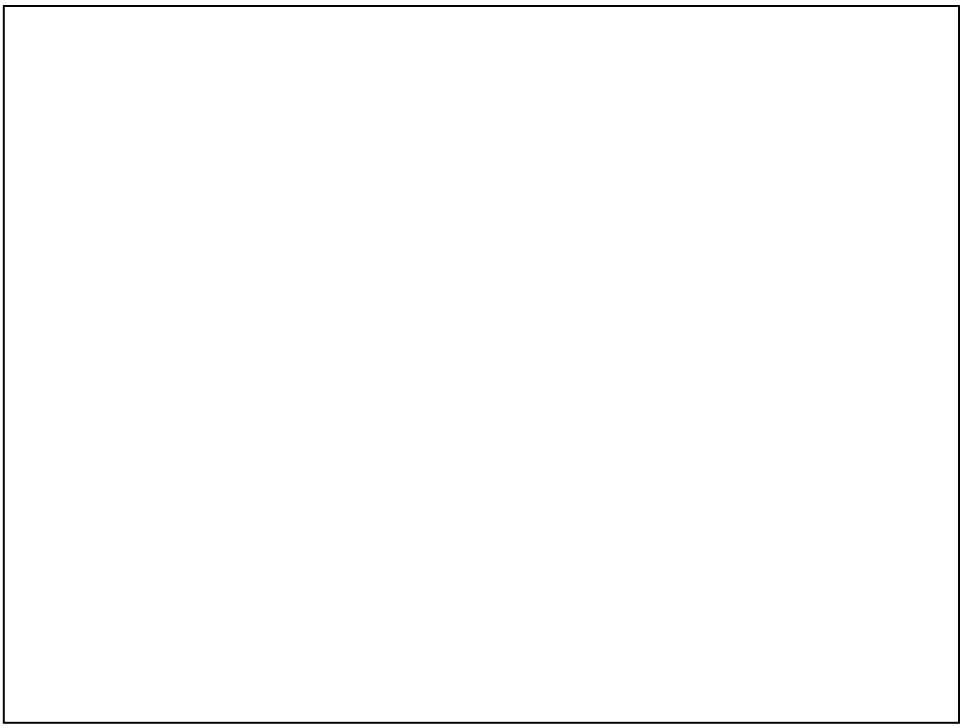

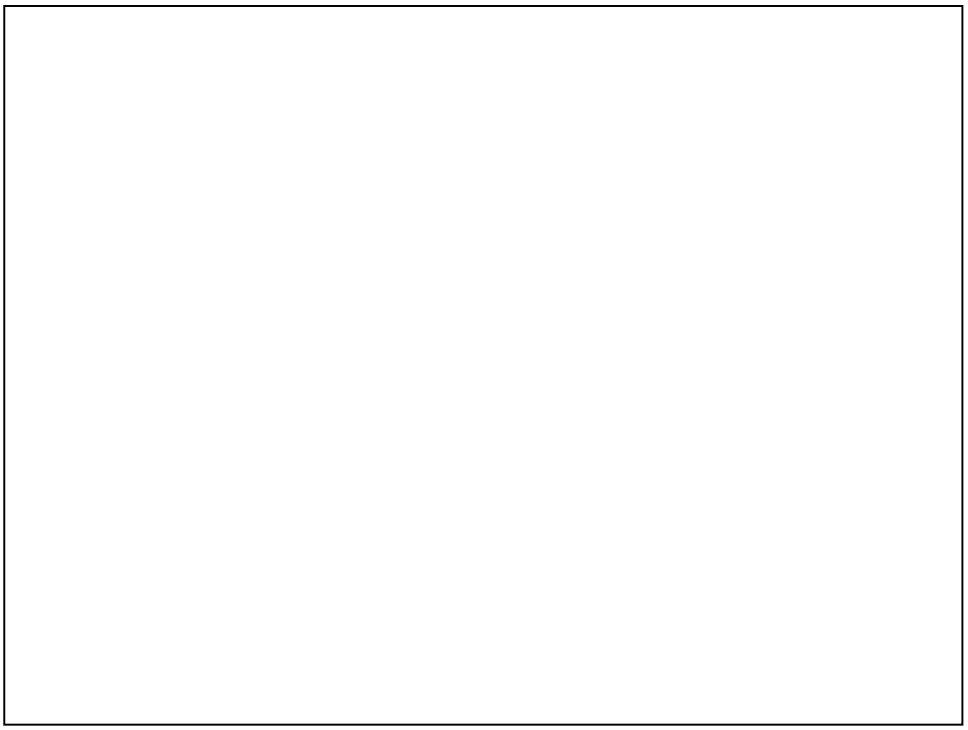

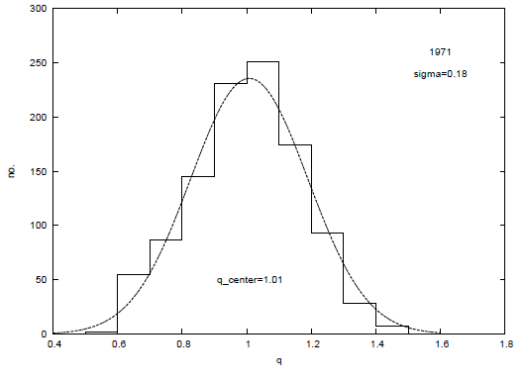
1971
sigma=0.18
q_center=1.01
no.
q
300
250
200
150
100
50
0
0.4
0.6
0.8
1
1.2
1.4
1.6
1.8

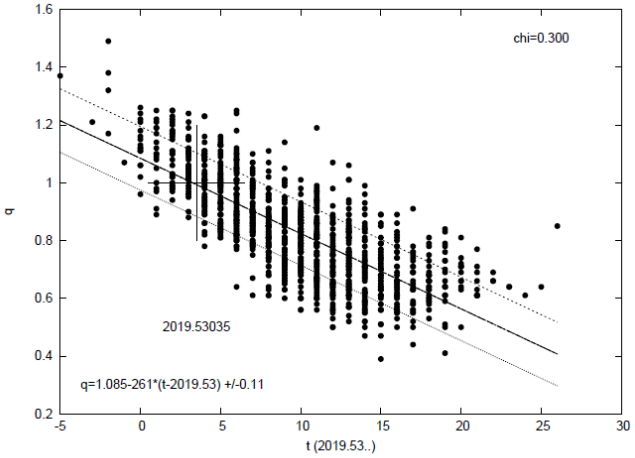
chi=0.300
2019.53035
q=1.085-261*(t-2019.53) +/-0.11
q
t (2019.53..)
1.6
1.4
1.2
1
0.8
0.6
0.4
0.2
-5
0
5
10
15
20
25
30